Electrical ageing of insulating polymers : approach through electroluminescence and cathodoluminescence analyses

Bo Qiao

THÈSE

En vue de l'obtention du

DOCTORAT DE L'UNIVERSITÉ DE TOULOUSE

Délivré par :
l'Université Toulouse III – Paul Sabatier
Discipline ou spécialité :
Génie Electrique

Présentée et soutenue par :
Bo QIAO
Le *16 Octobre 2015*

Titre : *Une approche du vieillissement électrique des isolants polymères par mesure d'électroluminescence et de cathodoluminescence*

Title : *Electrical ageing of insulating polymers: approach through electroluminescence and cathodoluminescence analyses*

JURY

Dr. Gilbert TEYSSEDRE	*Directeur de thèse*
Pr. John FOTHERGILL	*Rapporteur*
Dr. Pilar TIEMBLO MAGRO	*Rapporteur*
Dr. Christian LAURENT	*Examinateur*
Dr. Mohamed BELHAJ	*Examinateur*
Dr. Martinus WERTS	*Examinateur*

Ecole doctorale : *Génie Electrique, Electronique et Télécommunications (GEET)*
Unité de recherche : *LAboratoire PLAsma et Conversion d'Energie (LAPLACE) UMR 5213*
Directeur de Thèse : *Gilbert TEYSSEDRE*
Rapporteurs : *John FOTHERGILL et Pilar TIEMBLO MARGO*

À ma famille

Remerciements

Avant tout, je tiens à présenter toute ma gratitude à mon chef Monsieur Gilbert TEYSSEDRE, chercheur au CNRS, responsable d'équipe Diélectriques Solides et Fiabilité (DSF). Il travaille sur le développement des techniques de luminescence dans les isolants polymères sur la structure chimique et physique, les phénomènes de dégradation, la charge d'espace et les propriétés de transport de charge. Il a fait un excellent travail dans ce domaine. Il est très gentil, modeste, très accessible, et très admiré. J'ai acquis beaucoup pendant les trois ans, ce qui affecterait toute ma vie. Le remercier de ses mots et des démonstrations et me conduit au Palais Scientifique.

Que Monsieur Christian LAURENT, mon conseiller, chercheur au CNRS, le directeur de la Laboratoire de Plasma et Conversion d'Energie (LAPLACE) UMR5213, qui travaille sur des projets expérimentaux et de modélisation relatif au transport et au vieillissement des diélectriques. Il est une grande figure et des gros muscles (il aime le sport et il est un expert en planche à voile.). En même temps, il est très gentil et sourit beaucoup, plein de charme de la personnalité. J'aime parler avec lui sur des questions académiques.

J'ai bien de la chance d'avoir eu deux administrateurs à la fois sympathique, de forte personnalité et avec une prestance académique.

Je remercie le jury: Pr. John FOTHERGILL (rapporteur), Dr. Pilar TIEMBLO MAGRO (rapporteur), Dr. Mohamed BELHAJ (examinateur) et Dr. Martinus WERTS (examinateur).

J'adresse sincèrement mon remerciement à Séverine LE ROY, Bernard DESPAX et Kremena MAKASHEVA, qui m'ont beaucoup aidé et conseillé au cours de ma thèse.

Je remercie également F. Baudoin, L. Berquez, L. Boudou, V. Griseri, S. Le Roy, JJ. Martinez-Vega, D. Marty-Dessus, D. Mary et C. Villeneuve-Fauredu de groupe DSF pour leur aide au cours de mes trois années dans le groupe.

En outre, je tiens à remercier nos ingénieurs du LAPLACE, Benoît SCHLEGEL et Benoît LANTIN, qui m'ont appris à utiliser le matériel scientifique et qui m'ont aidé à faire face à certains problèmes lors de mes expériences.

Merci de l'Université Paul Sabatier (UPS) de Toulouse, le Centre National de Recherche Scientifique (CNRS), Laboratoire de Plasma et Conversion d'Energie (LAPLACE), des diélectriques solides et fiabilité (DSF), qui fournissent un environnement académique excellent et confortable et une atmosphère conviviale.

Merci à mon chef au cours de la Maïtrise, Pr. Xurong Xu, Pr. Suling ZHAO, et Pr. Zheng Xu.

Merci à mes collègues et amis en France: Aman, Florian, Laurent, Amal, Quyen, Xiaolin, Abderrahmane, Qi, Chenjiang, Yuan, Feng, Bertrand, Lucie, Nga, Jeremy, Mous, Yang, Haonan, Xuan, Sihem, Ningying, Jordi, Bang, Duc, Tiantian, Thomas, Paul, Lumei, Thibaut, Neko, John, Alessandro, Jacopo, Kevin, Rick, Petr, Louis, Alice et ainsi de suite, qui m'accompagnent au cours de ces trois ans et me font sentir joyeux. J'en garderai des merveilleux souvenirs.

Enfin, je tiens à remercier ma famille pour leur soutien inconditionnel et vital au cours de ces années.

Acknowledgements

Firstly, I would like to thank my supervisor Dr. Gilbert TEYSSEDRE, the director of Solid Dielectrics and Reliability (DSF) group. He works on the development of luminescence techniques in insulating polymers with focus on chemical and physical structure, degradation phenomena, space charge and transport properties. He has done a great work on this domain. He is very kind, modest, very approachable and being admired greatly. I acquired a lot during the three years, which would affect my whole life. Thank him for his words and demonstrations and leading me to the Scientific Palace.

And Dr. Christian LAURENT, my advisor, the director of Laboratory on Plasma and Conversion of Energy (LAPLACE) UMR5213, who works on experimental and modeling activity relating to charge transport and ageing in dielectrics and is well acknowledged. He has a tall figure and strong muscles (he loves sports and is an expert in windsurfing.). At the same time he is very kind and smiles a lot, full of personality charm. I like to talk with him on academic questions and social problems.

I am very lucky having two directors with both personality charm and academic influences.

I thank the jury: Pr. John FOTHERGILL (reviewer), Dr. Pilar TIEMBLO MAGRO (reviewer), Dr. Mohamed BELHAJ (examiner) and Dr. Martinus WERTS (examiner).

I thank Séverine LE ROY，Bernard DESPAX and Kremena MAKASHEVA, who help me a lot and give me instructions during my Ph.D. period.

I also thank F. Baudoin, L. Berquez, L. Boudou, V. Griseri, S. Le Roy, JJ. Martinez-Vega, D. Marty-Dessus, D. Mary and C. Villeneuve-Faure from group DSF for their help during my three years in the group.

Additionally, I would like to thank our engineers in LAPLACE, Benoît SCHLEGEL and Benoît LANTIN, who teach me to use some machines in the lab and help me dealing with some problems during my experiments.

Thank University Paul Sabatier (UPS) of Toulouse, National Center for Scientific Research (CNRS), Laboratory on Plasma and Conversion of Energy (LAPLACE), Solid Dielectrics and Reliability (DSF), which provide an excellent and comfortable academic environment and friendly atmosphere.

I thank my supervisor during my Master period, Pr. Xurong Xu, Pr. Suling ZHAO, and Pr. Zheng Xu. They led me to start my research career and also helped me a lot during my Ph.D. period.

Thank my colleagues and friends in France: Aman, Florian, Laurent, Amal, Quyen, Xiaolin, Abderrahmane, Qi, Chenjiang, Yuan, Feng, Bertrand, Lucie, Nga, Jeremy, Mous, Yang, Haonan, Xuan, Sihem, Ningying, Jordi, Bang, Duc, Tiantian, Thomas, Paul, Lumei, Thibaut, Neko, John, Alessandro, Jacopo, Kevin, Rick, Petr, Louis, Alice and so on, who accompany me during these three years and make me feel joyful. These are going to be happy memories.

Last but not least, I would like to thank my family for their unconditional and vital support during these years.

致谢

我首先感谢我的授业恩师 Gilbert TEYSSEDRE 博士，DSF 组的主任，同时是我的论文指导老师。他在高压绝缘电介质的老化和空间电荷传输及测试手段科研领域有极高的造诣，取得了丰硕的成果，同时他个性随和谦逊，平易近人，在我心目中高山仰止。三年的耳濡目染，让我受益终生。感谢博士期间他的辛勤教诲，通过口传心授以及亲自示范的方式把我带入了科学技术的殿堂。

还有我的授业恩师 Christian LAURENT 博士，LAPLACE 研究所的主任。他在我的研究领域有更丰富的经验，取得了杰出的成就，获得了世界各地各位同仁的广泛认可。他既有高大的身躯和健硕的肌肉（他热爱运动，是一名帆板运动员），同时经常面带微笑极其和善，极其富有人格魅力，我很享受和他一起讨论研究问题。

我很庆幸遇到两位人格魅力和学术能力都极好的老师。

感谢答辩委员会评审委员（两位 reviewers 和两位 examiners）：来自英国的 City University London 副校长、聚合物老化领域的权威 John FOTHERGILL 教授，来自西班牙 Spanish National Research Council 的聚合物材料及化学发光学专家 Pilar TIEMBLO MAGRO 博士，法国雷恩的 Martinus WERTS 博士和图卢兹的 Mohamed BELHAJ 博士。

感谢 Séverine LE ROY，Bernard DESPAX 和 Kremena MAKASHEVA，三位老师在我研究期间提供了大量的帮助和指导。

感谢 DSF 组的 F. Baudoin, L. Berquez, L. Boudou, V. Griseri, S. Le Roy, JJ. Martinez-Vega, D. Marty-Dessus, D. Mary 和 C. Villeneuve-Faure 各位老师给予了我很多帮助和指导。

感谢实验室工程师 Benoît SCHLEGEL 和 Benoît LANTIN 对我实验仪器使用的悉心指导，以及帮我解决各种实验上遇到的问题。感谢已经退休的 Alain BOULANGER。

感谢图卢兹大学（UT），图卢兹第三大学（UPS），法国科学研究院（CNRS），等离子与能量转换实验室（LAPLACE）及固体电介质与稳定性研究（DSF）研究组。其为我博士期间的研究工作提供了良好舒适的科研环境和友好和谐的科研氛围，让我能够专心地工作学习，并且取得出色的成果。

另外，感谢我硕士期间的导师徐叙瑢院士，及赵谡玲教授和徐征教授，在我博士期间对我的科研工作和在法国的日常生活仍给予大量的关心和指导。尤其徐先生逾九十高龄仍常和我通电话询问我的科研进展，并就一些核心的科研问题发表见解和我讨论，让我受益匪浅。

感谢我在法国期间的各位朋友同事，Aman, Florian, Laurent, Amal, Quyen, Xiaolin, Abderrahmane, Qi, Chenjiang, Yuan, Feng, Bertrand, Lucie, Nga, Jeremy, Mous, Yang, Haonan, Xuan, Sihem, Ningying, Jordi, Bang, Duc, Tiantian, Thomas, Paul, Lumei, Thibaut, Neko, John, Alessandro, Jacopo, Kevin, Rick, Petr, Louis, Alice 等，陪伴了我度过了三年的学习生活时光，让我在异国他乡生活得很快乐。这是一段美好的终身难忘的回忆。

最后衷心地感谢我的家人给予我的大力支持。

Table of Contents

Abbreviations and Symbols

Au - Gold

BCT - Bipolar Charge Transport

BOPP - Bi-axially Oriented Polypropylene

CCD - Charge coupled device

CHL - Chemiluminescence

CL - Cathodoluminescence

cps - Counts Per Second (cp2s, Counts per 2 seconds)

EL - Electroluminescence

FL - Fluorescence

HVAC - High Voltage Alternate Current

HVDC - High Voltage Direct Current

ITO - Indium Tin Oxide

LDPE - Low Density Polyethylene

LIMM - Laser intensity modulation method

LNT - Liquid Nitrogen Temperature (-185 ℃ in practice)

MEH-PPV - Poly[2-methoxy-5-(2-ethylhexyloxy)-1,4-phenylenevinylene]

PDs - Partial Discharges

PE - Polyethylene

PEA - Pulse electro-acoustic method

PEEK - Polyether Ether Ketone

PEN - Polyethylene Naphthalte

PET - Polyethylene Terephthalate

PHL - Phosphorescence

PL - Photoluminescence

PM - Photomultiplier

PP - Polypropylene

PTFE - Polytetrafluoroethylene (Teflon)

QDs - Quantum Dots

RL - Recombination-induced Luminescence

RT - Room Temperature

sccm - Standard Cubic Centimeter per Minute

SCLC - Space Charge Limited Currents

SPs - Surface Plasmons

XLPE - Cross-Linked Polyethylene

ZnO - Zinc Oxide

General Introduction

Insulating polymers are used in a variety of applications in electrical engineering, such as cables, generators, transformers, capacitors, from personal computers to car manufacturing, from living facilities to military installations [1, 2]. Electrical ageing and breakdown in insulating polymers is of fundamental interest to the researchers, the design engineers, the manufacturers and the customers. In this respect, Partial Discharge (PD) is a harmful process leading to ageing and failure of insulating polymers. However, with the development of the materials and apparatus, PDs can be weakened or avoided in some situations, e.g. extra high voltage cables, capacitors, etc. Therefore, there is urgent demand for understanding electrical degradation mechanisms under high energy particles or electric field intensity, pushing the limit of electrical properties in insulating polymers.

Electroluminescence (EL) along with cathodoluminescence (CL), is an exciting field of research for probing insulating polymers, because it gives insight into electrical ageing and breakdown process, since firstly reported in 1967 by Hartman [3]. They are original techniques, contributing to uncover the nature of charge transport mechanisms and electrical ageing. It provides a very interesting information, of photophysical nature, revealing excited states in the polymer, coupled to the electrical behavior of the material, especially with charge carriers in the material that are at the origin of the excitation through the exchange of kinetic or potential energy. Various physical and chemical mechanisms have been involved in the aging of electrical insulations under DC and AC stress [4, 5]. Electroluminescence (EL) is a phenomenon involving physical processes such as charge injection, extraction, and transportation, but also chemical reaction through excited states. Electric fields can produce excited or ionized states, some of which have a non-zero probability for light emission during their relaxation and for chemical reaction in their excited states. Hence, on one hand, EL can be a probe of charge excitation and recombination processes, on the other hand, it may provide information on the nature of defects and luminescent sources. EL is associated with electrical ageing and could provide the signature of excited species under electric field. Because interfacial electronic states are very important in charge transfer at the electrode-dielectric interface, it should impact on the EL features, especially under AC stress. Therefore, EL can also gather information and be used to probe the physical/chemical processes occurring inside dielectrics or at the metal-dielectric interface.

However, the essence of EL and the links between EL and electrical ageing or breakdown are still debatable. Hence, CL is a supplementary technique with another excitation source for probing insulating polymers. Insulating polymers, such as polyolefins, have a large band gap (approximately 9 eV), with deep trapping centers mainly due to structural defects, impurities, or additives. EL can originate from hot electron carriers and/or recombination of charge carriers. CL is excited with electron beams and can provide information with more energy level as a reproduction of EL. Investigations are carried out to identify the excitation processes.

This work was developed in Diélectriques Solides et Fiabilité (DSF) research group of Laboratoire Plasma et Conversion d'Energie (LAPLACE), University of Toulouse III Paul Sabatier, Toulouse, France. The scholarship for the Ph.D. of Bo QIAO is supported by China Scholarship Council (CSC).

The dissertation is divided into the following six parts:

Chapter 1: introduces the insulating polymers and their electrical applications, reviews the state of the art of luminescence processes in insulating polymers, such as photoluminescence, electroluminescence, cathodoluminescence, chemi-luminescence and charge recombination-induced luminescence. The electrical ageing, degradation and breakdown processes of insulating polymers are presented. The diagnostic techniques for electrical ageing or pre-breakdown signals are developed, such as space charge measurement and electroluminescence for probing the dielectrics. The relationship between electroluminescence and electrical ageing is addressed. The objectives of this work approaches to inferring the electrical ageing mechanisms are introduced at the end of this chapter.

Chapter 2: introduces the experimental materials, several insulating polymers, such as Polyethylene, Polypropylene and Polyethylene Naphthalte. The experimental methods and setups, such as gold and Indium Tin Oxide (ITO) coating setups, luminescence excitation setups and other inspection equipment.

Chapter 3: investigates the electroluminescence (EL) in Bi-axially Oriented Polypropylene (BOPP), evidences the excitons formation under stress, and analyzes their relationship to electrical ageing. The samples are prepared with sandwich structure metalized with gold electrode. EL is detected under both DC and AC electric stress. The field dependence of EL and time dependence of current under DC stress, and the field dependence and phase-resolved EL under AC stress, are carried out and discussed. Through spectral analyses the common spectra of both Polypropylene and Polyethylene infers that their EL mechanisms follow the same route and come from the same or similar luminescent centers.

Chapter 4: specially investigates the impact of the electrode during the EL measurement of insulating polymer films. In this chapter, Polyethylene Naphthalalte (PEN) thin films are deposited with two type of electrodes: i.e. gold and ITO. The PEN films metallized with gold are also measured with a red-censoring optical filter cutting wavelength longer than 620 nm. All the measurements are carried out on two electrodes (gold and ITO) of PEN films and compared to gold electrode with red optical filter. The cross-validation proves that the red emission of the spectra comes from the gold electrode. Furthermore, the red emission of the spectra come from the Surface Plasmons effect at the surface or interface of the electrode.

Chapter 5: further studies the cathodoluminescence (CL) of the insulating polymers with electron beam energy up to 5 keV. The CL spectra of polyolefin such as Polyethylene and Polypropylene are similar with the same wavelength of the peaks at approximately 570

nm and shoulders, which is also the same with EL of these molecules. The source of each peak and shoulders in both CL and EL spectra are identified. With the identified elementary components we reconstructed the CL and EL spectra and discussed the mechanisms of both CL and EL. Two aromatic polyesters, i.e. Polyethylene Naphthalte and Polyether Ether Ketone are irradiated with electron beams and evidenced that the CL spectra is a reproduction of EL spectra.

General conclusion and perspectives: conclude the achievements in this work and anticipate the future works in this domain.

Chapter 1
State of the Art

1.1 Insulating polymers and electrical applications

Polymers are frequently found in our surroundings from personal computers to car manufacturing, from living facilities to military installations. More specifically, some insulating polymers are widely used with their electrical insulating properties to electrical engineering applications [6]. Polymers play a very significant role as insulating media with electrical properties because of their ease of processing, mass production, cost effectiveness and stress withstanding. They are either purely amorphous materials, or partly crystalline. Structural disorder, as well as chemical disorder, containing by-products, chemical defects of the polymeric chain, etc, and interfaces between crystalline or amorphous units [7], are unavoidable factors that contribute to their electrical and photo-physical properties, and provide them with complex behavior. Polymers are often manufactured for strengthened properties, for example, cross linked Polyethylene (XLPE) is produced to achieve higher dielectric strength and thermomechanical stability.

1.1.1 Polymeric materials in electrical engineering

Polymers are always developed with special chemical and mechanical properties to meet some particular requirement, in spite of which, the electrical properties should overshadow the other properties. There are two kinds of polymers according to their electrical properties: conducting (or semiconducting) polymers and insulating polymers.

It is well known that the metal has a strong electronic conductivity, whereas most of the polymers are on the contrary, underlying their use as excellent insulators. However, there still exist some conductive or semi-conductive polymers which have a narrow band gap. Conductive polymers, more precisely, intrinsically conducting polymers, such as polyacetylene (Its high electrical conductivity was discovered by Hideki Shirakawa, Alan Heeger, and Alan MacDiarmid in the 1970s [8] and recognized by the Nobel Prize in Chemistry in 2000) and phenylene vinylene (PPV, a famous family of semiconducting polymers and extensively used in organic light emitting diodes), are organic polymers that conduct electricity, which have metallic conductivity or can be semiconductors. Most of the conductive polymers are not pure polymers but compounds, while even polymers themselves are not pure at all because of their degrees of polymerization and catalyst and impurities during the manufacturing process. The electrical and photo-physical properties can be fine-tuned using the methods of organic synthesis and advanced dispersion techniques. Conductive polymers or conjugated polymers have drawn attention of scientists and encouraged the rapid growth of this field. Since the late 1980s, organic light emitting diodes (OLEDs) and organic photovoltaic cells have emerged as important applications of semiconducting polymers [9-13]. Consequently, the electroluminescence features in materials for OLEDs has been investigated extensively and deeply [14-17]. For instance, I worked on OLEDs during my Master period [18], using synthetic size-controlled ZnO quantum dots (approximately 7 nm) to improve the luminous efficiency of MEH-PPV light

emitting diodes. In general, in OLEDs there are still two basic problems or challenges: the "luminescent efficiency" and "stability" of materials and devices. The "luminescent efficiency" can be improved by specially designed structure such as electron or hole injection layers and transport layers, or by special materials such as using phosphorescent materials to replace fluorescent materials with higher luminescent efficiency. The "stability" or in another words "electrical ageing" is also a basic issue for insulating polymers in electrical applications. The ageing mechanism of semiconducting polymers and insulating polymers can be merited from each other.

On the other hand, the insulating polymers are famous for their applications as insulators and dielectrics, which are materials whose internal electric charge do not flow freely and make it very hard to conduct an electric current under electric field. Of course a perfect insulator does not exist, because defects are still present that assist charge transport. Also, conduction of insulations may become substantially non-linear at high electric field, with significant current leakage. But generally the limitation of insulations in terms of electrical stress is the breakdown phenomenon when the applied voltage (or rather electric field) exceeds a certain value. Some materials are designed to serve as safe insulators under low or moderate voltages, while some are developed to be used under high or extra-high voltages (HV or EHV). With the booming development of high-voltage direct current (HVDC) in Europe and Asia [19-23], it is pressing to develop researches on ageing and breakdown mechanisms and develop insulator with high electrical insulation properties. Hence, the electrical ageing and breakdown of insulating polymers is still an area of much interest for scientists, engineers, enterprise developers and consumers. Although the bulk conductivity of most polymers is very low, it is important and common to evaluate insulating materials through electrical strength, resistivity, dielectric losses and permittivity using different measurement methods. In the present Ph.D. research work, we propose to investigate the mechanisms of material ageing and pre-breakdown phenomena of insulating polymers using electroluminescence along with other luminescence techniques. The optical information gained in the approach relates physical/chemical signatures of the material to excitation of the species by electrical charges.

1.1.2 Electrical applications and development of insulating polymers

The development of electrical insulating polymeric materials is closely associated with the development of electrical apparatus [1]. The latest electrical apparatus require some electrical insulating polymeric materials with high thermal and electrical properties. In turn, the advanced electrical insulating polymeric materials improve the performance and service time of electrical apparatus.

Up to 1920s, only naturally raw products such as rubber, asphalt, mica, cotton or fabric were generally used as insulations. As for electrical industry mineral oil-impregnated paper was utilized in transformers, capacitors, and underground cables at voltage up to 70 kV [24]. Then the first synthetic insulating materials, named phenolic (Bakelite®) and alkyd resins,

were utilized in insulating varnishes. The insulating polymers show gradually their advantages on traditional and latest specific electrical applications, for example the development of widely used paper-insulation and polymer-insulation seen in Figure 1-1 for cable industry. Polymer insulation has been gradually taking place of oil-impregnated paper especially in HVAC cables [25]. There are intensive ongoing researches for extension of polymer insulation to HVDC, as it is widely believed that polymer-insulated cables offer significant advantages over the traditional oil-impregnated paper cables.

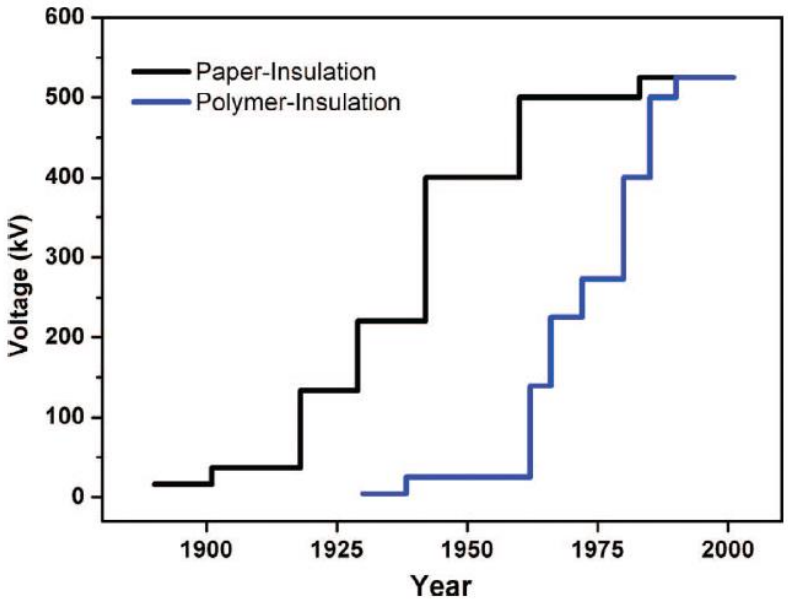

Figure 1-1 Evolution in time of paper and polymer insulation rating voltage. Polymer-insulated medium-voltage AC cables appeared in the late 1960s, from [1].

The insulating polymer films are used as dielectrics of capacitors and resonators. Commercially manufactured capacitors typically use a solid-dielectric material with high permittivity as the intervening medium between the stored positive and negative charges. Insulating polymers are used for capacitor application, not for their high dielectric permittivity but for the low film thickness providing high density of stored energy. For instance, the state-of-the-art in high energy density metalized film capacitors employs commercially Bi-axially Oriented Polypropylene (BOPP), with a high breakdown strength at about 600 kV/mm [26], low dielectric losses, and high availability. A dielectric resonator is an electronic component that exhibits resonance of the polarization response for a narrow range of frequencies, using more and more specific insulating polymeric materials.

The insulating polymers have also been widely used as insulators on electrical equipment such as cables, transformers, circuit breakers, and so on, to support and separate conductors without allowing current through themselves, more precisely, without electrical failure. For example, cross-linked Polyethylene (XLPE) has been widely used in high voltage cables, such as the booming HVDC systems.

A general historical description upon the research carried out contributing to the development of high-field polymer dielectric materials during last 50 years has been made in the literature [1]:

- From 1960s to 1970s, this is the early days of modern synthetic polymeric insulation. Some polymers with excellent dielectric strength such as cross-linked Polyethylene (XLPE) were invented and fundamental studies were brought into focus.
- From 1970s to 1980s, it was realized that polymeric insulation age under functional stress and came what was called the treeing era. Electrical and water trees were investigated in order to understand the electrical ageing in dielectrics.
- From 1980s to 1990s, appeared some new concepts in high-field phenomena, such as band theory for describing the electronic properties of partially crystalline materials and field-limiting space charge for describing conducting in polyolefins. It was also the dawn of space charge measurement, i.e., the direct measurement of internal charge density distribution in bulk insulation. Several techniques such as laser-induced method and pulsed electroacoustic method were introduced. We shall present these techniques in the course of this chapter.
- From 1990s to 2000s, polymeric insulations dedicated to HVDC applications appeared as a new need [27]. The insulating materials for HVDC cables were investigated deeply, such as XLPE. Mechanisms and theories of space charge and electrical ageing were simulated and studied.
- From 2000 to present, came the nano age [1]. The booming of study on nanocomposite materials clearly mark the decade. In addition, lessons learned from space charge measurements, e.g., the bipolar nature of transport and significant injection of electronic carriers, and from electroluminescence measurements, e.g., charge recombination, have been used in an attempt to provide a complete description of insulating polymers.

Hence, throughout the history of the research of insulating materials, the research trends are from macroscopic to microscopic [28], from simple polymer to composite [29], from ordinary application to high performance [25].

Until now, with the development of materials and apparatus, electrical ageing, degradation, and breakdown especially under high or extra-high voltage are still of great importance to investigate. In this case, luminescence appears as a family of techniques useful to probe insulating polymers and specifically to understand the mechanisms of electrical ageing. We systematically studied the various aspects of luminescence processes and carried out the implementation of the measurements in insulating polymers to uncover the luminescence mechanisms and relationship with the initiation of electrical ageing.

1.2 Luminescence processes in insulating polymers

Luminescence is light emission due to excitation sources not due to heat, in another words "a form of cold body radiation". According to various excitation sources, there are several methods allowing the production of luminescence from dielectrics: Photoluminescence (PL, including Fluorescence and Phosphorescence, UV induced luminescence) [30, 31], Electroluminescence (EL, electro induced luminescence) [32-34], Cathodoluminescence (CL, or called electron beam induced luminescence, EBIL) [35-37], charge Recombination induced Luminescence (RL) [31, 38, 39], Chemiluminescence (CHL, thermo oxidation ageing induce luminescence) [40], Triboluminescence [41], and Thermoluminescence. Luminescence is generated respectively from the excited states produced by UV photo absorption, electric field, high kinetic electron beam, energy release due to recombining charges, thermal energy/chemical reaction, and mechanical energy. PL, CHL, RL, EL, and CL have features as shown in Table 1-1 as demonstrated bellow. All the luminescence techniques below have been applied for the characterization of insulating polymeric materials. The detailed information on luminescence excitation setups and measurement methods will be given in Chapter 2.

Table 1-1 Overview of luminescence techniques in insulating polymers, adapted from [42].

Luminescence type	**Promotion of excited state**
Photoluminescence PL	Absorption of photon (mild UV)
Chemiluminescence CHL	Chemical reaction (typical: oxidation of polyolefins)
Recombination induced luminescence RL	Recombination between trapped carriers (no kinetic energy)
Electroluminescence EL	Mixture of excitation processes induced by electric field
Cathodoluminescence CL or Electron beam induced luminescence	Hot electron impact and processes induced by irradiation

1.2.1 Photoluminescence - optical excitation

Photoluminescence is light emission from the materials after the absorption of photons (electromagnetic radiation). This process can be described quantum mechanically as: the material absorbs photons, to be excited to excited states at high energy level, then release back to the ground state, meanwhile emitting light. The time between absorption and emission may vary from femtoseconds to milliseconds or even to minutes or hours under special circumstances. The relative short and relative long time between absorption and emission lead to fluorescence and phosphorescence respectively. The emitted light has a lower energy and therefore longer wavelength than the excitation light. The mechanism of photoluminescence has been known for many years and pertains to classical physical theory.

1.2.1.1 Fluorescence

Fluorescence occurs when an orbital electron of a molecule, atom or nanostructure releases back to its ground state by emitting photons after being excited to a higher quantum state.

Excitation process: $$S_0 + hv_{ex} \rightarrow S_1 \quad (1\text{-}1)$$

Light emission process: $$S_1 \rightarrow S_0 + hv_{em} + heat \quad (1\text{-}2)$$

Here, hv is photon energy with h (Planck's constant) and v (frequency of the light). State S_0 is called the ground state while state S_1 is its first excited state. During the emission process, not all the energy is converted to light emission, some of which can undergo with non-radiative relaxation, dissipated as heat. In spite of that, relaxation of S_1 can also occur through interaction with a second molecule through fluorescence quenching. Molecular oxygen is an extremely efficient quencher due to its unusual triplet ground state in phosphorescence.

The emission efficiency is defined by the quantum yield, Y as:

$$Y = \frac{number\ of\ photons\ emitted}{number\ of\ photons\ absorbed} = \frac{k_f}{\sum_i k_i} \quad (1\text{-}3)$$

Here, k_f is the rate constant of spontaneous emission of radiation, $\sum_i k_i$ the sum of all rate of excited states release. Because the excitation states are only singlet states in fluorescence, its quantum yield Y is always less than 1 (100%).

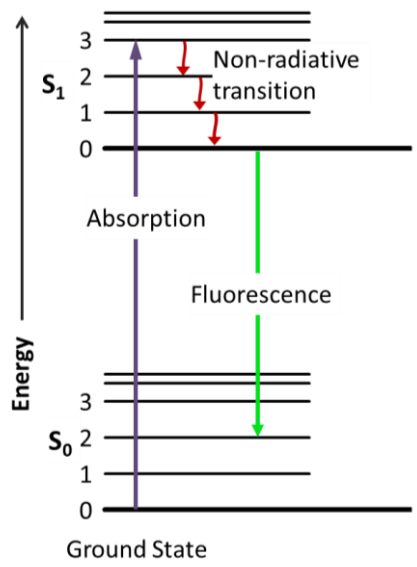

Figure 1-2 Fluorescence process of the materials [43].

1.2.1.2 **Phosphorescence**

Phosphorescence occurs when materials do not emit light immediately after being excited, due to the energy transition in quantum mechanics. Hence phosphorescent materials can "store" absorbed energy for a certain time.

Excitation process: $S_0 + hv_{ex} \rightarrow S_1$ (1-4)

Transition process: $S_1 \rightarrow T_1$ (1-5)

Light emission process: $T_1 \rightarrow S_0 + hv_{em} + heat$ (1-6)

Here, hv, S_0, S_1, and heat mean the same as in formula (1-1) and (1-2), while T_1 is a triplet state, S a single state.

During the phosphorescence process, the material is excited to higher energy states, then undergo an intersystem crossing into energy state of higher spin multiplicity, usually triplet states, $S_1 \rightarrow T_1$, see Figure 1-3. The transition $T_1 \rightarrow S_0$ is normally a spin-forbidden transition, which is why the lifetime of triplet states (phosphorescence) is longer than that of singlet states (fluorescence).

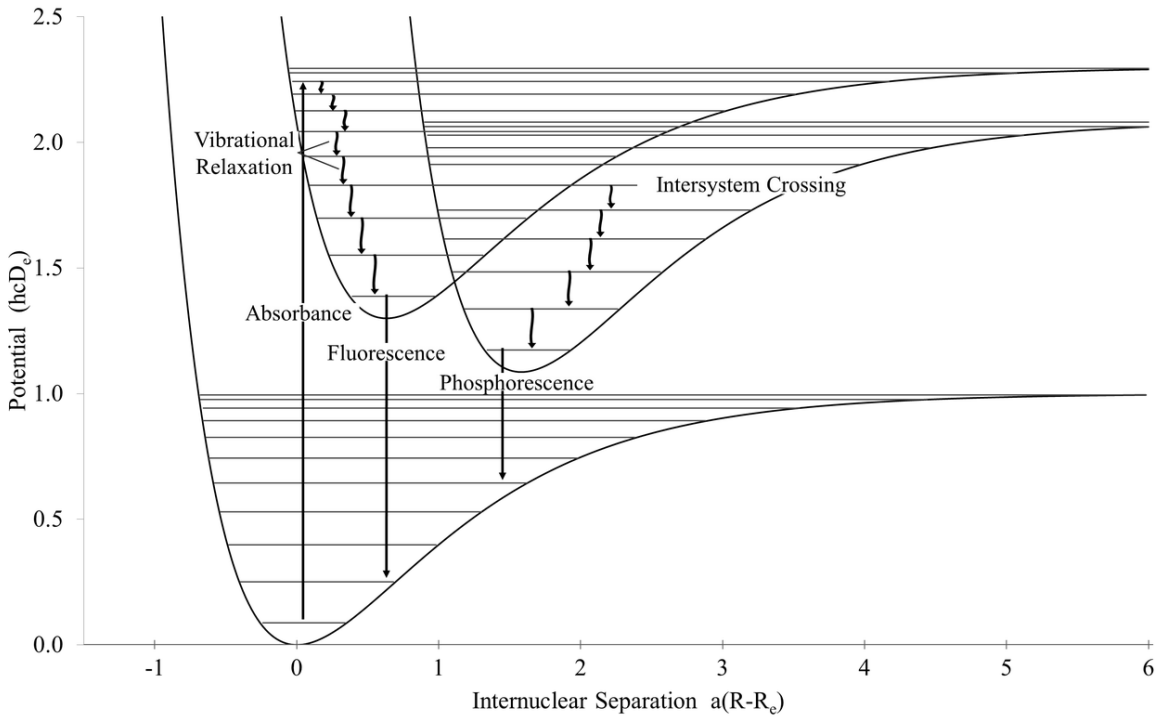

Figure 1-3 Fluorescence and phosphorescence processes of the materials [43].

1.2.2 Electroluminescence - electric field excitation

Electroluminescence is an electro-optical phenomenon under electric field. Electric stress performs as the excitation source. It is an optical output of recombination of injected electrons and holes and a series of physical/chemical processes. Electroluminescence in organic semiconductors was firstly reported in 1963 [44] and exploited as organic light emitting devices. On the other hand, electroluminescence in insulating polymers was firstly reported in 1967 [3]. So far, EL in Polyethylene (PE) [45], Polypropylene (PP) [46], Polyethylene terephthalate (PET) [47], Polyethylene Naphthalte (PEN) [48], Polytherimide (PEI), Polyimide (PI), Polyethersylfone (PES), Polyvinyl Chloride (PVC), et. al. [1, 2], have been observed and studied. The mechanisms of EL in insulating polymers are demonstrated bellow.

1.2.2.1 Electroluminescence mechanism in insulating polymers

In electroluminescence (EL), electrical energy is transformed into photons. In order to radiate in the visible portion of the spectrum, the luminescence center must have an excited state of ≥ 2 eV higher than the ground state. Two processes are of interest: how the radiative system is excited and the energy relaxation or light generation.

a) Excitation process

With electric field as excitation source, it follows different excitation processes. The energy band diagrams of insulation, semiconductor and conductor are shown in Figure 1-4. We consider firstly the effect of electron promoting from the valence band to the conduction

band (band-to-band transition) or from the ground state impurity level to the conduction band which occurs in semiconductors with a band gap of about 1-3 eV. It could not play any role in large band gap materials (beyond 5 eV) that are insulators. Therefore, the excitation energy has to be brought by other processes. There are two possibilities for that.

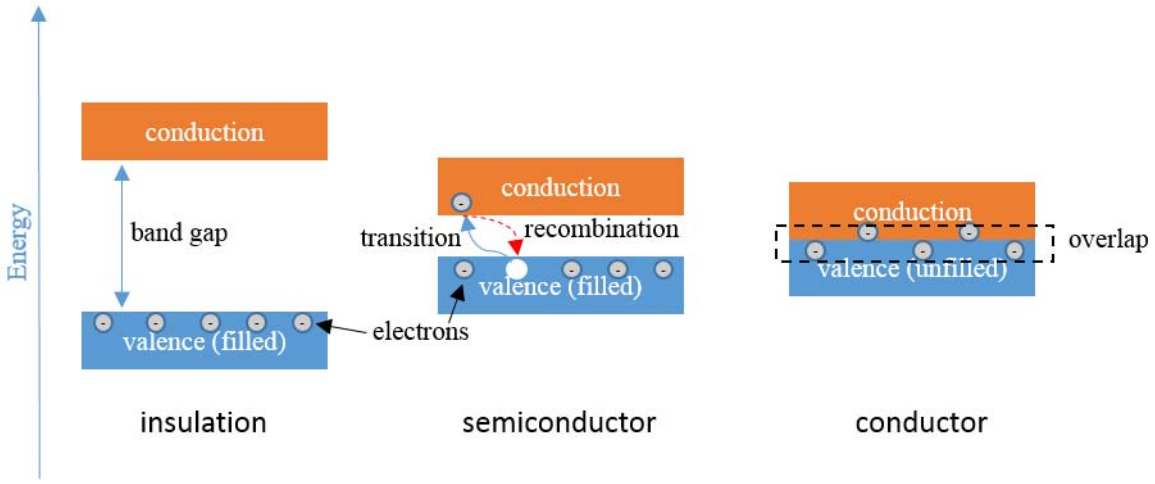

Figure 1-4 Energy band diagrams of materials

One excitation process is the inelastic collision of energetic electrons, a so-called hot electron. The kinetic energy is directly involved in the excitation process.

The other excitation process is bipolar charge carrier generation and subsequent electron-hole recombination which does not involve carrier kinetic energies, but does involve their potential energies [7]. The excitation process in insulating polymers occurs at localized given molecular orbit or at luminescent centers, leading to the formation of excitons. An exciton is a bound state of an electron and a hole that are attracted to each other by the electrostatic Coulomb force, which is regarded as an elementary excitation that can transport energy.

b) Relaxation process

Relaxation of excited groups can follow two different pathways involving radiative and non-radiative transitions [49]. The radiative and non-radiative transitions both have physical, i.e. reversible pathway and chemical, i.e. irreversible pathway as shown in Figure 1-5. Along the non-radiative pathway, excitons release to thermal energy through oscillations. Along the physical radiative pathway, a molecule “AB” is excited into a non-dissociative states “AB*” and returns to its ground states by a reversible process during which light is emitted as energy release. Hence, the wavelength spectrum of light emission is a direct reflection of the energy release. Along the chemical pathway, the intermediate processes occurs before the relaxation of the excited states. An important question in the analyses of EL in insulating polymers is the identification of the emitting groups. In case of chemical pathway, it could provide a key to understand ageing mechanism at play. In case of physical pathway, EL

reveals the presence of excited states which can potentially initiate chemical reactions, in parallel to the physical relaxation pathway. So in both case, EL is considered as a potential ageing warning.

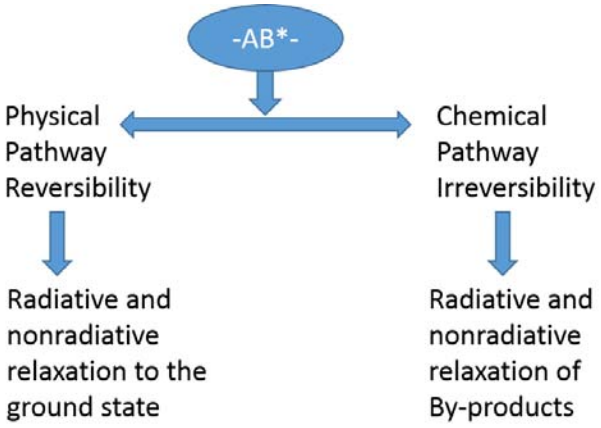

Figure 1-5 Energy release of an excited molecule

The most frequent transitions during relaxation processes [49] are demonstrated below:

(1) Fluorescence emission, from singlet to singlet transition involving two electrons with opposite spin number:

$$^{1}AB^{*} \rightarrow AB_0 + {}^{1}hv \quad (1\text{-}7)$$

(2) Phosphorescence emission, from triplet to singlet transition involving two electrons with the same spin number:

$$^{3}AB^{*} \rightarrow AB_0 + {}^{3}hv \quad (1\text{-}8)$$

(3) Complex formation with fluorescence or phosphorescence of an excimer (excited state of a pair of molecules):

$$^{1}AB^{*} + AB_0 \rightarrow {}^{1}(ABAB_0)^{*} \quad (1\text{-}9)$$

$$^{1}(ABAB_0)^{*} \rightarrow + AB_0 + AB_0 + {}^{1,3}hv \quad (1\text{-}10)$$

(4) Complex formation with fluorescence or phosphorescence of an exciplex:

$$^{1}AB^{*} + CD_0 \rightarrow {}^{1}(ABCD_0)^{*} \quad (1\text{-}11)$$

$$^{1}(ABCD_0)^{*} \rightarrow + AB_0 + CD_0 + {}^{1,3}hv \quad (1\text{-}12)$$

(5) Relaxation by internal conversion:

$$AB^{*} \rightarrow AB_0 + nkT \quad (1\text{-}13)$$

(6) Relaxation by quenching:

$$AB^{*} + Q \rightarrow AB_0 + Q^{*} \quad (1\text{-}14)$$

(7) Relaxation by energy transfer:

$$AB^{*} + CD_0 \rightarrow AB_0 + CD^{*} \quad (1\text{-}15)$$

where:

AB_0 and CD_0 stand for molecular ground states,

AB* and CD* stand for molecular excited states,

^{1,3}AB* stand for the first excited singlet or triplet state,

^{1,3}hv is the photon energy radiated by fluorescence (1) or phosphorescence (3), kT is the thermal energy, Q is a quencher.

c) Possible luminescent centers

The pure carbon chain with C-C or C-H single bonds in insulating polymers cannot perform as luminescent centers in UV-visible domain, because the energy level transitions in these bonds are $\sigma \rightarrow \sigma^*$ and $n \rightarrow \sigma^*$ transitions at extreme ultraviolet domain with high energy. Hence, the chromophores should be some unsaturated bonds, like $\pi \rightarrow \pi^*$ transition in C=C bond and other conjugated structures. Furthermore, some auxochromes like -OR, -NR_2 and -CH_3 (R stands for any group) will influence the absorption with red shift or blue shift. In insulating polymers like polyolefins, there are two types of possible chromophores which play the role of luminescent centers: one is intrinsic molecular chromophore groups that exist in the carbon chain, the other is additives, impurities or by-products that are extrinsic centers in the materials.

Therefore, in a polyolefin polymer like Polyethylene or Polypropylene, there is normally no emission from the repeat unit due to the aliphatic structure of the chains. So, if luminescence is detected, it is necessarily due to some types of possible chromophore groups in the carbon chain of Polyethylene as shown in Figure 1-6: carbonyl, dienone, hydroxyl, double bond, conjugated double bond and vinyl. Some additives and residues can be present in materials due to compounding or to processing techniques. Examples are antioxidant and residues associated with peroxide crosslinking of Polyethylene as shown in Figure 1-7, which provides another possible family of luminescent centers.

However, which chemical structure is actually excited and act as the chromophore under electrical field is still unknown according to previous works. It is difficult to localize the definite luminescent centers by experimental and simulations. Nevertheless, spectral analyses can help to investigate the source of the light emission. Works are carried out to uncover the nature of luminescent centers in these insulating polymers.

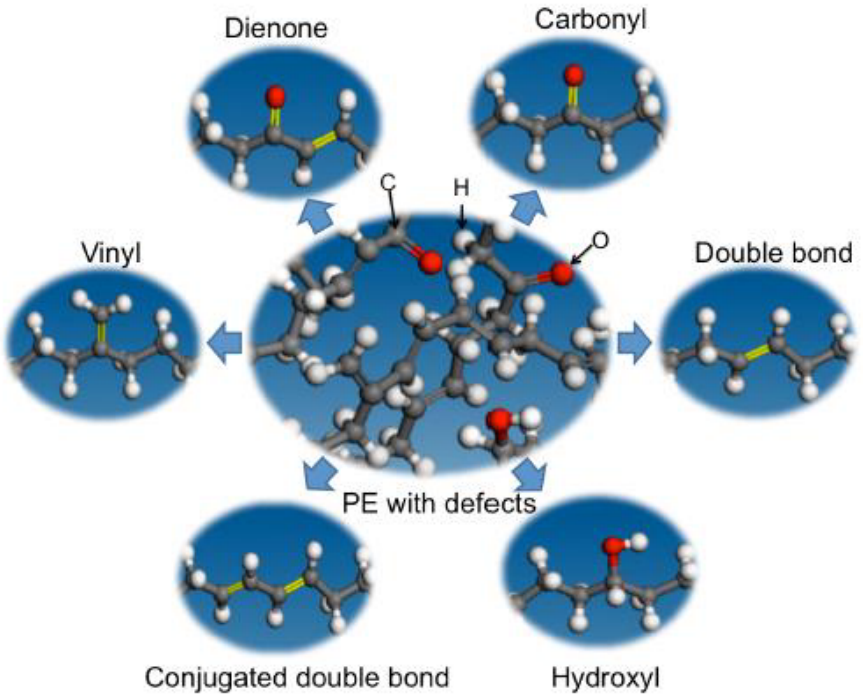

Figure 1-6 Six typical chromophore structures that may occur in the carbon chain of Polyethylene: carbonyl, dienone, hydroxyl, double bond, conjugated double bond and vinyl. Taken from [50].

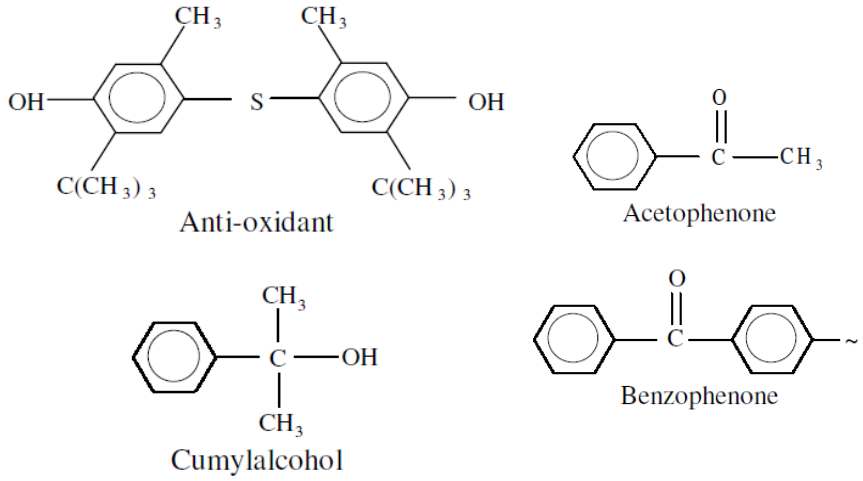

Figure 1-7 Chemical structure of possible additives and residues.[39, 51]

1.2.2.2 Comparison of EL in insulating polymers and in organic semiconductors

In semiconducting polymers used in OLEDs, two basic problems or challenges are the luminescent efficiency and stability of materials and devices [52, 53]. The EL in insulating polymers aims to investigate the stability or electrical ageing of polymers. Hence, they are investigated for different applications. The comparison between EL in insulating polymers and EL in organic semiconductors according to conductivity, intensity of light emission,

device structure, DC vs. AC, spectral analyses, luminescent centers and electric field is shown in Table 1-2.

Table 1-2 Comparison between EL in insulating polymers and EL in organic semiconductors.*

	Dielectric EL	Organic semiconductor EL
Conductivity	Very low*	Between insulators and conductors*
Device structures	Sandwich structures and others	Sandwich structures and others
Thickness of EL layer	Commonly 10-250 µm	Commonly 10-100 nm
Intensity of light emission	Relative low signal	Strong light emission
Electrical field	Tens to hundreds kV/mm*	Tens to hundreds kV/mm*
DC vs. AC	EL intensity much stronger under AC than under DC	Normally under DC
Spectral analyses	No fluorescence contributions	Emission spectrum correlated to fluorescence and/or phosphorescence
Luminescent centers	Chromophore groups in carbon chain or additives or residues	Chromophore groups in polymers

*The electrical and EL properties of both dielectrics and organic semiconductors vary depending on materials nature.

a) Device structures

EL insulating polymers and EL in organic semiconductors are both measured by fabricating sandwich structures as shown in Figure 1-8. OLEDs have other function layers, such as electron/hole injection layers and barrier layers to improve the luminescent efficiency. The Al and ITO electrodes are normally used in OLED for cathode and anode, respectively. In dielectric EL, structure like Au-insulating polymer-Au are most often carried out under electric stress owing to the good conducting quality of the electrode.

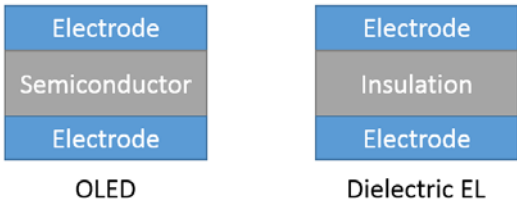

Figure 1-8 Basic OLED device and Dielectric EL structure. Commonly the thickness of semiconductor is 10-100 nm; the thickness of insulation is 10-250 μm.

b) Luminescent centers and intensity

For the luminescent centers in insulating polymers, there may exist some types of unavoidable chemical chromophore groups in the carbon chain of polyolefins and other insulating polymers and some unavoidable additives during the manufacturing process. These groups or additives may play a role as luminescent centers distributed in insulating polymers. However, the intensity of the light emission is very weak. Sensitive and effective optical detection methods have to be developed while the difficulty is related to their implementation in a high voltage environment. Partial discharge or gaseous discharge has to be avoided, by immersing the samples in a liquid insulating medium, or by increasing the chamber pressure, or by evacuating the chamber down to secondary vacuum. Three main topics in dielectric EL are still debatable: namely the excitation mechanisms, the nature of luminescence centers, and the relationship between EL and ageing.

However, in organic semiconductors there are numerous chromophore groups in the molecular structures such as conjugated structure in conjugated polymers [16, 17, 54, 55]. This makes organic semiconductors emit much stronger intensity of light. In order to be used in OLED, the improvement of luminescent efficiency along with tuning the emission wavelength is of great interest to study.

c) Spectral analyses

In semiconducting luminescent polymers, the absorption, photoluminescence, and electroluminescence peaks have a close relationship with each other, which can be seen in Figure 1-9. During the photo-physical processes, either with single luminescent peak or with multi peaks, the materials absorb light with a higher energy (shorter wavelength), excited by photons, then a series of energy transfer processes, emitting light (photoluminescence) with a lower energy (longer wavelength). Under electric stress, the materials emit light with a little red shift and similar spectra curve compared to PL, which infers that electric excitations operate with the same function as photon excitations. In bipolar injection model, the electrons inject into the luminescent materials from cathode, and transfer along with Lowest Unoccupied Molecular Orbital (LUMO) energy levels to the luminescent centers; the holes are injected into the luminescent materials from anode, and transfer along with Highest Occupied Molecular Orbit (HOMO) energy level to the luminescent centers. The

recombination of electrons and holes generates excited states, which go back to the ground level with releasing light emission.

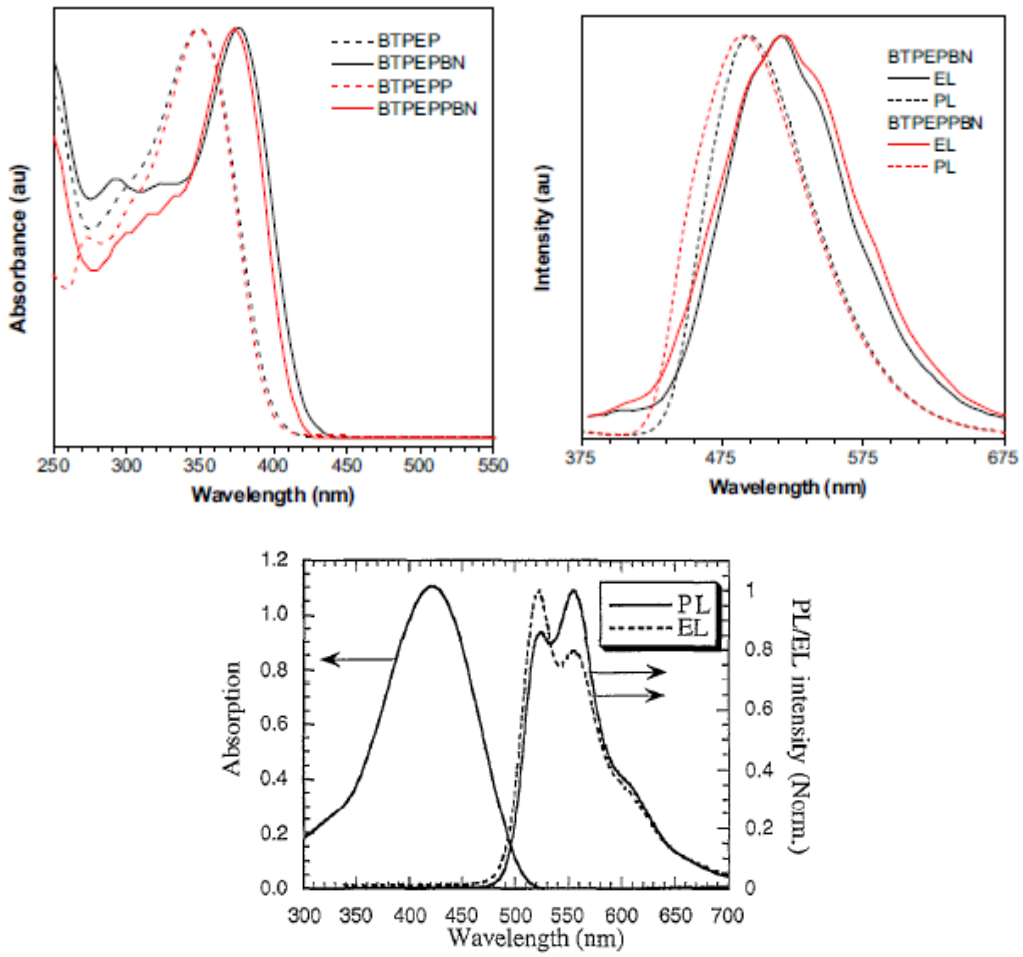

Figure 1-9 Absorption, photoluminescence, and electroluminescence of some luminescent polymers, with single luminescence peak in BTPEP-family materials, taken from [56]; or multi luminescence peaks in PPVs materials, taken from [57].

On the contrary, in insulating polymers, the electroluminescence has little relationship with fluorescence, according to the research progress until now. Under high electric field about tens to hundreds of kV/mm, the process of the electron exciting the luminescent center cannot be interpreted on the basis of the photo-physical properties of the materials, which is different with the case of semiconducting polymers. The example of Polypropylene (PP) is shown in Figure 1-10 and Figure 1-11 results being issued from the present thesis. From photoluminescence measurements in Figure 1-10, the fluorescence peaks at 328 nm and the phosphorescence appears at about 472 nm. The electroluminescence in Figure 1-11 appears dominated by a crest at approximately 580 nm. As far as OLEDs are concerned, it is claimed that due to spin state consideration, the probability of obtaining triplet state following a recombination event is normally 3 times higher that obtaining a singlet state. So normally,

OLEDs should emit mainly in the phosphorescence region. Quenching by oxygen could be one of the reasons for the lower apparent efficiency for fluorescence-type EL. The reason for the absence of fluorescence in the EL spectrum of insulations is not really known at present. It could be due to a different excitation process, e.g. impact excitation with an energy transfer less than the expected value for obtaining a singlet state or to the low possibility of recombination on luminescent species at the origin of fluorescence. For instance, electroluminescence in insulating polymers can be reproduced when the materials are irradiated with an electron beam (Cathodoluminescence, CL), which was firstly evidenced in the literature [45].

The withstanding of materials - electrical ageing of both insulating polymers and organic semiconductors is of significance to investigate and to improve. Hence, what is the nature of electroluminescence in insulating polymers, and the relationship between electroluminescence and electrical ageing, will be investigated in this work.

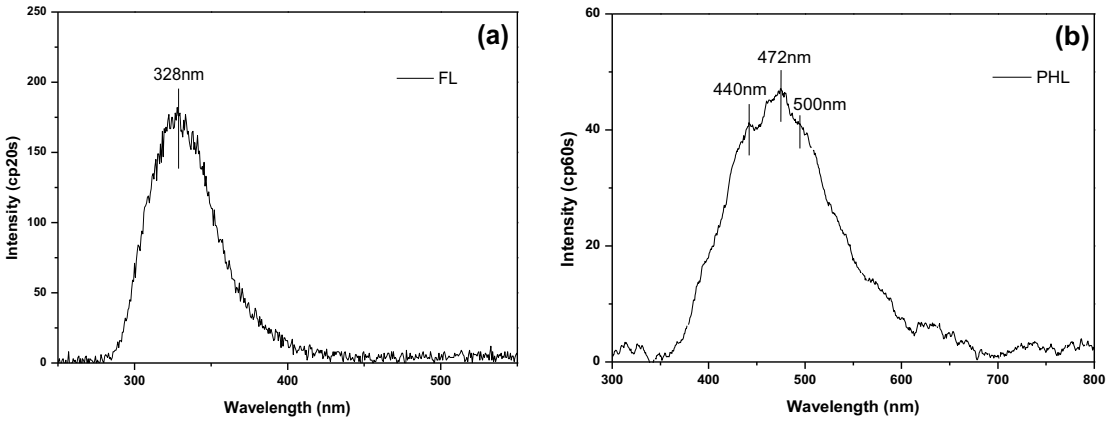

Figure 1-10 Photoluminescence of Polypropylene, (a) fluorescence excited at 230 nm at room temperature, (b) phosphorescence excited at 250 nm at liquid nitrogen temperature, [58].

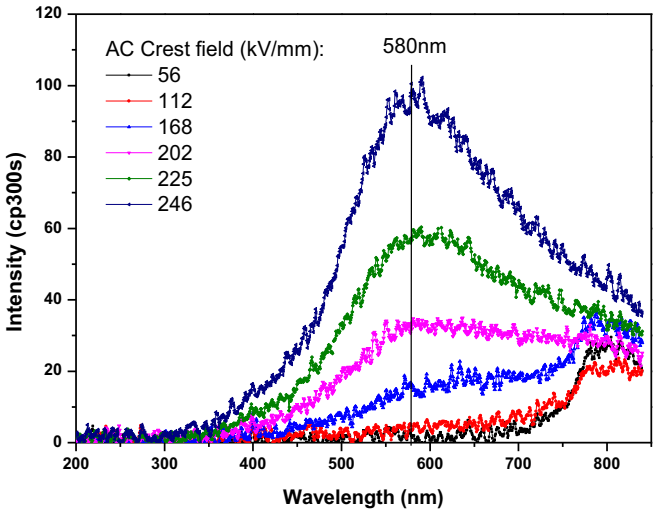

Figure 1-11 Electroluminescence spectra of Polypropylene film under 50Hz AC stress, [58].

The dissertation mainly focuses on insulating polymeric materials. Nevertheless, some of the physical and chemical mechanisms in conducting or semiconducting polymers can be transferred and adapted to the mechanisms in insulating polymers, while the study of electroluminescence in insulating polymers can also contribute to understanding the nature of EL and its relationship with ageing.

1.2.2.3 Development of electroluminescence measurement methods

In the first reports on EL from insulating polymers [32, 59, 60], the electrode configuration was needle electrode inserted in a polymer as shown in Figure 1-12 a. The electrode configuration is easy to be carried out and well contacted with each other. The field is divergent field from the needle electrode to the plane electrode. There are several drawbacks in using needle electrode configuration: First, the emission is localized to the region close to the tip and overall emission is generally weak. Second, the field is highly divergent, which prevents analyses of the process with controlled field. Third, care should be taken when molding the needle as voids can be present at the vicinity of the tip. Finally, material deterioration can occur around the tip leading to change in time of the analyzed light.

Various electrode configurations are illustrated in Figure 1-12 besides the needle plane geometry for divergent field. In Figure 1-12 b, this is a concentric ring form geometry for divergent field. In Figure 1-12 c, this is a plane geometry for uniform field, while the light emission is detected in the direction perpendicular to the direction of electric field. In Figure 1-12 d, this is a plane geometry, while the light emission is detected in the direction parallel to the direction of electric field.

Electrode configuration as Figure 1-12 b with an inner and an outer electrode has been used in [61] to investigate the EL from surface layer of insulating polymer. The polymer configuration is so much like the dielectrics applied in the cables. At the same time, the field is divergent.

Electrode configuration as Figure 1-12 c has been employed for investigating the surface EL phenomena under stepped AC voltage [62], since the surface/interface plays an important role during the EL phenomena. The configuration has also some obvious advantages of optical and imaging detection. However, complex surface processes may occur.

For a deeper insight into excitation and relaxation mechanisms, efforts are put for collecting more light intensity. This is achieved in EL experiment under uniform field configuration by using polymer films metalized with semi-transparent electrodes sandwich structure [63] as Figure 1-12 d. Both two brass electrodes have polished surfaces. The lower electrode is a disk, while the upper one is a ring with an inner diameter of 20 mm where light emission is detected. Semi-transparent layers are most often made of gold, typically 30 nm in thickness, as a good compromise between optical transmission and electrical conductivity and lack of oxidation of the electrodes. The light emission, detected through a ring electrode arises from an area of several cm^2, and is more easily detected as with needle electrode.

Because of the uniform field and uniform light emission, the theoretical model is easier to be built and the charge injection and transport and EL mechanism are easier to be analyzed.

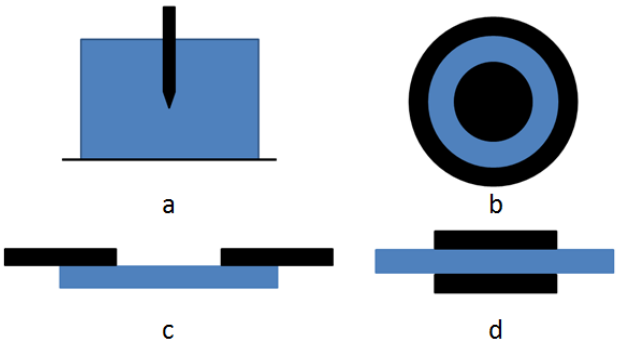

Figure 1-12 Electrode configuration cross section for EL measurement (the black stands for electrode, while the blue stands for insulating polymer). (a) Needle-panel electrode, (b) Concentric ring electrode, (c) Surface EL, (d) Uniform field electrode.

1.2.2.4 **Historical overview of electroluminescence in dielectrics**

In 1967, Hartman *et al.* [3] firstly studied the light emission from polymer films such as Polyethylene, Polyimide, PET, and PTFE under electric field at room temperature. Authors inferred that the electrons are introduced by the field either from the electrodes or from the bound states within the polymer.

In 1977 and 1979, AC electroluminescence and breakdown of Polyethylene adjacent to the tip of a needle electrode were found at liquid nitrogen temperature (77K) by Shimizu, *et al.* [32, 64, 65]. The luminescence was considered to be caused by the recombination between positive and negative charges injected from the point electrode, instead of by partial discharges.

In 1980 and 1981, light emission was detected at the tip of a needle electrode inserted in a polymer under divergent field by using a photomutiplier (PM) and an image intensifier, cooled to -20 ℃, by Laurent and Mayoux [59, 66]. This work confirms that trapped gases play an important role and that space charge is at the initiation of radiative phenomena. Later in 1985, the density of the injected and trapped carriers was estimated to be 10^{17} /cm^3. The nature of the light emitting centers seems to be related to the structure of the polymer bulk because different polymers have different luminescence spectra [67].

In 1986 and 1987, both near ultraviolet and visible light emission in Polyethylene subjected to highly divergent field at room temperature were reported by Bamji *et al.* [60, 68]. It was suggested that UV radiation causes photo-degradation of the polymer which results in both scission and formation of a micro-void in which partial discharge can occur and cause tree propagation. It was realized later that UV-light was due to discharge in the ambient. In 1993, the thermoluminescence and electroluminescence were both recorded in Polyethylene at

elevated temperature, while the luminescent centers for the two processes are quite different [69].

In 1988, EL in epoxy was recorded under impulse voltage by Stone *et al.* [70]. In 1994, EL in Polyethylene 2,6 Naphthalate was investigated under uniform field, DC and AC stress and pulsed voltage by Mary *et al.* [71]. In the next few years, other insulating polymers such as Polypropylene (PP) [40], Polyvinyl Chloride (PVC), and Polytetrafluoroethylene (PTFE) [72] were investigated.

In 1993, two basical types of thin film light emission – photon radiation from the polymer itself and from the metal electrode (Surface Plasmons) - were distinguished in metal-insulator-metal structures by Laurent *et al.* [73]. The question of light emission from Surface Plasmons is discussed later on in the chapter.

In 1998, the spectra of light emission in polyolefins were particularly analyzed by Teyssedre *et al*. [38]. The spectral features are closely associated with the electroluminescence mechanism. The chemical nature of the luminescent centers was discussed by a comparison with the photoluminescence spectrum.

In 1999, Tiemblo, *et al*. [74-79] investigated chemiluminescence in Polypropylene at great length, which provide a spectral features of light emission entirely through chemical route. The intensity and spectra distribution of EL depending on ageing time was achieved [80], which give another evidence to the relationship between EL and electrical ageing.

In 2000, photo-, cathodo- and electro- luminescence spectra were compared between them, whose relationship with electrical ageing was investigated [31].

In 2004, charge carries transport in XLPE was characterized by both transient space charge and electroluminescence measurement [81]. Light emission was interpreted as an interfacial phenomena, probably a hot carrier effect associated with heterogeneities in the interface.

In 2008 and 2009, Bamji *et al.* summarized luminescence and space charge in polymeric dielectrics [82, 83]. He described the characteristics of electroluminescence in polymeric insulation subjected to AC voltage and showed its relevance to space charge injection. The electroluminescence was also distinguished from other types of luminescence. In 2008, evidence of hot electron induced chemical degradation in electroluminescence spectra in polymer was found by Teyssedre and Laurent [45]. Electroluminescence and electrical ageing can be associated in an implicit scheme, opening the way for defining safety limit in terms of electric stress applied to a material for a given application.

In 2011, EL measurements of Polyethylene in different gas environments were investigated. The presence of gas molecules plays a crucial role on the formation of EL in insulating polymers [84]. A charge transport model allowing the description of EL in PE films under AC stress is proposed. Experiment and simulation fit nicely and the time dependence of EL intensity is accounted by the charge behavior [85-87].

In 2012 and 2013, Laurent *et al.* summarized charge dynamics and its energetic features in polymeric materials [42, 88]. Two models have been introduced describing bipolar space charge limited current in transient and steady states. The nature of electroluminescence was discussed in order to understand its relationship with electrical ageing.

In 2014, electroluminescence of a Polythiophene molecular wire suspended between a metallic surface and tip of a scanning tunneling microscope was studied by Reecht *et al*. [89]. Though Polythiophene is conductive polymer, it directly proves the theoretical simulations with single molecule wire, paving the way towards single molecular optoelectronic components and electroluminescence mechanisms.

More and more efforts on experiments and simulations are made to uncover the nature of EL in insulating polymers and its direct relationship with space charge, electrical degradation, ageing and breakdown.

1.2.3 Cathodoluminescence - electron beam excitation

The Cathodoluminescence (CL) phenomenon is a luminescence processes that occurs after the excitation of matter by an electron beam [90]. CL is a contactless spectroscopic technique based on detection of infrared (IR), visible, and ultra violet (UV) luminescence excited by energetic electrons [91]. CL analyses enables characterization of materials with high spatial resolution. With the development of electron microscopy, the image and spectroscopy of CL have proven to be a useful technique for chemical, electrical and structural analyses of luminescent materials. Historically, luminescence spectroscopy has been a widely used sensitive tool to characterize the nature of excitons, impurities and native point defects in electrical materials.

Electron beam in vacuum can be accelerated by electric and magnetic field in an electron gun to achieve a high energy. Exposure of a solid to an electron beam with several keV energy induces a number of processes in the specimen, which lead to the formation of secondary and backscattered electrons, and also generate characteristic radiation and X-ray, and Auger electrons [90]. The secondary electrons and backscattered electrons analyses has also been used in scanning electron microscope (SEM) and transmission electron microscope (TEM). However, CL is just the light emission from the material under electron beam irradiation as shown in Figure 1-13.

The cathodoluminescence process consists three steps:

1) The energy loss of impinging electrons;
2) The excitation of luminescent centers;
3) The emission of photons.

The deceleration of electron beam generates secondary electrons and plasmons with an energy of 20-30 eV. The secondary electrons do not leave the sample in turn generate electron-holes pairs [90]. It is noteworthy that upon excitation of luminescence by an

electron beam, the energy of excitation considerably exceeds the bandgap width of any material. Therefore, the excitation is inherently similar to the optical excitation in the region of fundamental absorption and electro excitation under electric stress. The excitation of luminescent centers can occur not only via direct excitation of a center, but also as a result of radiative and non-radiative transitions from higher lying energy states. As a consequence, CL spectra often demonstrate a larger amount of emission bands than other luminescence spectra, which will also be proved in our work.

The energy losses of electrons due to their deceleration in the materials are estimated theoretically accounting the absorption energy and reflection processes in a wide energy or wavelength range. When the insulating polymers are radiated in the electron beams, visible light -cathodoluminescence, can be detected and spectrally analyzed along the other luminescence techniques.

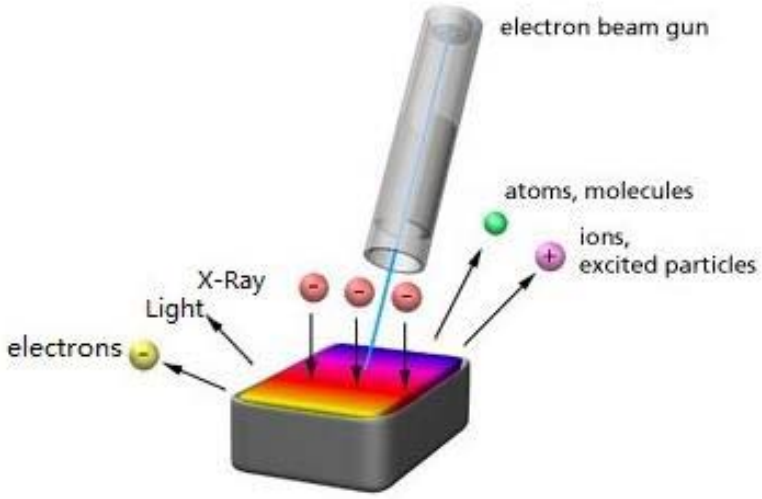

Figure 1-13 Schema of formation of electrons and radiations with electron beam excitation on the surface of the sample.

1.2.4 Other luminescence excitation sources

1.2.4.1 Chemiluminescence - chemical process

Chemiluminescence is the light emitted during a chemical reaction. It is a well-known process in polyolefins where oxidation reactions lead to the formation of C=O bonds (triplet ground state). Owing to thermal degradation of polyolefins being studied with aim of understanding its kinetics and its mechanism, Chemiluminescence (CHL) [74, 76, 77, 92-95] phenomenon in polyolefins has been particularly investigated, but there is still no clear and conclusive description of how the degradation occurs. Tiemblo, *et al*. have investigated Chemiluminescence in Polypropylene at great length [74-79]. During CHL measurement, the samples were heated in a special-design multi-purpose chamber. The samples were

deposited in a glass vessel in contact with the heating resistor, in isothermal conditions for time up to 8 h and temperature up to 165℃. The light emission was continuously registered, during the sample heated with a heating resistor.

The light is generated during the last step of chemical reaction from C=O* to C=O with a typical signature at 415 nm [74]. The CHL curves correspond to the spectra performed along the oxidation process. The overall intensities shown by the spectra evolve with time in the same way as in the integral CHL curves. Consequently, CHL is corresponding to the thermal oxidation of the insulating polymers.

1.2.4.2 **Recombination luminescence - recombination process**

Radiative recombination of charge carriers on luminescent centers is one of the main mechanisms for light excitation mediated by an electrical stress. In EL, charges are recombined either following impact ionization by hot carriers or due to bipolar injection (electrons injection from the cathode and holes injection from the anode) [39, 96, 97]. Recombination luminescence can be detected through placing the samples contacting to a cold plasma for surface treatment as an alternate way for material charging [38]. Plasma-induced luminescence (PIL) is recorded after excitation by the plasma discharge. The PIL has complex contributions according to different test and treatment time. Chemiluminescence, UV-induced luminescence, and recombination-induced luminescence all can be decomposed after the plasma treatment [78, 79]. The part of the recorded signal recorded long (tens of seconds) after discharge switch off has been proven to arise from recombination-induced luminescence as it is the sole possible excitation mechanism. Again, the emissions due to RL appear in the phosphorescence domain; they appear as due to chromophores present in the material, but the spectrum does not match that of EL. The spectra due to recombination luminescence have been achieved and analyzed in Polyethylene, Polypropylene, and epoxy resin among other materials [38, 39, 96-98]. Dynamic bipolar charge recombination model has been put forward to understand the mechanisms of recombination process [99]. The recombination luminescence are recorded after discharge switch off. Because the recombination mechanism has also a close relationship with light decay kinetics, these luminescence techniques can be used to infer chemical nature of the luminescent centers acting as recombination centers.

In order to investigate the recombination induced luminescence (RL) , setup as shown in Figure 1-14 [96] was designed. The surface of the sample is subjected to a cold plasma for charge deposition. The sample is contacted with a temperature controlled holder able to operate at a temperature from that of liquid nitrogen to 180℃. A cooled photomultiplier and a CCD camera are used to investigate the EL characteristics and spectral distribution.

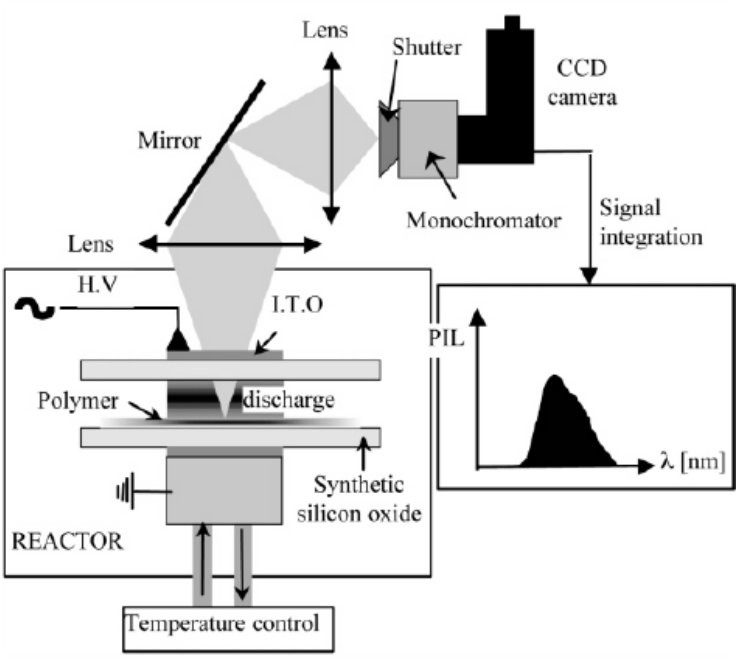

Figure 1-14 Recombination induced luminescence measurement setup, from [96].

1.2.4.3 **Surface Plasmons effect - electrode interface process**

Surface Plasmons (SPs) is an effect that always exists during the electroluminescence measurement of the gold-metalized insulating films. Surface Plasmons (or more precisely surface plasmon polaritons, SPPs) are electromagnetic excitations that propagate along the interface between a metal and a dielectric medium. In order to explain the SPs effect, let's make a stone thrown into the water as an analog. A stone thrown into the water produces waves spread out symmetrically in all directions along the surface of the water. When two stones are thrown into the water at different places and times, the symmetry patterns of the propagating wave can be changed. Similarly, Surface Plasmons bounded to a metal/dielectric interface can be excited by different sources [100]. SPs are polarized along the surface of the metal, closely related to the roughness of the interface as shown in Figure 1-15.

The electroluminescence from a metal-insulator-metal or metal-insulator-ITO centered at about 750 nm has been observed by Canet and Laurent [73, 101, 102]. It exists theoretically at all the metal-insulator rough interfaces under electrical field, which influences light emission excited by electric field. It is called light-emission tunnel junctions which is due to the metal electrode, contrasting to the thin-film devices light emission which is due to the film itself. The space-charge limited current provides excitation conditions of Surface Plasmons at the positively biased electrode surface above the trap-filled limit voltage. An electron tunnel loses its energy to a collective excitation of junction, then in the presence of the surface roughness, it may radiate. Otherwise, the electrons are injected by elastic tunneling and they enter the metal as hot carriers. The hot-carriers distribution relaxes through emission of photons, thermalized electrons, or emission of SPs which couple to

external radiation through surface roughness. Anyhow, the light emission has no relationship with the insulators in the interlayer. When a semi-transparent electrode is used, both surfaces can contribute to the light emission.

The spectral distribution of light emitted by SPs depends on the surface roughness of electrode itself and the energy distribution of charge injection/extraction produced by the field. Hence, the roughness of electrode surface and the field applied on it are two key factors. Under AC stress, due to alternative injection at the surface of electrodes, high density of carriers always exists here. So under AC low field, the energy distribution meets the requirement of SPs. However, under DC stress, charge injection starts, then due to screening effect, the current density of injected carriers is much less than in the AC case, which makes it very difficult to emit light. Consequently, the SPs from Ag or Au electrode has been verified under AC electric stress [46, 103, 104]. In chapter 4, we comprehensively investigated the impact of the nature of the electrode.

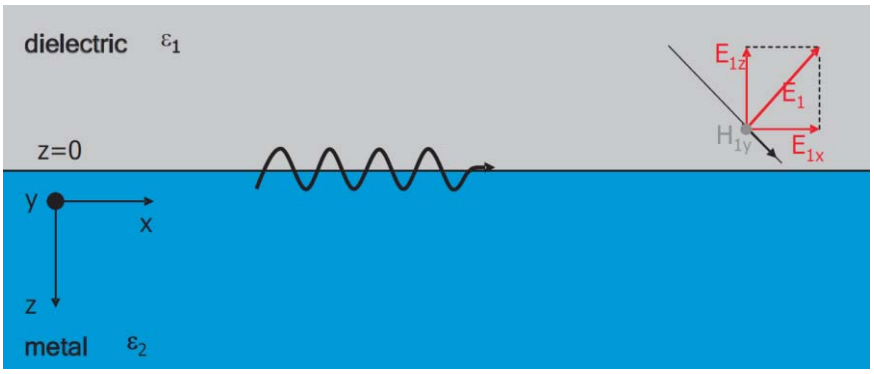

Figure 1-15 The interface along the x-y plane between a metal (bottom) and a dielectric (top).

1.3 Electrical ageing, degradation, and breakdown

Since the electrical insulating polymeric materials are closely associated with electrical apparatus, the devices failure can be studied through focusing on electrical stress –induced processes pertaining to polymeric materials. As will be shown below, such processes are split into those representing intrinsic limits of materials, such as short term breakdown, which should normally not occur under service conditions with appropriate design, and those resulting from slow evolution of the material, termed ageing, which are more subtle to analyze and to anticipate: ageing can be considered as acceptable if it does not lead to failure of the insulation within the expected life of the system. In many parts of the world, in particular in the industrializing countries such as Brazil, China, India and South Africa, the growing demand of energy has already led to transmitting electric power of several Gigawatt (GW) across distances of thousands of kilometers. As a consequence, there exists an urgent demand for understanding the electrical ageing of insulations used in these electrical applications. Therefore, there is great interest in understanding the ageing, degradation and breakdown of electrical insulation in an effort to improve its long term withstand (lifetime or service time) and efficiency. However, after more than 50 years of research the gap between electrical breakdown of insulating polymeric materials and engineering breakdown is still tremendously large even fruitful efforts have been taken.

1.3.1 Classification and mechanisms of electrical ageing

1.3.1.1 Ageing, degradation and breakdown based on time to failure

As refer to electrical ageing, we have distinguished three situations: ageing, degradation, and breakdown, according to the time to failure as shown in Figure 1-16. Though there is not perfectly clear distinction between these processes, one can separate them, as depicted in the figure according to their time scale of occurrence. The book “Electrical degradation and breakdown in polymers” by Dissado and Fothergill [105] systematically demonstrates the physical and chemical structures of polymers and their breakdown mechanisms. The electrical breakdown is a process occurring within 1 second or less, the electrical degradation from a few seconds to a few days, the electrical ageing from a few days to years. The electrical breakdown happens when subjecting the material to intense electric field, without providing the time for the material to change under the effect of the electrical stress.

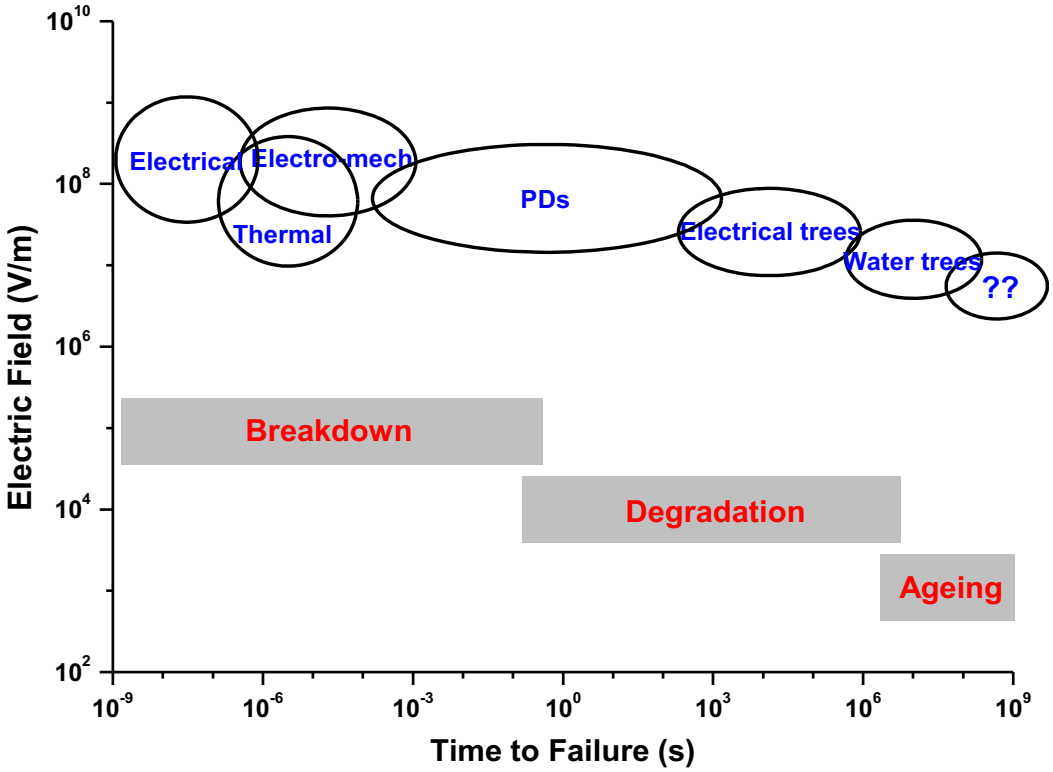

Figure 1-16 Indicative times and electric fields over which various electrical breakdown and degradation mechanism are operative, adapted from [105].

In electrical degradation, with a milder stress, there is an effective deterioration of the material through one of the mechanisms explained in the following. The difference between breakdown and degradation is that breakdown is sudden and catastrophic, after which the insulation can not withstand the service voltage, whereas degradation is a process that take places during a period of time. We can distinguish them from the effect, speed, evidence, place, and size as shown in Table 1-3. The degradation exists with electrical trees and water trees [105]. If these trees are sufficiently conductive, it may also lead to breakdown. Failure has full probability to occur, and this goes with an effective degradation, such as erosion of the material. Finally, ageing encompasses a family of hypothetical processes likely to produce a weakening of the material. At the same time, the processes are not as well identified as for breakdown or degradation, and it is difficult to diagnose. Its size can be nano scale or molecular scale and has many potentially contributory factors and uncertainty. The ageing rate is assumed to increase in region of high space charge concentration, high electric stress, and free volume that allow high local current. Its identification and impact on insulation performance need to be known, as it may represent the major part of the insulation life when the earlier failure processes have been fixed.

Table 1-3 Characteristics of Breakdown, Degradation and Ageing Processes, adapted from [106].

	Breakdown	**Degradation**	**Ageing**
Effect	Catastrophic, insulation cannot be used afterwards	Leads to breakdown	May lead to degradation
Speed	Fast: occurs in << 1s	Less than required service life: hours – years	Continuous process: whole service life
Evidence	Direct observation: normally by eye-hole through insulation	Observable directly: may require microscopy or physic-chemical techniques	Difficult to observe: may even be difficult to prove existence
Place	Continuous filament: bridge electrodes	Occurs in weak parts: may form fractal structures	Assumed to occur through insulation
Size	>mm: dependent on energy of event	>µm: may form larger structures	>nm, molecular scale
Examples	Thermal, electromechanical, mixed mode avalanche and intrinsic	Electrical trees, water trees, partial discharges	Bond scission and nano-voids formation non-electrical changes (oxidation)

The consequence of ageing phenomena is materialized, at the macroscale, by life laws, as used for example for the electrical insulations used in high voltage cables: $L = AE^{-n}$ where E is the applied field, A and n are parameters that are tentatively estimated based on hypothetical ageing models. The value of the exponent n is very important in life estimation, and it is one of the main quantities required by designers and for specification purpose. It is therefore necessary to understand the mechanism behind the ageing process in order to diagnose, prognosticate, and improve its electrical properties and lifetime.

1.3.1.2 Ageing, degradation and breakdown - kinetic energy of carriers

Hot electrons i.e. carriers with kinetic energy, play a significant role in electrical breakdown processes of polymers, which will also be shown in the electrical tree growing process in Figure 1-18. Hot electrons are particles that attain a kinetic energy from being accelerated by a high electric field. Hot electrons or holes, where "hot" means $E_{kin} \gg k_T$, can generate excited states under electric stress. The term "hot electron" was originally introduced to describe non-equilibrium electrons or holes in semiconductors. More broadly, the term describes electron distributions by the Fermi function, but with the elevated effective temperature. If the power input into the electronic system exceeds the rate of energy loss, then the carriers heat up and their velocity distribution $f(v)$ deviates significantly from the equilibrium Maxwellian form. The time-dependent distribution function $f(t, r, v)$ can be determined by solving the Boltzmann transport equation,

$$\frac{\partial f}{\partial t} + \mathrm{v} \cdot \frac{\partial f}{\partial r} + a \cdot \frac{\partial f}{\partial v} = \left(\frac{\partial f}{\partial t}\right)_{coll} \tag{1-16}$$

where a is the acceleration and the collision integral is the right hand is a linear functional on f.

Hot electrons are very mobile because of its high effective temperatures. Therefore, hot electrons can tunnel through the materials instead of recombining with holes or conducted to a collector. Consequently, it can excite and/or damage the dielectric materials, which is called "hot carriers degradation". Hot electron process is a pathway leading to electrical breakdown. The hot electrons in insulating polymer can arise from high energy electron beams (a few keV) or high electric field (from tens to hundreds of kV/mm), which are both investigated in this work. In addition, hot electrons is also of great importance for studying of all modern semiconductor devices. For example, hot-carrier injection into the gate dielectric in silicon field-effect transistors is somehow a nuisance. This unwelcome effect gives rise to degradation of transistor characteristics and may lead to circuit failure [107]. It is also the saturation of drift velocity under high electric stress.

For the electrical breakdown process, there are three main pathways that are considered to lead to final breakdown, namely "electrical", "thermal", and "electro-mechanical", as shown in the breakdown period of Figure 1-16.

The three pathways of electrical breakdown are listed in Table 1-4. Firstly, the application of high voltage can cause localized electron avalanches in the materials, which is named "intrinsic breakdown". Secondly, large and continuous current through the sample generate thermal energy to melt and to oxidize local area to cause breakdown, which is named "thermal breakdown". Thirdly, electric field causes mechanical stress in the material which directly damages the sample, named "electro-mechanical breakdown".

Table 1-4 Pathways to electrical breakdown.

Breakdown	Pathway to breakdown
Intrinsic breakdown	Avalanche of electrons
Thermal breakdown	Thermal runaway
Electro-mechanical breakdown	Mechanical stress

Within the above processes, intrinsic or avalanche breakdown is directly triggered by the kinetic energy of the carriers. Intrinsic breakdown refers to the electric field which will cause breakdown of a "perfect" material in a very short time, for example, without the effect of

high field ageing. The literature [108] reviews the historic advancement of intrinsic breakdown theories in detail.

Electron avalanche is a process in which a number of kinetic electrons are subjected to strong acceleration by an electric field, subsequently collide with other atoms and ionize them (impact ionization). The released additional electrons accelerate and collide with further atoms, releasing more electrons. In order to evaluate the rate of avalanche of electrons, M is given as a multiplication factor of initial electrons:

$$M = \frac{1}{1-\int_{X_1}^{X_2} \alpha dx} \tag{1-17}$$

where X_1 and X_2 are the positions that the multiplication is being measured between, and α is the ionization constant. Considering the electric field and substituting the voltage gradients into the equation, it results in:

$$M = \frac{1}{1-\left|\frac{V}{V_{BR}}\right|^n} \tag{1-18}$$

where V is the applied voltage, V_{BR} is the breakdown voltage and n is an empirically derived value. It can be seen from the formula that the multiplication factor is highly dependent on the applied voltage. When the applied voltage increases to near breakdown voltage, the multiplication factor approaches infinity, resulting as breakdown. Breakdown is not the sole process in which the kinetic energy of carriers is critical to the materials. Let's consider the diagram in energy of Figure 1-17 in which processes in the dielectric are derived according to the energy of the carriers.

When we consider the kinetic energy of electrons in the materials as shown in Figure 1-17, under kinetic energy of 0 eV it is considered trapped charges in the materials. Then above a kinetic energy at about 8 eV intrinsic breakdown occurs. Hence, there is a threshold kinetic energy for electrical ageing, furthermore, there is a threshold electric stress for electrical ageing. In general, the position of the electrode Fermi level within the band gap and relative to impurity states can critically affect the breakdown field.

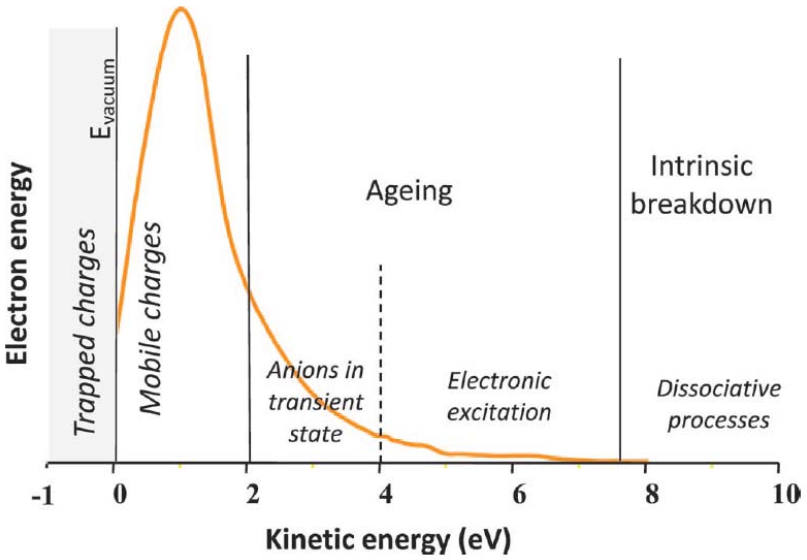

Figure 1-17 Schematic representation of the electron energy distribution in a large bandgap insulator under an electric field, taken from [7].

1.3.1.3 Electrical tree growth - electrical ageing and degradation processes

In presence of cavities within the insulation, discharges within the gaseous medium present in cavities, so-called 'partial' discharges (PDs) since they do not bridge the gap between the electrodes, produce alteration of the walls of the voids and subsequent growth of the voids, as a form of degradation process, which leads to breakdown. However, in the case of a cavity-free polymer, how does the electrical ageing indeed take place and grow? In this situation, electrical ageing takes place above a critical level of stress. It grows through a number of different stages as shown in Figure 1-18 before leading to ultimate failure of the dielectric. At the initial stage, electric field induced space charge center lead to alteration of the microstructure and of the local chemical composition, which play a role as nano-voids enlarge to micro voids. It is thought that degradation at a microscopic scale leads to the formation of micro voids which can develop into larger cavities, up to the point where the cavity size is just enough to sustain micro discharges which will ultimately lead to the failure through the propagation of an electrical tree.

The initiation of the degradation of polymers is still unclear or debatable. So far, local molecular re-configurations and chemical changes are considered to play an important role. Furthermore, it is significant to diagnose the initiation of electrical breakdown. It was evidenced experimentally that threshold of light emission is inferred to the onset of the electrical ageing, which will be demonstrated in section 1.3.3. Electrical stress can initiate material degradation reactions through energetic processes such as “partial discharges” and/or “hot electrons”. “Partial discharges” take place depending on the time scale and specific situation, such as micro void formation or enlargement. “Hot electrons” and other sources could generate excited states and become a common feature in the early stage of electrical ageing.

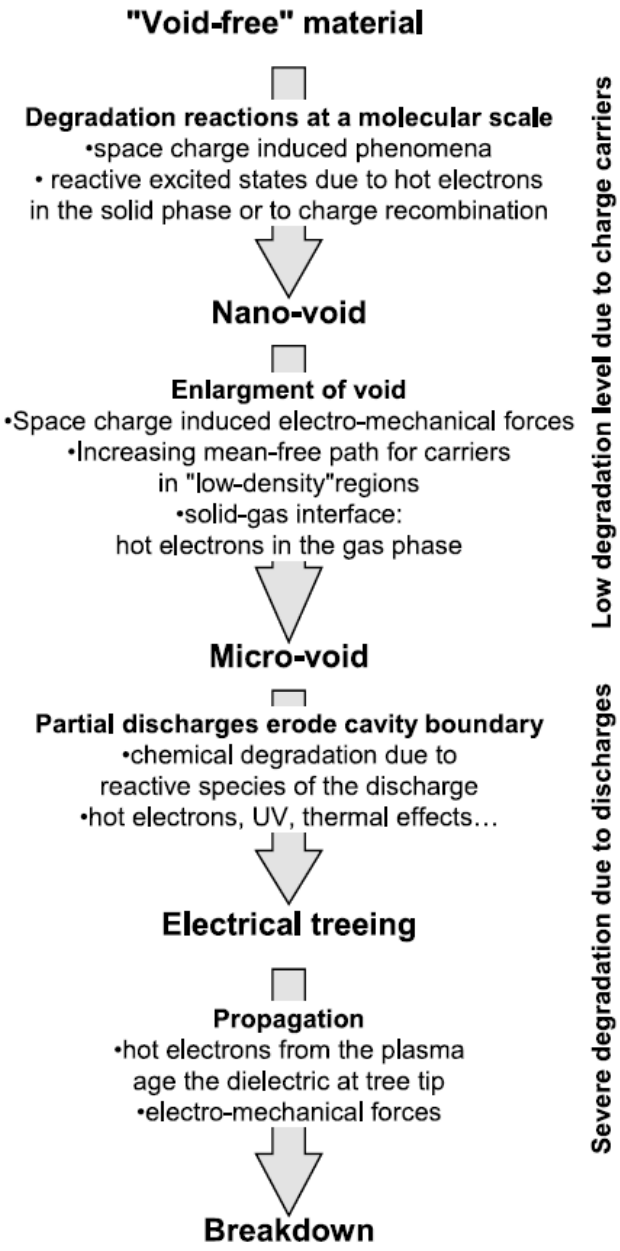

Figure 1-18 Postulated steps in electrical ageing for a cavity-free polymer submitted to an electric field in the absence of partial discharges in the surrounding medium, taken from [4].

1.3.2 Electrical ageing or pre-breakdown diagnosis

Search for pre-breakdown warning signs in insulating polymers has been the subject of a great deal of work in the past few decades [45]. Electric and acoustic signals emitted in the presence of discharging in internal cavities or during electrical treeing propagation have been used for long time to diagnose defects and to monitor ageing. Partial discharges and treeing phenomena are considered to be the main sources of the electrical degradation and breakdown of polymers used in high voltage applications. Numerous works have been carried out to solve the problem. Nowadays, long-term material degradation in discharge-

free situation is of more and more importance due to the improvement of the production processes and demand for higher efficiency and high energy density. It has been more and more important to search for pre-breakdown signals. The methods to diagnose pre-breakdown warning signs are shown in Table 1-4.

One available way that has been opened in recent years is the space charge diagnosis in electrical ageing. However it is still not deeply understood and how it affects ageing is still debatable. Widespread approach has been carried out through comparing the space charge distribution under different electric field, temperature, and environment.

Another way is to probe ageing is to investigate the light emission of materials under electric stress which is called electroluminescence. Under electric field, some excited states have a non-zero probability to relax visible photons because the energy involved in covalent bond breaking is roughly of the order of a few eV, i.e., in the range of visible wavelength. Electrical ageing is accompanied by a change in the physical, chemical and structural features of the dielectric. By investigating the characteristics of light emission under an electric stressed material, it is possible to unravel the leading deterioration process in insulating polymers.

Electrical ageing does not start throughout the polymer volume but a localized process, which can also been evidenced by chemical analyses, such as thermal gravimetric analyses (TGA) and infrared (IR) spectra analyses. Ageing proceeds through the molecular dissociation of some of the original constituents of the material and the formation of the new chemical bonds, which can be detected with chemical analyses.

Table 1-4 Methods to diagnose electrical ageing or pre-breakdown warning signs.

Methods	Characteristics
Partial discharge detection	From micro-void at atmosphere
Space charge diagnosis	Charge transport and accumulation
Electroluminescence test	Optical signals to uncover mechanisms

1.3.2.1 Partial Discharge detection

During diagnose the electrical ageing of insulating polymers under electric stress, partial discharge phenomenon always occur at atmosphere. The term “Partial Discharge” (PD) is defined firstly by IEC 60270 Partial Discharge measurement as a localized electrical discharge that only partially bridges the insulation between two conductors, which may or may not occur adjacent to a conductor [109]. PD always results from breakdown of gas in a cavity or electrical tree channel, or from breakdown along an interface or surface. The PD

phenomena exist extensively in the industrial electrical applications operating in atmospheric environment. The PD testing is widely applied in cable systems. A big challenge during diagnosis is that PD occurs always without immediate failure. Indeed, some sources of PD can continue for years before causing failure, which makes it more difficult to diagnose.

Discharge occurs in cavities and/or micro-channels. When the material is subjected to an electric field, owing to the existence of some cavities in its bulk, the field in the cavity is stronger than in its surrounding dielectric as shown in Figure 1-19. The amplification of the field varies depending on the shape and location of the cavity. As the voltage is raised, the field in the cavity increases rapidly and reaches its threshold, then the gas can breakdown. The resistance of the cavity changes from very high to zero, along with zero of the cavity field and transient change in the electric field distribution. However, the PD can't cause the material failure immediately but partial breakdown, until the electric tree grow through the dielectric and bridge the two conductors.

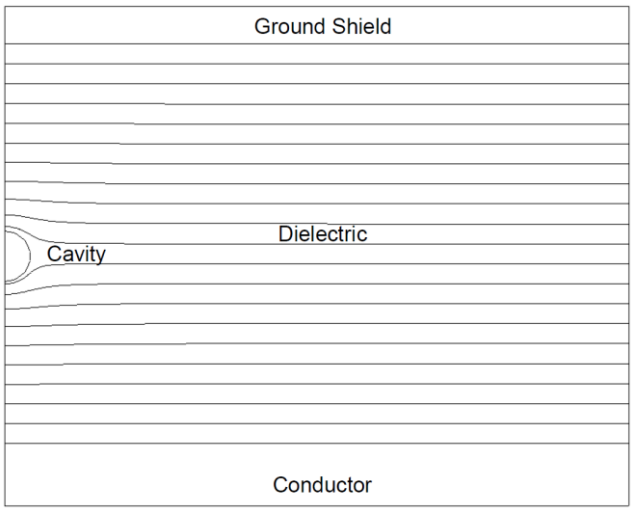

Figure 1-19 Equipotential plots for an 0.8 mm diameter cavity in an XLPE cable with 6.4 mm thick dielectric, from [109].

Along with the PD phenomenon, a transient current change results in a voltage pulse at a few nanoseconds (10^{-9}s), which propagates in both directions away from the PD source. Its nanosecond scale also limits the diagnostic task. Nevertheless, number of advances have been carried out [4, 109-122] since firstly reported with a wide-band Partial Discharge detector in 1975 [122]. When dealing with PD, three stages are needed to collect sufficient information for evaluation: detection, classification, and location [114]. Detection is usually performed with a classical discharge detector having a bandwidth of 250 kHz. It shows the presence and the magnitude of PD under observations. Classification recognizes the defects causing the discharges, e.g. internal or surface discharges, corona, treeing, etc. It is vital to estimate the harmfulness of the PD. Location is to locate the position of PDs in a dielectric.

This is very difficult to achieve and also differs from sample to sample, resulting in calibration difficulties.

According to the source of PD and the formation process of PD, the PD could be eliminated or at least relieved by dealing with the gas in the void and the interface or electrical tree. For example, putting the dielectric sample in a vacuum environment, pumping out the air from the void and interface, making a better dielectric interface, could relieve the PD at the maximum extent.

With the development of advanced materials synthesis processing and understanding of the mechanism of PD and electrical ageing, insulating polymers are pushed to their electric limit in order to meet the requirement of the high-voltage cables, high density capacitors, etc. Solutions have been implemented to strengthen the insulation against PD even when they are not avoidable.

1.3.2.2 **Space charge diagnosis**

When the polymeric insulation is under electric field, space charges accumulate in the insulation material. The space charges may distort the electric field profile and influence the steady-state current. When the space charge density is sufficiently high, the local field strength may be strong enough to exceed the breakdown threshold of polymeric insulation, leading to electrical breakdown or dielectric failure. Space charges have been recognized as harmful to DC applications, while they also play important role in long term electrical ageing of polymers under AC field. The electron energy distribution in an insulator under an electric field shown in Figure 1-17 has already been commented. Below the band edge, the trapped space charge has a very low mobility, while above the band edge, the space charge is mobile and electrons can gain kinetic energy from the electric field and be excited. Nevertheless, there still exists a gap between the space charge distribution and electrical ageing in insulating polymers.

In the last three decades, a significant effort has been directed to measure and model the internal space charge distribution in dielectrics. Internal space charges move under the influence of the electric field. At the same time, ionic dissociation can take place and charges can be transferred at these interfaces.

A significant effort has been done to understand the internal space charge distributions in dielectrics, due to the development of a number of methods which give detailed information on space charge distributions [123]. The space charge diagnostic methods have been addressed in Table 0-6 in the annexes at the end of the dissertation.

In 2014, Villeneuve-Faure *et al*. [124] developed a new method derived from atomic force microscopy (AFM) – the electrostatic force distance curve (EFDC), to realize 3D charge localization. It is a powerful method with high spatial resolution in 3 dimensions. The main advantage is its high sensitivity to charge localization. Boularas *et al*. [125] carried out simulation of electrostatic forces at play in the method to analyze force distance curves

modification induced by electrostatic charges. This is a great work toward the 3D charge localization.

With all these methods focusing on different materials, the internal space charge distributions can be directly carried out. Among that, the Pulsed electro-acoustic (PEA) method has been widely used in space charge measurement. Bipolar charge transport model (BCT) has been evidenced with both experimental and simulations along with the carriers injection at the electrodes. However, how these space charge make an effect under the electric field, and what is the relationship between the space charge and electrical ageing, are still debatable and need more experimental and simulation evidences by e.g. probing energetic processes associated to space charges.

Profiting by the development of the space charge measurement methods not only in space but also in time scale, a lot of works on space charge distribution measurement and simulation have been carried out. Some space charge transport and trapping theories such as mechanism for space charge limited currents (SCLC) and bipolar charge transport (BCT) model are demonstrated in the annex at the end of the dissertation.

1.3.3 Electroluminescence and electrical ageing

The dielectric materials could be subjected not only to electrical stress but also to thermal, mechanical, chemical and environmental stresses [2], which all make contributions to the electrical degradation, ageing, and breakdown. Among them, luminescence, especially electroluminescence can provide information for pre-breakdown or ageing warning signs and could be an important way to diagnose electrical ageing. Electroluminescence plays a significant role in the insulating polymer under field stress. In addition, the partial discharge can also give rise to transient luminescence and can also be employed to monitor the growth and propagation of electrical treeing and breakdown, while the electroluminescence is continuous, sensitive, and relatively stable under AC or DC field. Therefore, the light emission or electroluminescence is not due to partial discharge but chemical/physical processes internal samples.

EL is a technique to detect the initiation of electrical degradation and breakdown in insulating polymers. What's more, EL is, so far, the only direct experimental evidence of the existence of potentially dangerous excitation energy in insulating polymer during ageing. EL detected in many different polymers [126] under AC and DC field exhibits a threshold-like character, which means that the light emission increases super-linearly with the applied field above a critical value. Luminescence measurements were carried out in different insulating polymers, such as in Polypropylene as shown in Figure 1-20 for example. The voltage was increased in steps of a few hundred volts on a 18 μm thickness sample. The onset field for EL emission can be found at about 10kV/mm under AC stress in this example. Typically the field threshold reported for polymeric materials is of the order of 10 to 30 kV/mm under AC stress.

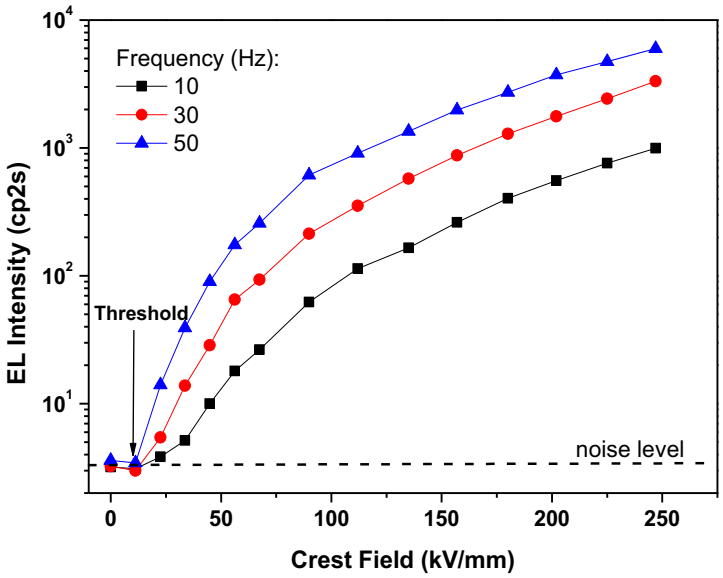

Figure 1-20 EL intensity vs. field characteristics Polypropylene under AC stress at different frequencies. EL Threshold is at about 10 kV/mm. The dotted line is the noise level of the measurement. Light intensity is given in photomultiplier counts per 2 seconds.

Under DC stress, field threshold is generally higher as listed in Table 1-5. The higher field threshold reported for DC is due to fundamentally different conditions for the excitation. With the hypothesis of EL due to charge recombination, EL under AC appears as a near-electrode effect, charges injected under one polarity in a given half-cycle of AC stress recombine with previously injected charges of opposite polarity during the previous half-period of stress. The description is somewhat substantiated by modelling of EL as a function of the AC waveform (square, triangle, sine, with or without offset) and voltage offset based on bipolar charge injection, trapping and recombination. With the model it was shown that the charge recombination would occur in a region within a few nm from the electrode [85, 87]. Conversely, under DC, EL excitation requires that charge of one polarity are transported through the bulk to meet and recombine with charges of the other polarity injected at the counter electrode.

The injected carriers are responsible for the subsequent EL. The EL is due to the recombination of carriers of opposite polarity - electrons and holes. During this process, the energy released through radiation or energy, which is the initiation of electrical ageing and breakdown [59, 127].

Table 1-5 Onset of electroluminescence in gold-metallized materials submitted to a DC field, adapted from [126].

Material	Field (kV/mm^{-1})
Low-density Polyethylene (LDPE)	110
Cross-linked Polyethylene (XLPE)	60
Bi-axially Oriented Polypropylene (BOPP)	200
Polyethylene terephthalate (PET)	400
Polyethylene Naphthalte (PEN)	150
Polyetherimide (PEI)	170
Polyimide (PI)	350
Polyethersulfone (PES)	350

The onsets of EL in different insulating polymers are different due to their intrinsic electrical properties. It is noteworthy that the insulating polymers have the onset EL characters under DC stress as in Table 1-5. It infers that EL corresponds to the onset of excitation mechanism which is universal among the insulating polymers. The onset of EL in some polymers may vary a little depending on material formulation.

In summary, EL onset voltage is a warning of electrical ageing which occurs at initial stage of electrical tree growth as shown in Figure 1-18. However, until now there is still no evidence for the exact relationship between EL and ageing. Bamji *et al.* [68] propose a degradation mechanism due to the UV contributions measured in EL of polymers. However, it seem that the UV they measured was due to discharges in the environment of the samples as no UV emission has been reported by other authors when carrying out measurements in vacuum. Zeller [128] considers the EL emission as a proof of the existence of excited states, but with no major implications for polymer ageing which rather would be related to the non-radiative chemical pathways. More evidences of both experimental and simulations should be furnished to support and uncover the correlations between EL and electrical ageing.

Hence, so far, the threshold of EL is a direct correlation between EL and electrical ageing. On the other hand, spectra analyses is an elegant way to understand physical or chemical process in the materials, which can be used to uncover the nature of luminescence and the relationship between EL and electrical ageing. This is also the main aim of the dissertation. With luminescence techniques, we can carry out light emission from each single process, such as recombination process and chemical reaction process, for analyzing. This provides

more information of EL, which proves EL is a multi-excitation involving physical and chemical processes under electric stress.

1.4 The aim of the dissertation: approach to inferring the electrical ageing mechanisms

Electrical pre-breakdown or ageing warning signs are very important because the engineering of insulating materials needs knowledge of safety service limits in terms of applied electric tresses, while all the polymers are known to be sensitive to electrical ageing that decreases their electrical abilities to sustain a certain electric field. Electric and acoustic diagnosis methods during the discharge of internal cavities have been developed to test the defects in materials and monitor ageing. However this is only used in the presence of local field enhancement and micro-voids. Nevertheless, the electrical ageing and degradation is thought to be due to charge trapping, charge transport, and charge recombination or energy dissipation.

Therefore, electroluminescence and cathodoluminescence, along with other luminescence techniques which will be used in the following, as approaches to inferring the electrical ageing mechanisms, are to uncover the nature of physical and chemical processes and bridge the gap between the space charge and electrical ageing in insulating polymers.

The excitons formation in insulating polymers will be evidenced. Field dependence under DC and AC stress, spectral and their component analyses, and spectral analyses between different samples will be carried out. The impact of the nature of the electrode will be analyzed, and the source of the light emission, i.e. interface states and Surface Plasmons, will be investigated. The cathodoluminescence and electroluminescence will be compared and investigated. Each component of spectra will be identified and spectral reconstruction will be carried out.

Chapter 2
Experimental Materials and Techniques

2.1 Experimental materials

2.1.1 Polyolefins

2.1.1.1 Polyethylene

Polyethylene (PE) is the most common plastic, and the one with the simplest chemical structure, a polyolefin, composed of monomers - C_2H_4 -, with the chemical formula $(C_2H_4)_nH_2$. The mechanical properties of PE depend significantly on the extent and type of branching, the crystal structure and the molecular weight. Until now, different categories of PE have been synthesized based mostly on their density and branching, such as Ultra-high-molecular-weight Polyethylene (UHMWPE), Ultra-low-molecular-weight Polyethylene (ULMWPE), High-molecular-weight Polyethylene (HMWPE), High-density Polyethylene (HDPE), High-density cross-linked Polyethylene (HDXLPE), Cross-linked Polyethylene (XLPE), Medium-density Polyethylene (MDPE), Linear low-density Polyethylene (LLDPE), Low-density Polyethylene (LDPE), Very-low-density Polyethylene (VLDPE), Chlorinated Polyethylene (CPE), etc [2, 129]. These materials are designed for special or extreme applications.

The tested PE samples in the dissertation are, on the one hand, peroxide cross-linked PE, termed XLPE films. It was peeled from a HV cable having a 15 mm thick insulation layer. Such XLPE cables are issued from EU project Artemis [130] in which database for electrical ageing markers were looked for. The thickness of XLPE film is 150 µm. It is available in roll form up to 15 m long and 8cm wide. Samples are stored in plastic bags at atmospheric pressure.

The other PE being investigated is additive-free LDPE films of 50 µm thickness. The samples were provided by ABB.

Figure 2-1 XLPE insulation in a power cable.

There exist some types of defects in the carbon chain of Polyethylene which have been shown in Figure 1-6 in chapter 1: carbonyl, dienone, hydroxyl, double bond, conjugated double bond and vinyl [50] for example. Some additives [39, 51] are often added in the sample, especially antioxidant that prevent attack of the polymer by dissolved oxygen at the processing stage (e.g. during polymer crosslinking at high temperature 190 °C) or in service conditions as materials are designed to continuously endorse temperature of 90°C In case of

peroxide cross linked PE, crosslinking by-products are dissolved in the polymer such as cumylalcohol, acetophenone, or α-methylstyrene and also water and hydrogen. Some of these by-products have also been shown in Figure 1-7 in chapter 1.

2.1.1.2 **Polypropylene**

Polypropylene (PP) is another polyolefin, composed of monomers $-C_3H_6-$, with the chemical formula $(C_3H_6)_nH_2$, widely used in industries since invented in the early 1950s. The commercial production of PP began in 1957 in USA and 1958 in Europe [131, 132]. It is a thermoplastic polymer widely used in a variety of applications including packaging, textiles, and electrical equipment components, such as capacitors and electrical accessories. It is liable to chain degradation from exposure to heat, UV radiation, and under electric field. Samples are extruded between two rolls and manufactured in thin films for capacitor applications with high breakdown strength.

When Polypropylene film is extruded and stretched in both the machine roll direction and across machine roll direction, it is called Bi-axially Oriented Polypropylene (BOPP). All the PP measurements are carried out in the dissertation on BOPP films of 17.8 μm thickness supplied by KOPAFILM, Germany. The films were provided with different roughness for the two faces, to favor oil impregnation. There are some large (from rough outside of the BOPP roll as seen in Figure 2-2) and small (from smooth inside of the BOPP roll as seen in Figure 2-2) crater-like structures on the two surfaces of the BOPP films, which will be discussed in detail in chapter 3. The only known additives contained in the BOPP films under study are penta-erythritoltetrakis (3,5-di-tert-butyl-4 hydroxyhydrocinnamate) and calcium stearate [133]. The former is known as Irganox 1010, which is a sterically hindered phenol used as an antioxidant to abstract unstable radicals. Calcium stearate is a lubricant and an acid scavenger used to neutralize any hydrochloric acid generated from reactions between the hindered phenol and residual chloride-containing catalyst [133].

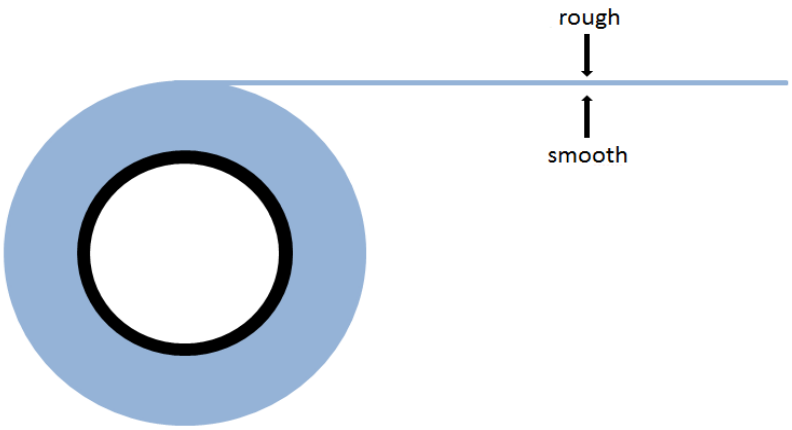

Figure 2-2 Diagram of Bi-axially Oriented Polypropylene roll.

2.1.2 Polyesters

2.1.2.1 Polyethylene Naphthalte

Polyethylene Naphthalte (PEN, Poly(ethylene 2,6-Naphthalte)) is a polyester with good barrier properties and a static dielectric constant of 3.4. It is an aromatic polyester of the same family as Polyethylene Terephthalate (PET) but with two aromatic rings instead of one, as shown in Figure 2-3, making it a candidate for replacement of PET with higher thermal stability [134]. The PEN samples tested in the dissertation are transparent, with a thickness of 25 μm, supplied by Dupont (Dupont Teijin Films Teonex® Q51).

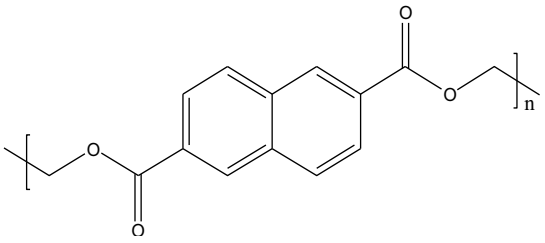

(a)

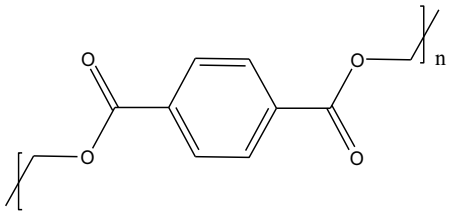

(b)

Figure 2-3 Chemical structure of (a) Poly(ethylene-2,6-Naphthalte) (PEN) and (b) Polyethylene terephthalate (PET).

2.1.2.2 Polyether Ether Ketone

Polyether Ether Ketone (PEEK) with chemical structure as shown in Figure 2-4 is a thermoplastic polymer in the polyaryletherketone (PAEK) family, used in bearings, pumps, and cable insulation, due to its robustness. The PEEK samples tested in the dissertation are transparent with a thickness of 50 μm, supplied by Goodfellow Cambridge Limited.

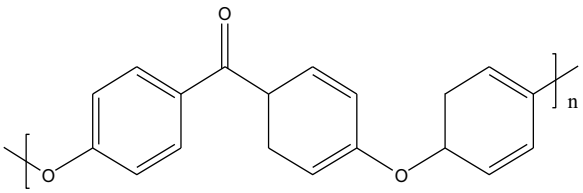

Figure 2-4 Chemical structure of Polyether ether ketone.

2.2 Experimental setups

In the dissertation, the Edwards system and Univex 350 G system are utilized to deposit gold (Au) and Indium Tin Oxide (ITO), respectively. Atomic Force Microscope and Optical Microscope are used to characterize the surface of the polymer films. Ultraviolet-Visible Spectrophotometer is used to measure the transmission and absorption of the polymer film and electrodes. The luminescence analyses system is a lab-made test bench to measure the photoluminescence (including fluorescence and phosphorescence), electroluminescence, and cathodoluminescence from solid materials.

2.2.1 Samples preparation

2.2.1.1 Gold metallization setup

During current and EL measurements, electrodes must be deposited on samples to apply a controlled electric field. Besides, the deposited electrodes must be partially transparent in the UV-visible domain in order to collect light. In Figure 2-5, it is the picture of Scancoat 6 SEM sputter coater for gold metallization from Edwards. The system is a compact bench-top sputter coater designed to coat a wide variety of specimens with a high quality, conductive metal (such as gold) film. The films are deposited uniformly (the center area of the metallization is a little thicker than its edge), even over re-entrant surface, as a deposit rate of 0.1 nm/s.

The insulating polymer films are provided with gold electrodes having a diameter of 50 mm and thickness of 30 nm (the center area is about 30 nm, while the edge area is about 26 nm.). The parameters of the sputtering process are listed in Table 2-1. The sputtering rate is about 0.1 nm/s. The sputtering pressure is about 0.15 mbar in Argon gas. The voltage and current are 1 kV and 10 mA, respectively.

Figure 2-5 Gold metallization setup, Scancoat 6 from Edwards.

Table 2-1 Parameters of the sputtering process of gold.

Sputtering	Value
Rate	0.1 nm/s
Gas	Argon
Pressure	0.15 mbar
Voltage	1 kV
Current	10 mA
Time	300 s

2.2.1.2 **Indium Tin Oxide coating setup**

In Figure 2-6, we can see the Univex 350G glove box system made by Oerlikon Leybold Vacuum used to deposit Indium Tin Oxide (ITO) on the surface of polymer films. Figure 2-6 a (1) shows the control system, including the operating system in Figure 2-6 b and power controller in Figure 2-6 c, while Figure 2-6 a (2) shows the deposit system, in which the polymer films are provided with ITO electrode.

During the deposition processes, the temperature of the polymer films, the electric power on the ITO target, and the flow rate of Argon and Oxygen could be adjusted to achieve the best conditions for deposition. The parameters of the sputtering process are shown in Table 2-2.

Table 2-2 Parameters of the sputtering process of ITO.

Sputtering	Value
Temperature	30 °C
Rate of Argon	50 sccm*
Rate of Oxygen	1.2 sccm*
Pressure	5.5×10^{-3} mbar
Power	150 W
Time	18.5 min or 33.5 min*

** "sccm" means standard cubic centimeter per minute.*

** Sputtering time 18.5 min and 33.5 min are set for thickness of 110 nm and 200 nm, respectively.*

In the dissertation, the ITO (diameter 50 mm) thickness of 110 nm and 200 nm are deposited on the PP and PEN respectively in order to achieve the best transparency and conductivity. The transparency of ITO is approximately 89%, while the surface electric resistance per centimeter is approximately 30 Ω/□.

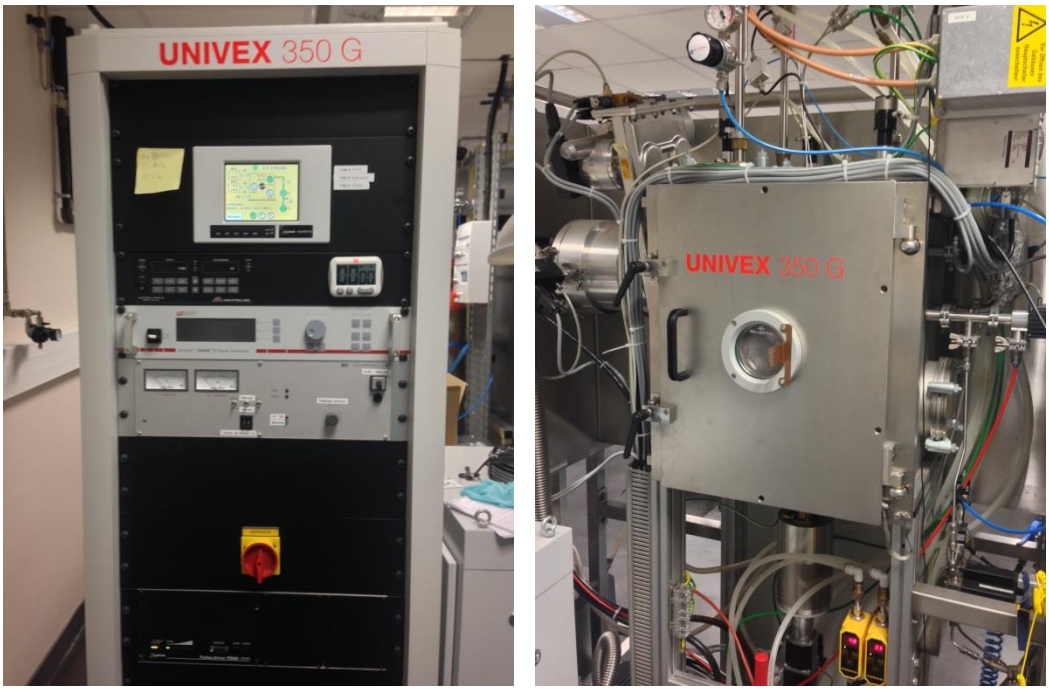

a: Full view of ITO experimental setup

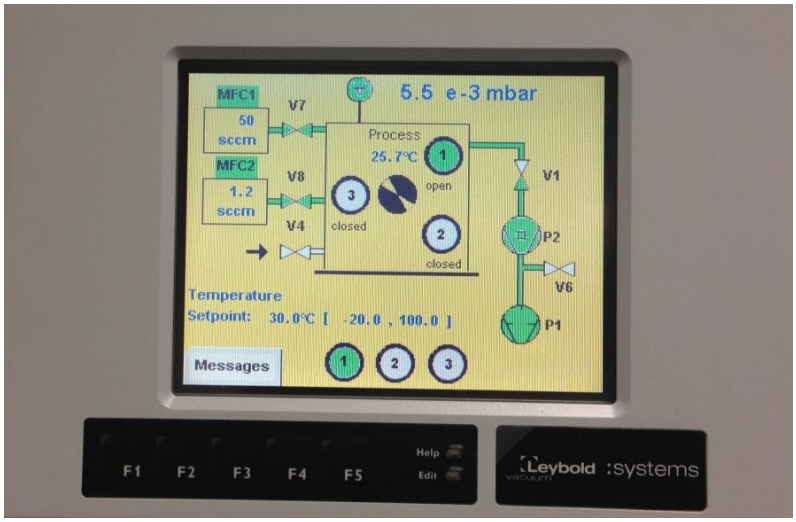

b: Operating system

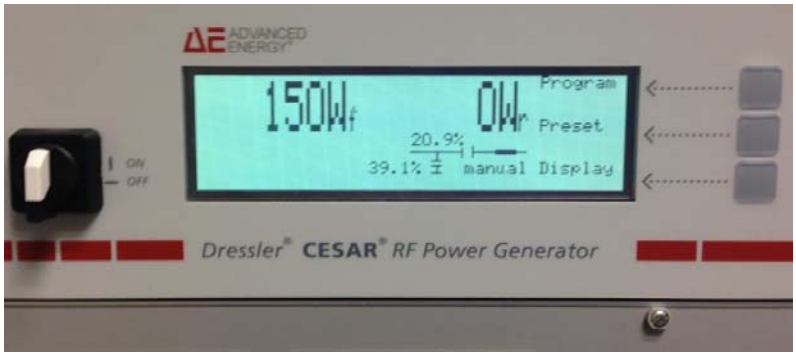

c: Power controller

Figure 2-6 Univex 350G ITO-deposition experimental setup.

2.2.2 Luminescence setups

All the luminescence experiments were carried out in a special-design multi-purpose chamber as shown in Figure 2-7. It mainly contains five systems:

1) excitation source system (electric field, electron beams, photons, and plasma),
2) optical detecting system (PM system and CCD camera system),
3) optical path controlling system,
4) temperature controlling system,
5) and pumping system.

The excitation source system and the testing system are two core parts for luminescence measurements, while the other systems are auxiliary components.

The testing system also contains three parts according to the optical axis: optical axis No.1 photo and electron beam excitation sources; optical axis No.2 a cooled photomultiplier (PM) working in photon counting mode for integral light detection; optical axis No.3 a grating monochromator (4.5 nm in resolution) coupled to a liquid nitrogen cooled charge coupled device (CCD) camera for spectral analyses which covers the wavelength range from 230 nm to 840 nm. It is a light proof dark chamber connected to a turbo-molecular double pumps system to achieve high vacuum at 10^{-7} mbar in order to avoid gaseous discharges during measurements. Samples can be placed on the holder which contact to a heating resistor, a nitrogen reservoir, and a temperature sensor, to control the temperatures from liquid nitrogen temperature up to 180 °C. The multi-purpose chamber is designed to accommodate different kinds of luminescence excitation as described below.

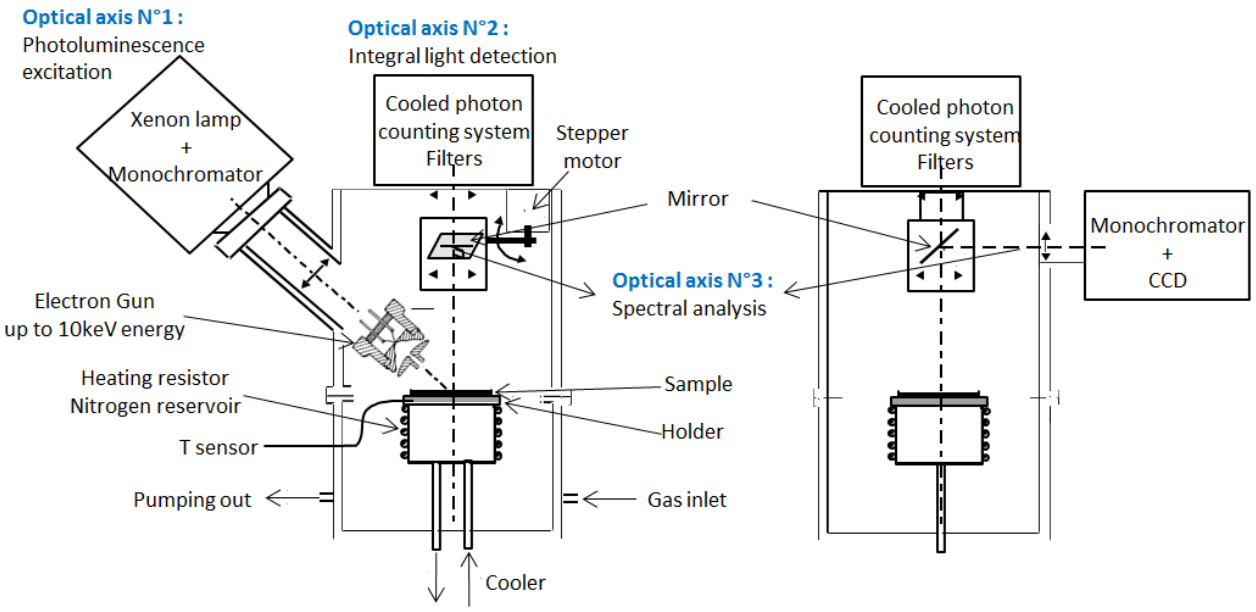

Figure 2-7 Luminescence experimental setup.

2.2.2.1 Three Excitation sources

a) Electric field excitation

During electroluminescence (EL) measurement, the configuration of Figure 2-8 was installed in the chamber and put under high vacuum. All the measurements are carried out at room temperature. Light detection is carried out by two systems -PM and CCD. The two electrodes HV ring electrode (inner diameter 30 mm) and ground flat electrode (diameter 50 mm) are connected to the high voltage and ground respectively. The ring electrode allows the light emission analyses from the center of the sample.

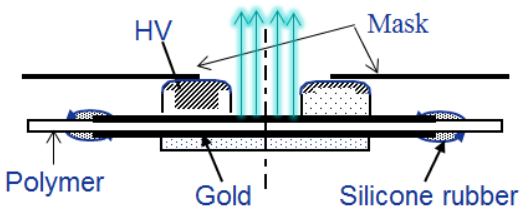

Figure 2-8 Configuration of EL measurement.

Direct current (DC), alternating current (AC) and pulse current (PC) are applied to the dielectrics. The AC and DC power supply system are shown in Figure 2-9 and Figure 2-11, respectively. The AC power supply consists of an oscillograph, a pulse/function generator and a high voltage amplifier (20 kV amplification from Trek, Germeny). The amplification factor is 2000. Three kinds of AC voltage waveform (Sinusoidal, square and triangular) as in Figure 2-10 of AC can be used to investigate the EL characteristics. The phase of AC voltage can be synchronized with the computer which can achieve the phase-resolved EL of the materials. The phase-resolved EL of insulating polymers will be analyzed in Chapter 3 and Chapter 4. The DC power supply is a 35 kV source from Fug, Germeny. DC current is measured using a Keithley 617 programmable electrometer. The DC voltage by increase-steps of a certain value as shown in Figure 2-12 is applied to the materials. With this equipment and PM system, the EL characters and current vs. field, phase-resolved EL, and spectra can be diagnosed. With CCD camera the spectra can be achieved under both DC and AC electric field.

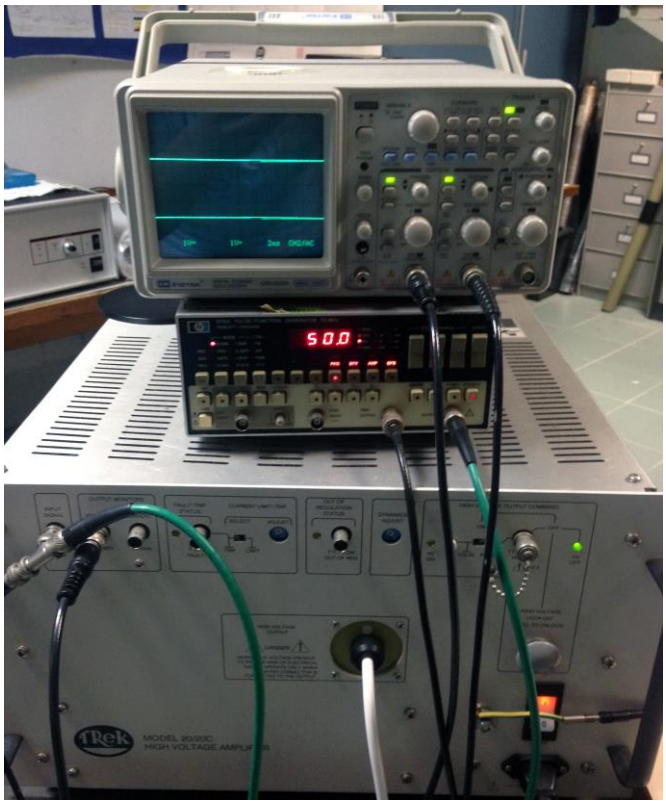

Figure 2-9 AC power supply. From top to bottom: an oscilloscope, a pulse/function generator and a high voltage amplifier. The amplification factor is 2000.

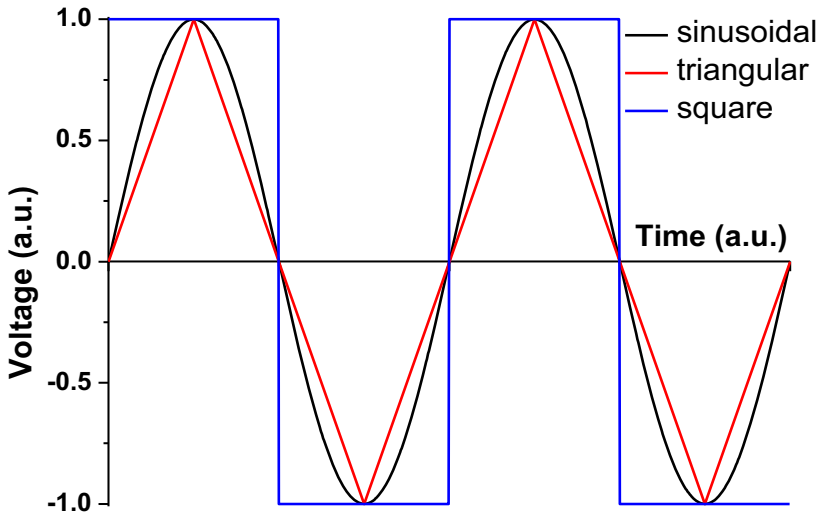

Figure 2-10 Three kinds of voltage waveform.

Figure 2-11 Keithley 617 programmable electrometer and DC power supply (voltage up to 35 kV, current up to 1 mA).

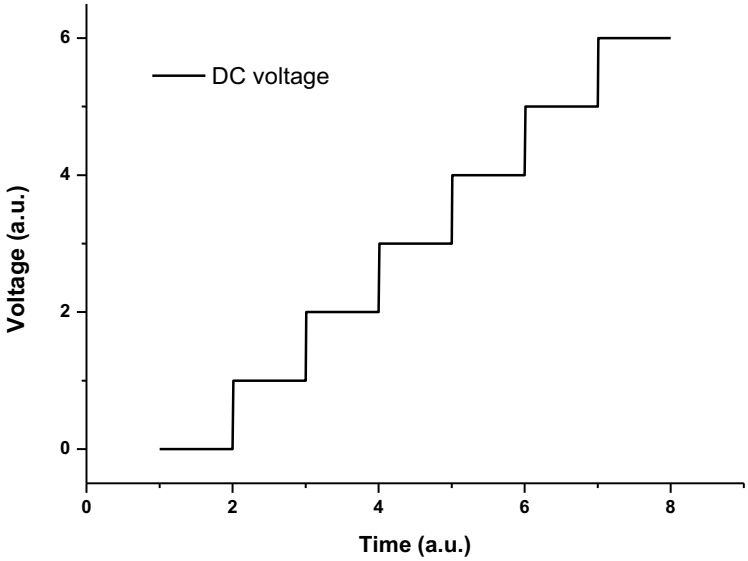

Figure 2-12 Applied DC voltage by increase-steps of a certain value.

b) Optical excitation

During photoluminescence (PL) measurement, the samples mounted into the chamber at ambient atmosphere were excited by a xenon source coupled to an irradiation monochromator as shown in Figure 2-13. The Xenon lamp has a power of 150 W from Jobin-Yvon. It is coupled to an excitation monochromator (double pass monochromator HD10UV from Jobin-Yvon with 1200 lines/mm). The bandwidth of the excitation light source is 4 nm. The xenon lamp was turned on with an exhaust gas system to exhaust ozone produced by the UV from the lamp. The excitation wavelength varies form 200 nm to 700nm and is set manually. The bandwidth of the irradiation window can be adjusted from 0.2 nm to 4 nm. Coupling between the sample, the excitation source, and CCD camera, was achieved by

optical path through the quartz lenses window of the chamber. In prior to testing samples in photoluminescence measurements, the chamber was evolved and filled in with Helium at atmosphere. PL measurements were performed at liquid nitrogen temperature especially for phosphorescence (PHL) and at room temperature especially for fluorescence (FL), respectively. The phosphorescence can be achieved according to the delay time through controlling the switch on/off of the shutter placed in front of the irradiation source.

There is a high pass filter at 300 nm in front of the CCD camera in order to cutoff the excitation light of wavelength shorter than 300 nm. The emission spectrum is integrated under different time (from 10 to 300 seconds) by the CCD camera, which proves enough to have a good resolution.

Another filter has a sharp cut-off at 620 nm enabling light detection with "red rejection". It is used in EL measurement as discussed in Chapter 3 and Chapter 4. Both of the two filters can be changed from outside, i.e. without opening the chamber.

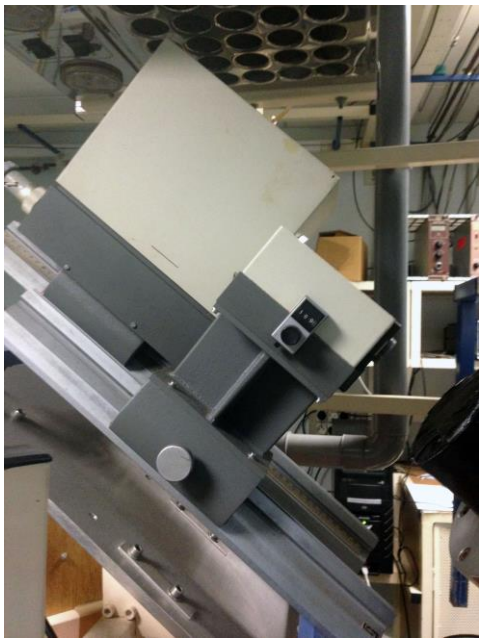

Figure 2-13 The xenon lamp with an excitation monochromator from Jobin-Yvon.

c) Electron beam excitation

During cathodoluminescence (CL) measurement, we use a home-designed electron beam gun as shown in Figure 2-14 mounted into the chamber as shown in Figure 2-7, providing electrons of up to 10 keV in energy. The filament is at high voltage and the anode at the ground. The distance between the electron gun and the sample on the holder is about 40 mm. The axis of the gun is at 50° to the normal of the sample plane rendering possible light detection along the normal to the samples. The beam current is about 0.5 μA. Experiment were also carried out under a vacuum better than 10^{-6} mbar, at ambient temperature.

Emission spectra and light intensity were recorded for different electron beam energies and for different radiation time with the same beam energy.

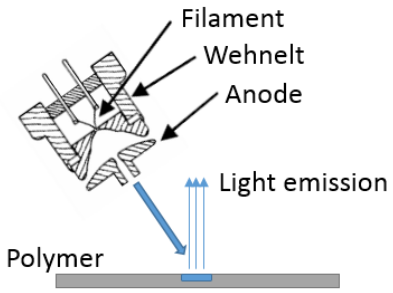

Figure 2-14 Schema of the core of the electron gun. The diameter of the hole at the anode is 1 mm.

Figure 2-15 shows the circuit diagram of the excitation source during the cathodoluminescence measurement. The AC voltage supply provides the energy to heat the filament and emit electrons from the metal by thermionic emission. Hence, the AC voltage or current dominates the number of excited electrons. The DC voltage supply accelerates the electron beams, which dominates the energy of excited electron beams. Hence, the electron beam average energy can be achieved according to the DC voltage. The capacitor is to avoid the burnout of the filament. R_1 and R_2 are to obtain the border of filament voltage. R_3 is to ensure that the Wehnelt of electron beam accelerator is biased negatively in respect to the anode (at ground).

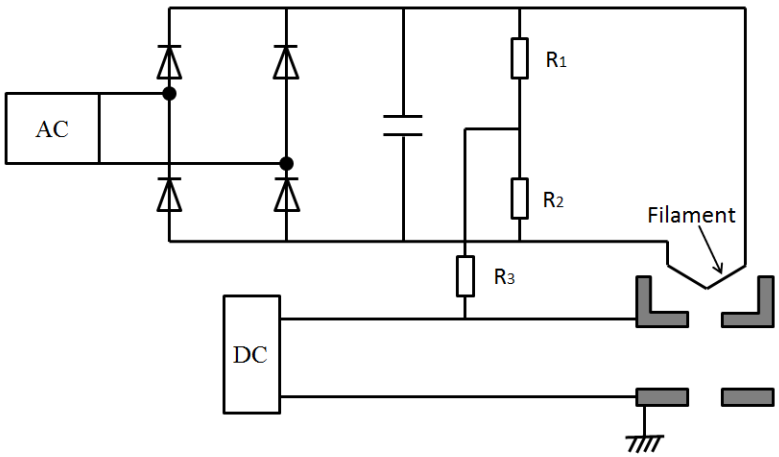

Figure 2-15 Circuit diagram of the excitation source (R_1=72.2Ω, R_2=72.2Ω, R_3=275kΩ.).

During the CL measurement, the AC and DC power supplier as shown in Figure 2-15 are to control the number and energy of the electrons, respectively. Prior to measurement, a calculation curve has been established, with the AC voltage source or the AC current provided by the electron gun. The DC current vs. AC voltage and current are plotted in

Figure 2-16 and Figure 2-17, respectively. From Figure 2-16 and Figure 2-17, the DC current increases very sharply with the increase of the AC current and AC voltage. There appears a threshold at about 1.1 A of AC current. From 1.1 A to 1.9 A, the DC current booms. On the other hand, the DC current increases little with the DC voltage. The counts of electrons are independent from their energy of 2-5 keV. Both the energy and the counts of electrons affect the intensity of light emission. The electron beam energies with several keV are used in the following. Hence, during the CL measurement of materials AC voltage of 120 V and current of 1.68 A are applied on the filament to achieve enough electrons.

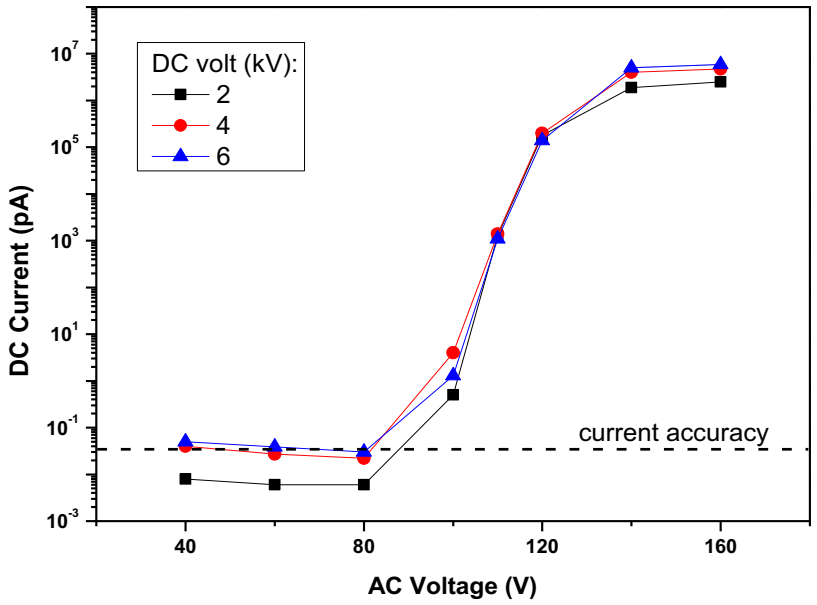

Figure 2-16 DC current vs. AC voltage.

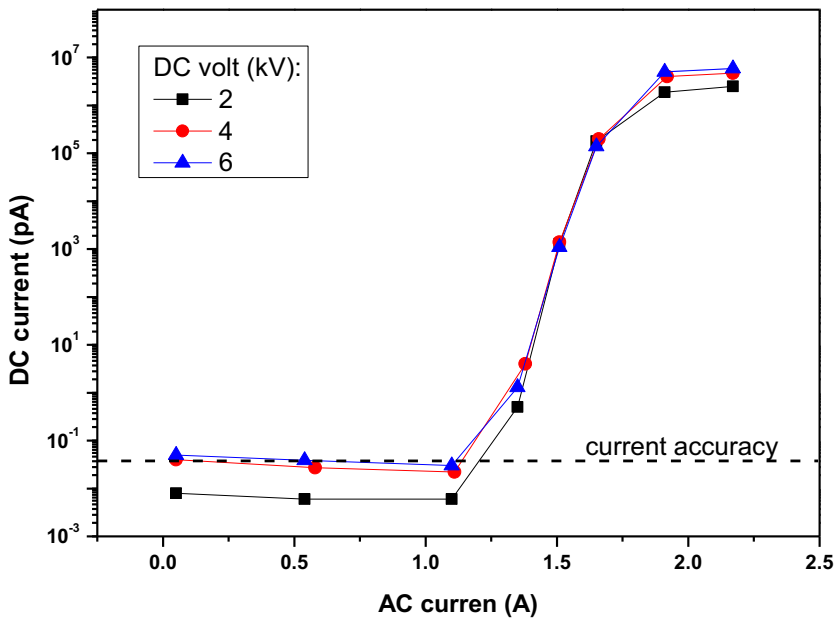

Figure 2-17 DC current vs. AC current.

During the CL measurement, the light emission in the red domain is detected due to incandescence of the filament. Examples of spectra are shown in Figure 2-18. They were obtained on the electrode (anode) in the absence of sample. For an AC voltage of 0.5 kV, it is only due to incandescence and no electrons exit the electron gun. The emission spectrum due to incandescence has been corrected from the CL spectral distribution irradiated with electron beam energy up to 5 keV in the dissertation.

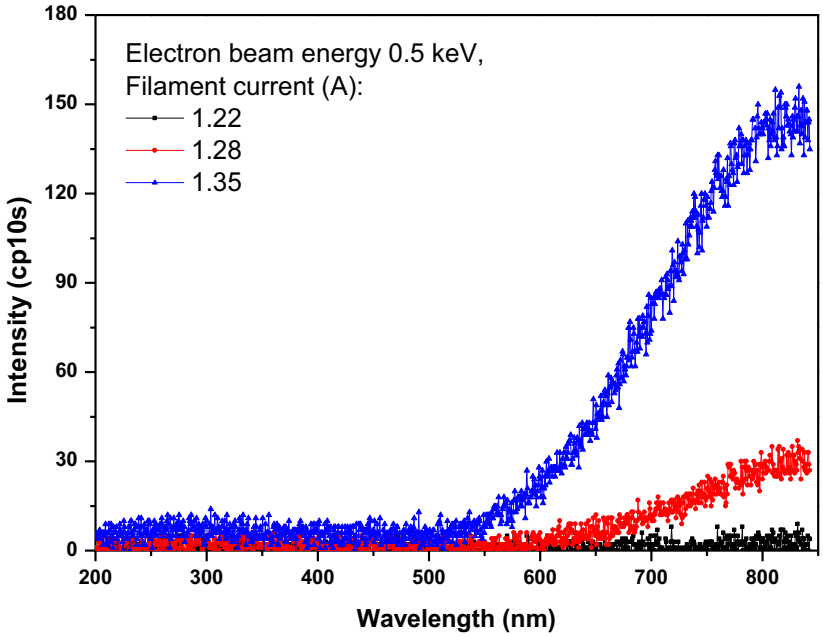

Figure 2-18 Spectra of filament, incandescence emission from the filament is at about 1.28 A.

2.2.2.2 **The photomutiplier detector - photons counting**

The photomultiplier (PM), type of Hamamatsu R943-02, as shown in Figure 2-19, is used to count photons emitted by the material. It allows to observe resolved luminescence in time. It operates at a controlled temperature of -30 °C by a Peltier cooling system. This temperature has the effect of reducing the thermal emission of electrons from the photocathode, which implies extremely low noise (a few counts per second). The spectral response of the photocathode of the photomultiplier does not vary a lot.

The signal transmitted by the PM is pre-amplified and then passes through a set of amplifier/discriminator and is finally transferred to a computer via a card of "fast" acquisition pulse counter from ORTEC. The integration time (dwell time) is variable from micro-seconds to several minutes. We have carried out with our materials, which is generally appropriate for photoluminescence, electroluminescence and cathodoluminescence along with other luminescence measurements.

Figure 2-19 The photomultiplier with cooling system of Hamamatsu R943-02.

2.2.2.3 **The monochromator and CCD camera - spectra acquisition**

The CCD camera (Charge Coupled Device) from Princeton Instruments (LN /CCD-1100-PB) works at a controlled temperature of -110 °C. This camera is associated with an imaging spectrograph (type: Jobin-Yvon CP200) which ranges at 200 lines/mm. It covers a spectral range between 190 nm and 820 nm. The sensitive part of the camera has a resolution of 1100 × 330 pixels, each covering on area of 24 × 24 μm, summing information over the 330 rows. The spectral resolution is 4.5 nanometers. The CCD camera works either in spectral detection mode or in imaging mode. The output of the monochromator extends over the length of the detector at 1100 pixels, i.e. a point per 0.573 nm.

Figure 2-20 CCD camera with cooling system from Princeton Instruments (LN / CCD-1100-PB).

2.2.2.4 **Ultraviolet-visible spectroscopy**

The Ultraviolet-visible spectroscopy is used to measure the absorption or transmission spectroscopy of the samples in the ultraviolet-visible spectral region. In the dissertation, we used Ultraviolet-visible spectrophotometer - HP8452A from Hewlett-Packard as shown in Figure 2-21. It is complementary to fluorescence spectroscopy, which derive from the absorption energy transition from excited state to the ground state. The absorption spectra and emission spectra could be considered together. The UV-vis spectroscopy covers the wavelength range from 190 nm to 820 nm both on absorption and transmission modes.

Figure 2-21 Ultraviolet-visible spectrophotometer, type of HP8452A.

Chapter 3
Electroluminescence in Bi-axially Oriented Polypropylene Thin Films and Relationship to Electrical Degradation

Synopsis

In this chapter, gold-metalized Polypropylene thin films are submitted to DC and AC electric fields and gold-metalized Polyethylene thin films are submitted to AC electric field in conditions where gaseous discharges in ambient are avoided emit light in the visible part of the optical domain. Phase-resolved EL is compared between different electrodes (gold and ITO) with/without filter. Two spectra components of the light with different features have been unraveled being due to the electrode and to the polymer itself.

The EL spectra along with photoluminescence and absorption spectra of polyethylene are compared with that of polyethylene. These excited states provide a route for a series of reactions associated with chemical degradation of the polymer during its ageing under high field. Finally, it will show that similar excited species are generated in Polyolefins pointing towards a generic origin of these excitations in the materials.

3.1 Introduction

The degradation mechanisms of polyolefin such as Polyethylene and Polypropylene under an electrical field are still the matter of debate. There is a reasonable understanding of the deterioration process in the situation where electrical discharges are present: chemical reactions are started following the interaction between the active species of the (partial) discharge –ions, energetic electrons, metastables, UV radiation etc., and the polymer [135]. For some applications under high fields –like capacitors and high voltage cables, the presence of partial discharges is to be absolutely avoided. In spite of that, the use of polymers is limited by their long term withstanding to electrical stress [136].

Different hypotheses have been put forward for explaining the ageing but none has found a firm theoretical and experimental basis. Electro-mechanical or electro-kinetic effects have been envisaged as ageing-driving mechanisms. Among electro-kinetic processes, some involve the relaxation of kinetic energy (hot carriers effects) or potential energy (charge recombination). Both imply the formation of excited states and therefore of light emission. The formation of excited states opening the way to chemical reactions, we investigated in this chapter the way whereby such excited states can be created, considering the field conditions (DC field, AC field with consideration of the phase patterns…) in which the material is excited and trying to infer their nature based on electroluminescence emission spectra.

3.2 Experimental

3.2.1 Samples

Measurements were carried out on Bi-axially Oriented Polypropylene (BOPP) films (see Figure 3-1) of 17.8 µm thickness supplied by KOPAFILM, Germany. These are "hazy" films with rough surfaces to promote impregnation of capacitors. Both surfaces of the films were metallized with semi-transparent layers of gold deposited by cold sputtering (thickness: 30 nm, diameter: 50 mm), or alternatively by sputtering transparent Indium Tin Oxide (ITO) layers (thickness: 110 nm, diameter: 50 mm). Observation of the film surfaces using an optical microscope in reflection and transmission mode clearly shows the differences in roughness and transparency of the two surfaces, respectively, cf. Figure 3-1 and Figure 3-2. In reflection mode and because of the small thickness of the films, it is not easy to distinguish features appearing on the both faces of the films (Figure 3-1 a and b). For this reason, films were gold-metallized providing pictures shown in Figure 3-1 c and d.

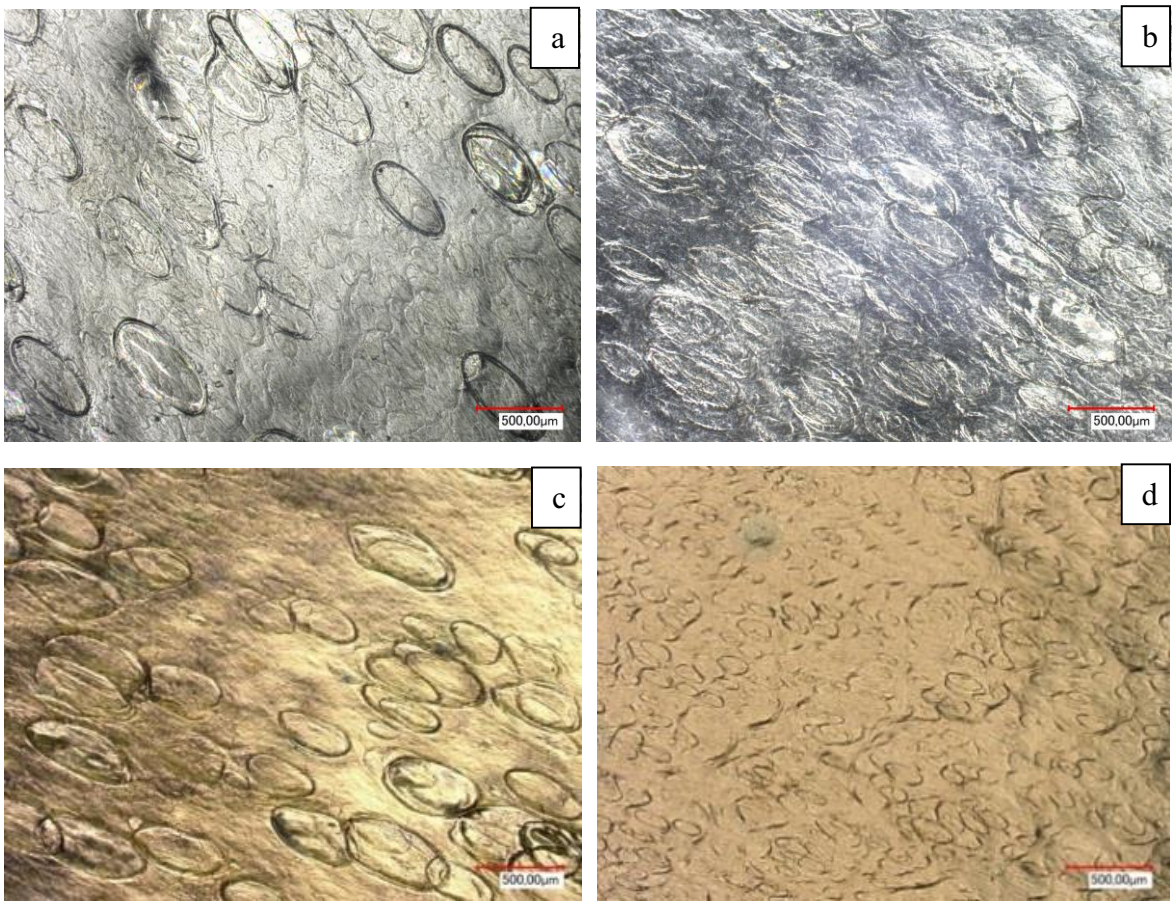

*Figure 3-1 Optical microscopy of **a:** BOPP film from the rough surface, **b:** BOPP film from the smooth surface, **c:** Au-BOPP-Au from the rough surface, and **d:** Au-BOPP-Au from the smooth surface. Reflection mode. The red marks indicate a scale of 500 µm.*

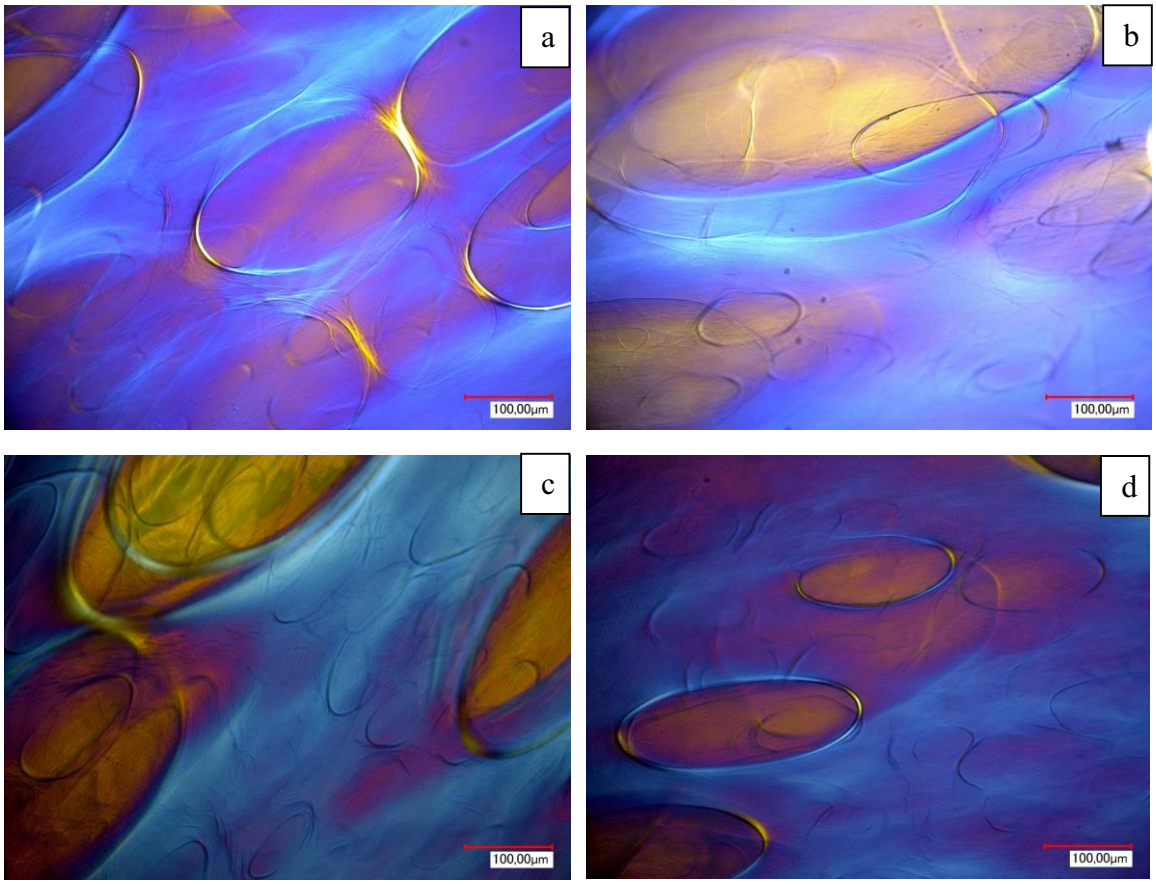

*Figure 3-2 Optical microscopy of **a:** BOPP film from the rough surface, **b:** BOPP film from the smooth surface, **c:** Au-BOPP-Au from the rough surface, and **d:** Au-BOPP-Au from the smooth surface. Transmission mode. The red marks indicate a scale of 100 µm.*

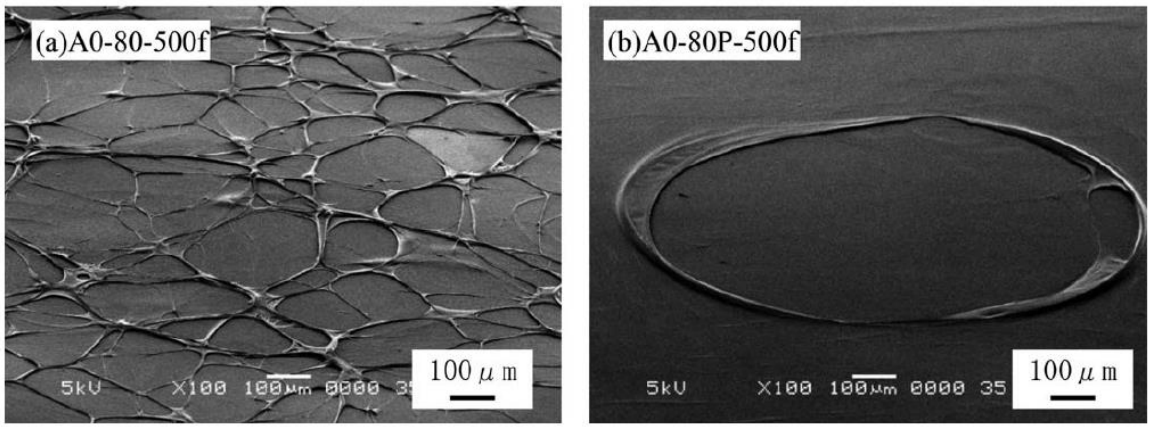

Figure 3-3 SEM image of the surface and the opposite side of BOPP sheet, taken from [137].

It can be seen clearly from Figure 3-1 there are elongated structures of different scale on each surface. Large (500 µm) and small (100 µm) crater-like structures define respectively rough and smooth surfaces. Their transmittance and thickness both vary in different film area as shown in Figure 3-2, which is due to the physical structure of BOPP. A number of studies on the surface morphology of BOPP films with crater-like structure have been

reported since the 1980s [138]. The SEM image of the surface and the opposite side of PP sheet can be seen in Figure 3-3. The depth of these structures formed during the stretching process of BOPP has a good relationship with the chill-roll temperature as shown in Figure 3-4. The shape of the crater is closely related to the shape of crystal grains formed at the surface of BOPP. β crystals with lower density in PP sheet change into α crystals with a higher density after stretching the sheet which contains both α and β crystals. An explanation to the formation of crater-like surface roughness of BOPP films is based on the difference between the densities of α and β crystals – however the complete mechanisms for crater formation are not yet fully elucidated [138]. By the way, the crater structure is possible to design as it is required by controlling the trans-crystal structure in the surface layer of PP sheet. The thickness, roughness, density, and components of BOPP range at different regions of crater because of the crystal grain.

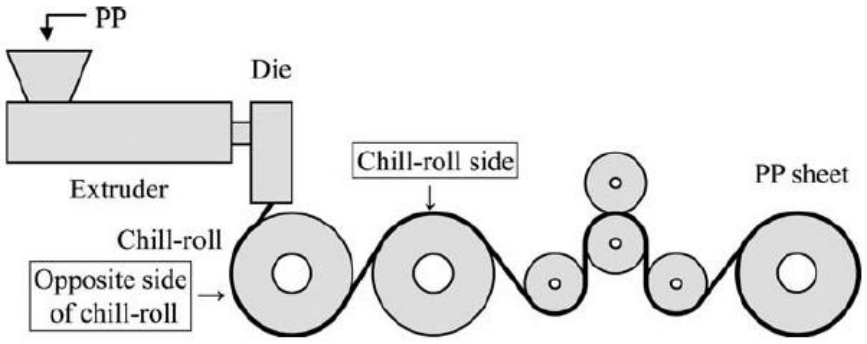

Figure 3-4 Schematic diagram of PP sheet forming machine, taken from [137].

3.2.2 Light analyses set-up

Light emission analyses was performed at room temperature under high vacuum (about $5x10^{-7}$ mbar) in order to avoid partial discharges in the ambient atmosphere. Light detection is carried out by two systems: a cooled photomultiplier (PM) working in photon counting mode for integral light detection, and a grating monochromator (4.5 nm in resolution) coupled to a liquid nitrogen cooled charge coupled device (CCD) camera for spectral analyses which covers the wavelength range from 300 nm to 850 nm. PP films with both sides metallized with semi-transparent gold or ITO layers were sandwiched between two brass electrodes (the rough surface of BOPP films on the top), as shown in Figure 2-8 in chapter 2. The upper electrode has a ring shape in order to allow light emission analyses under AC or DC field up to breakdown. Photoluminescence are also carried out in the same chamber with a xenon lamp coupled to an irradiation monochromator of wavelength from 200 – 700 nm. Transmittance is measured by an ultraviolet-visible spectroscopy as demonstrated in chapter 2.

3.2.3 Stressing

Owing to the high dielectric strength of BOPP, DC electric field values up to 420 kV/mm (DC stress) and 246.4 kV/mm (all the AC fields in the text are crest values) could be applied to the samples.

For DC stress, the voltage was increased by step of 14 kV/mm lasting for 600 seconds up to a level of 280 kV/mm, then by step of 28 kV/mm up to 420 kV/mm (or until breakdown occurs). Charging current and electroluminescence were recorded simultaneously along the process of voltage application.

For AC stress, when recording EL-field characteristics, the voltage was increased in steps of 11.2 kV/mm lasting 40 seconds up to a level of 67.2 kV/mm, then by step of 22.4 kV/mm to 246.4 kV/mm. Also phase-resolved EL patterns were recorded, resolving the phase of the AC signal into 200 segments and integrating the light for 400 seconds, i.e. for 2 seconds per segment.

3.3 Results

3.3.1 Field dependence of EL and time dependence of current under DC stress

Light emission is detected above a field of 300 kV/mm under DC electric stress as shown in Figure 3-5 where electroluminescence (EL) intensity is plotted at different voltage steps within 60 seconds after voltage application. EL exhibits a transient character with a decreasing intensity in a matter of some seconds after voltage application. However, a weak level of light is still detected at the end of these 60 seconds steps. The current as function of time under DC electric stress is plotted in Figure 3-6. The transient current decreases very fast during the first 100 seconds then decreases slowly. The current increases with the increment of the electric field, which is demonstrated more intuitively in Figure 3-7.

The field dependence of the light emission and current averaged over 30 seconds at the end of the voltage steps is shown in Figure 3-7. The current is increasing super-linearly with the increase of the field but the current-voltage characteristic has a slope that tends to decrease from 200 kV/mm and on. It can also be seen that the light starts to level off above 200 kV/mm, but stays near the base line (noise of the photomultiplier) even at 420 kV/mm.

Such behavior is typical of the DC EL detected in polyolefin films. It has been reported in [139] that DC EL in Polyethylene films has a transient character decreasing in a matter of seconds after voltage application and being undetectable after some time. Above a given field, a constant level of light emission is still detected at longer time. A discussion of this effect has been given in [139]. DC EL can be excited upon charge recombination or hot electron effects. However, in the absence of preexisting charges, bipolar recombination needs the crossing of fronts of charges of opposite polarity (charge transit time) and this would appear as a time shift between voltage application and light detection. A decaying transient EL appearing at the moment of voltage application is therefore hardly explainable by recombination mechanisms except in the case where ions accumulated near the electrodes recombine with injected carriers. Experimental evidence of such mechanism has not been given so far. Hot electrons on the other hand are likely to be generated above a sufficiently high field by injection of carriers from the electrodes, leading to a decreasing light emission due to field screening at the electrode as soon as injection is copious.

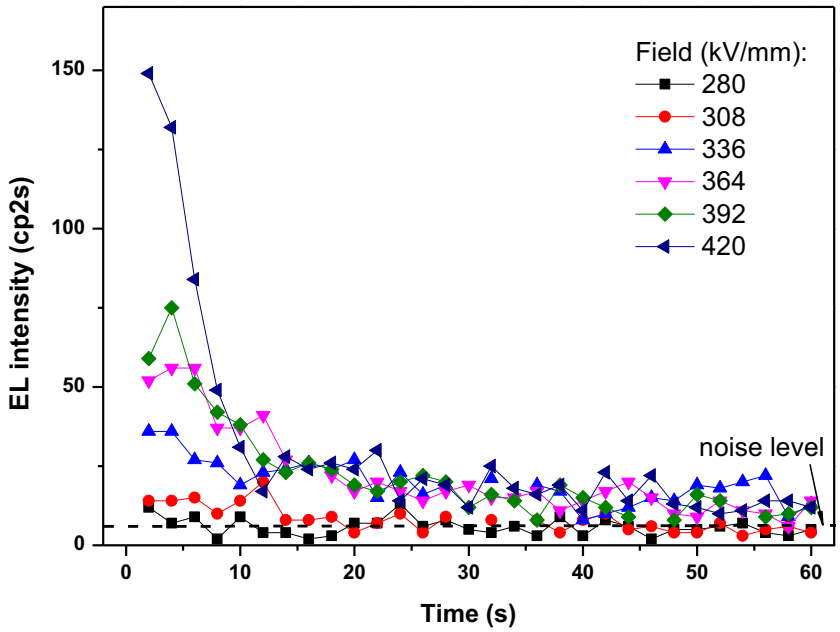

Figure 3-5 Electroluminescence vs. time within 60 seconds after voltage application under different DC fields (gold electrodes; cp2s stands for counts per 2 seconds dwelling time).

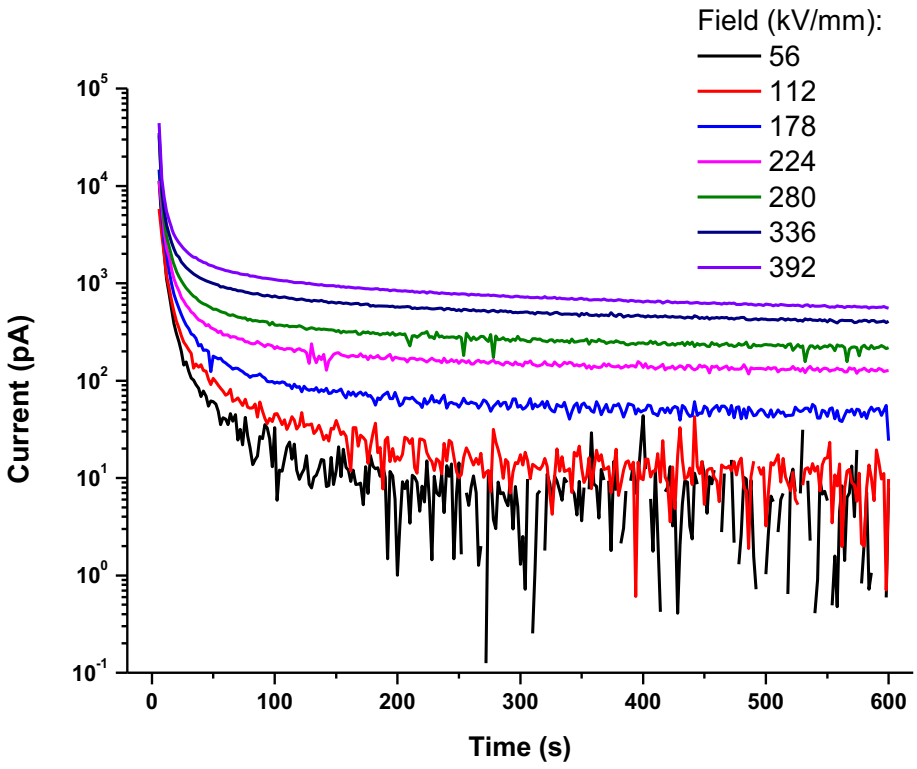

Figure 3-6 Current as function of time during the first 600 seconds. The current is measured on a 20 cm^2 electrode area.

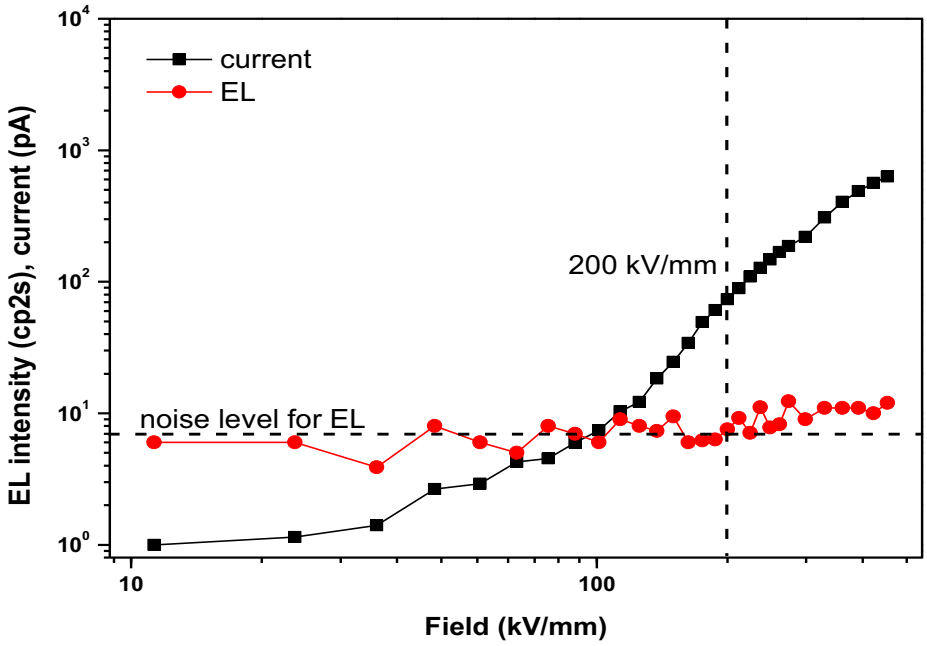

Figure 3-7 Current and electroluminescence vs. field (average values over 30 seconds at the end of each voltage step, gold electrodes).

Under such high electric fields, both mechanisms of charge recombination and hot electron effects could co-exist. The first could dominate at high fields where the field maximum is located in the bulk of the films (see [140]) and where the copious charge injection ends up with recombination domains located near both electrodes: this could lead to a continuous emission of light due to recombination domains continuously fed by the copious injection. On the other hand, hot electrons are particles that attain a kinetic energy accelerated by an electric field. Hot electron effects could dominate short after transient voltage and generates excited states (due for example to the step voltage application) because there is an unbalanced field at this moment.

Further indication in favor of a recombination-dominated electroluminescence at long time is provided by the shape of the current vs. voltage characteristic: the slope is decreasing from the field at which EL is detected and on. An analyses of the current-voltage characteristic of low density Polyethylene (LDPE) reported in [140] has shown that such shape is only reproduced in charge transport modeling when charge recombination is considered. It seems that qualitatively the same mechanism is at play in BOPP. However, the DC EL in BOPP thin films is much fainter and the threshold is much higher than in LDPE. This is maybe due to the higher dielectric strength, a lower current which leads to less probability of excitation, thinner thickness and probable lower contents of chemical defects in BOPP films.

Despite the high field strength, the detected DC-EL in BOPP is extremely faint and could not be further analyzed.

3.3.2 Field dependence and phase-resolved EL under AC stress

The AC-field dependence of the light emission at different frequencies of the AC voltage is shown in Figure 3-8 and Figure 3-9 (a) for two different Au-BOPP-Au samples. The threshold of EL in BOPP films is approximately 10 kV/mm. The EL intensity increases a little with the increase of the frequency. The EL emission is considered due to the injection and recombination of charges. The higher frequency makes it possible that more injection occurs at a certain time. The threshold does not change with the frequency, which is an intrinsic property of the material.

Although the light intensity and the shape of the characteristics vary, there is a common feature in that the curves exhibit a typical upward convex shape in the low field region (that we called “bump” for simplicity), increasing with an increase in frequency as indicated by the arrow in Figure 3-8 and Figure 3-9 (a). This “bump” has already been reported when testing different types of gold metallized polymer films under AC stress [126]. It was also shown that the “bump” in the EL-field characteristics can be suppressed by using a low band path optical filter as shown in Figure 3-9 (b) with a sharp cut-off at 620 nm enabling light detection with “red rejection”. The transmittance of the optical filter is shown as Figure 3-10 with a high light transmission rate of wavelength from 300 nm to 620 nm. It infers that the red component emission contributes the “bump” in the EL intensity vs. field curve.

It is clearly shown that the “bump” of the EL vs. field characteristic is associated with an emission in the red part of the spectrum and can be rejected by the filter in Figure 3-9 (a) and (b). This emission has been attributed in previous studies to the relaxation of Surface Plasmons excited by charge injection/extraction at the interface between gold electrodes and the material [126]. Surface Plasmons excited in metals can radiate light in the red part of the optical spectrum upon decay. A further evidence of the involvement of Surface Plasmons is provided by the fact that the “bump” is not detected when using ITO electrodes as shown in Figure 3-9 (c). Therefore, the comparison of BOPP films with Au or ITO electrodes has been done and plotted in Figure 3-9 (a) and (c). The ITO electrodes appear the same effect of suppressed of the “bump”, which implies that the “bump” is due to red component emission, more precisely due to Surface Plasmons effect of the Au electrodes. We will further address this effect in the chapter 4.

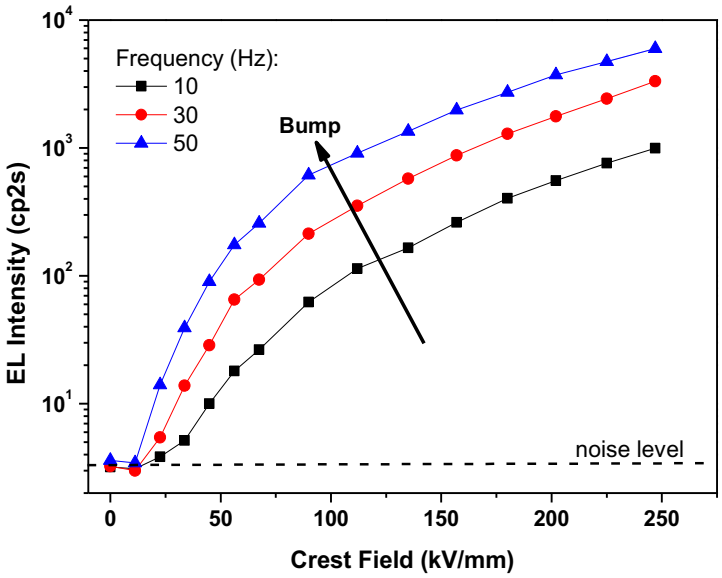

Figure 3-8 EL intensity vs. field characteristics of Au-BOPP-Au under AC stress at different frequencies. The dotted line is the noise level of the measurement. Light intensity is given in photomultiplier counts per 2 seconds.

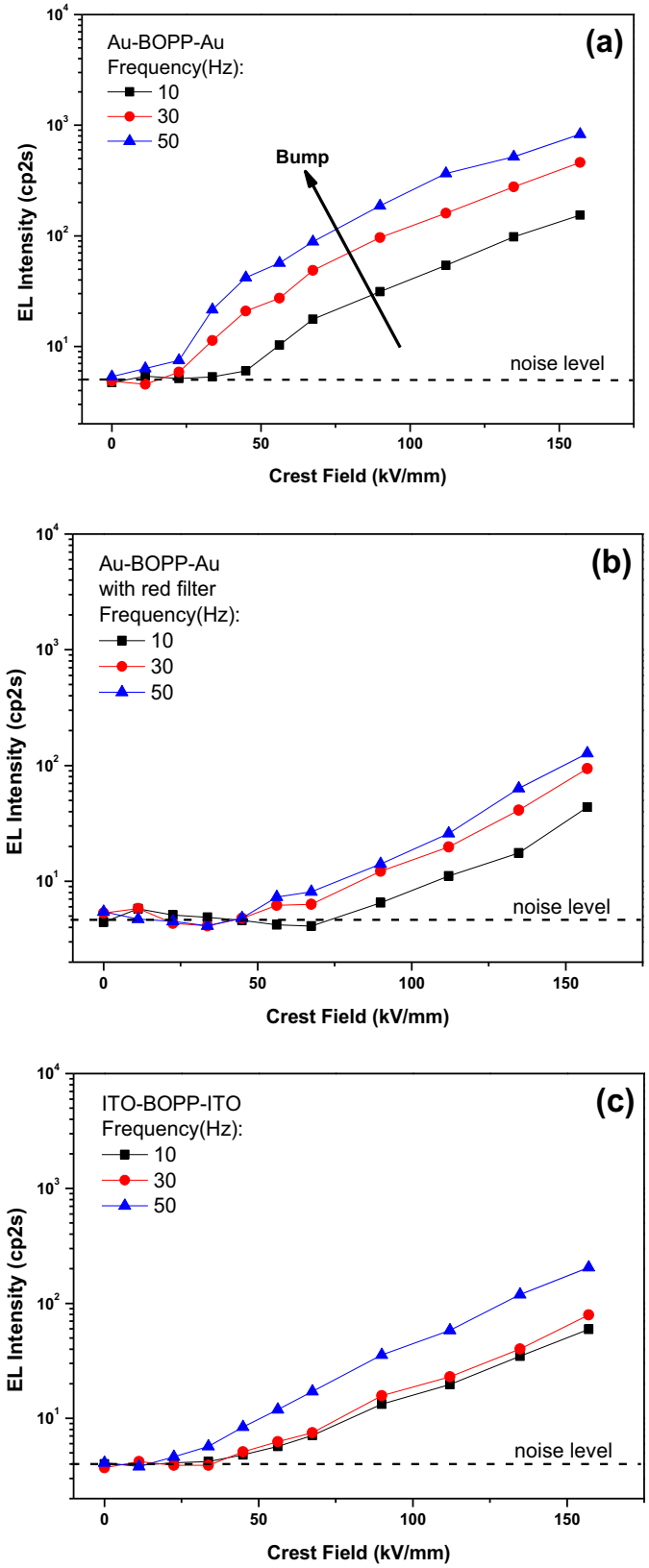

Figure 3-9 EL intensity vs. field characteristics of BOPP films under AC stress at different frequencies. (a) Au-BOPP-Au, (b) Au-BOPP-Au with filter, the light being detected with "red rejection", (c) ITO-BOPP-ITO. *The dotted line is the noise level of the measurement. Light intensity is given in photomultiplier counts per 2 seconds. The same sample was used for characteristics (a) and (b).*

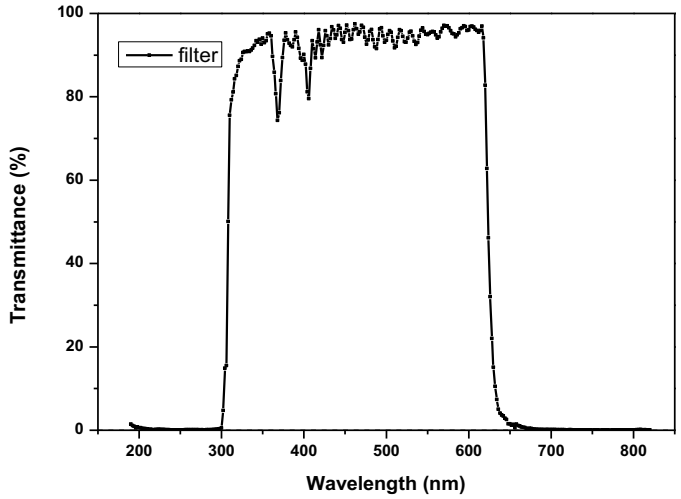

Figure 3-10 Transmittance of the filter.

In order to investigate the relationship of EL intensity and curve with voltage waveform, we carried out phase-resolved EL measurements. The AC phase-resolved EL is reported in Figure 3-11 for the same conditions as in Figure 3-9. Figure 3-11a shows a significant shift of the EL crest from 12.6 (112 kV/mm) to 13.2 (157 kV/mm) which is not detected when using a red filter, or when using ITO electrodes, i.e. when rejecting the emission due to Surface Plasmons effects. This further substantiates the existence of two contributions to the light emission with specific field dependency. Another striking fact is the dissymmetry in the amplitude of the EL peaks detected under positive and negative voltages when using the red filters or the ITO electrodes. This might also be related to the non-symmetric topology of samples surface for example. However, no such relation to the roughness could be shown. In fact, electroluminescence measurements on similar samples often revealed some discrepancies when focusing on the light intensity during each half cycle and we will not comment further this observation.

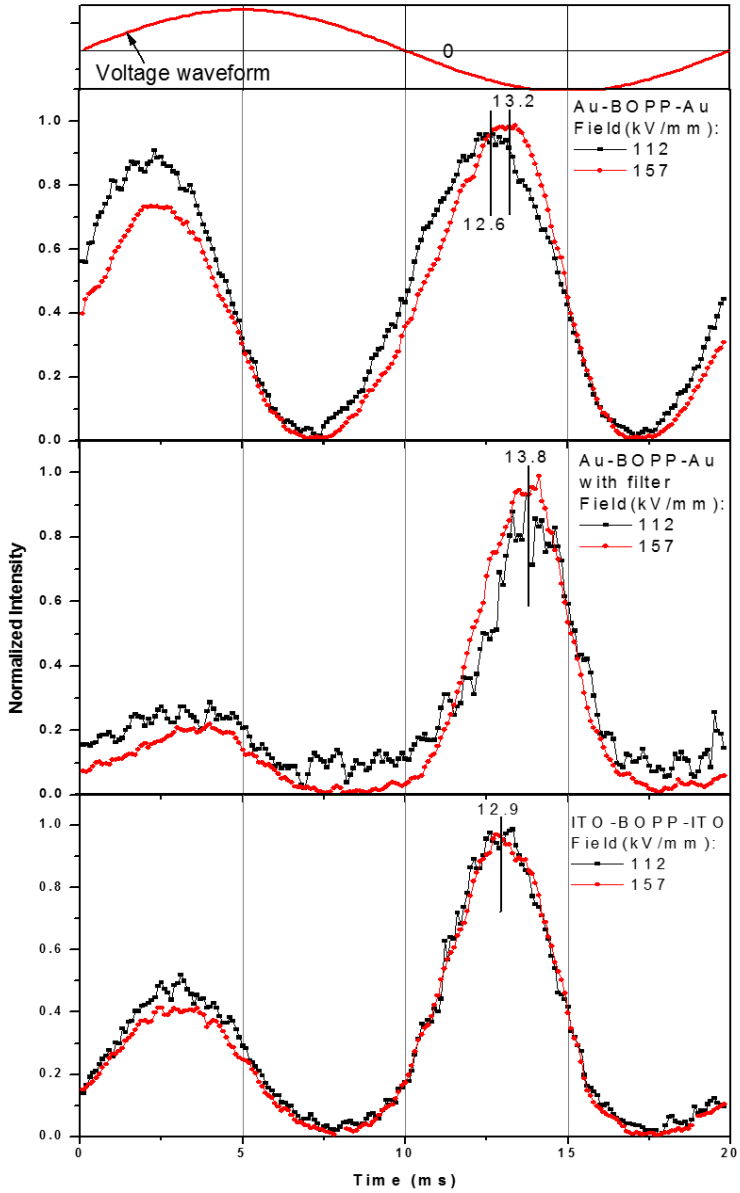

Figure 3-11 Phase-resolved EL of BOPP films under 50 Hz AC stress. Light intensity is normalized to 1 in the second half period. The same sample was used for Au-BOPP-Au with or without filter.

3.3.3 AC EL Spectral analyses

The EL is measured under a relatively high electric field, especially when acquiring spectra. Eventually breakdown occurs during EL recording; the fracture pattern was analyzed in some instances. For example, in BOPP films, the breakdown area is burnt and carbonized as shown in Figure 3-12. From numerous breakdown samples, we consider the edge of crater-like structure is the weakest area for electrical breakdown. The chemical structure is a reason for electrical breakdown.

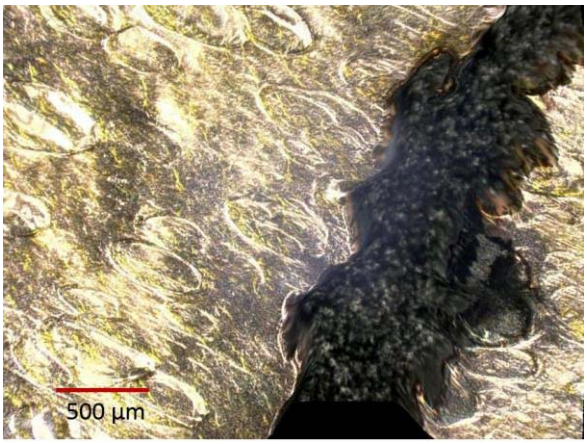

Figure 3-12 Optical microscopy of Au-BOPP-Au film after breakdown. Reflection mode. The width of the breakdown area is about 500µm.

Spectral analyses was not possible under DC stress due to the very low level of light. It has been realized under AC stress only. The emission spectra of Au-BOPP-Au samples are shown in Figure 3-13. The spectra in Figure 3-13 (b) are after eliminating the red emission at 56 kV/mm. The emission spectrum can be analyzed as composed of two contributions with different field dependencies: a contribution in the red part of the spectrum, centered at 800 nm and dominating the emission spectrum at low fields, and another one centered at about 570-580 nm, dominating the emission spectrum at high fields. The existence of the so-called "red component" has been reported in our different investigations of EL in metallized polymer films and was attributed to an interfacial effect involving Surface Plasmons [103, 126]. This will be discussed in detail in chapter 4. The peak of spectra at 570-580 nm is the bulk emission from the BOPP films.

The UV-vis transmittance spectra of BOPP films and BOPP films with gold electrodes are shown in Figure 3-14. BOPP mainly absorbs Ultraviolet light of wavelength lower than 250 nm and absorb little light in visible domain. Note that there exists amount of reflection of light on the surface of the BOPP films during the transmittance testing.

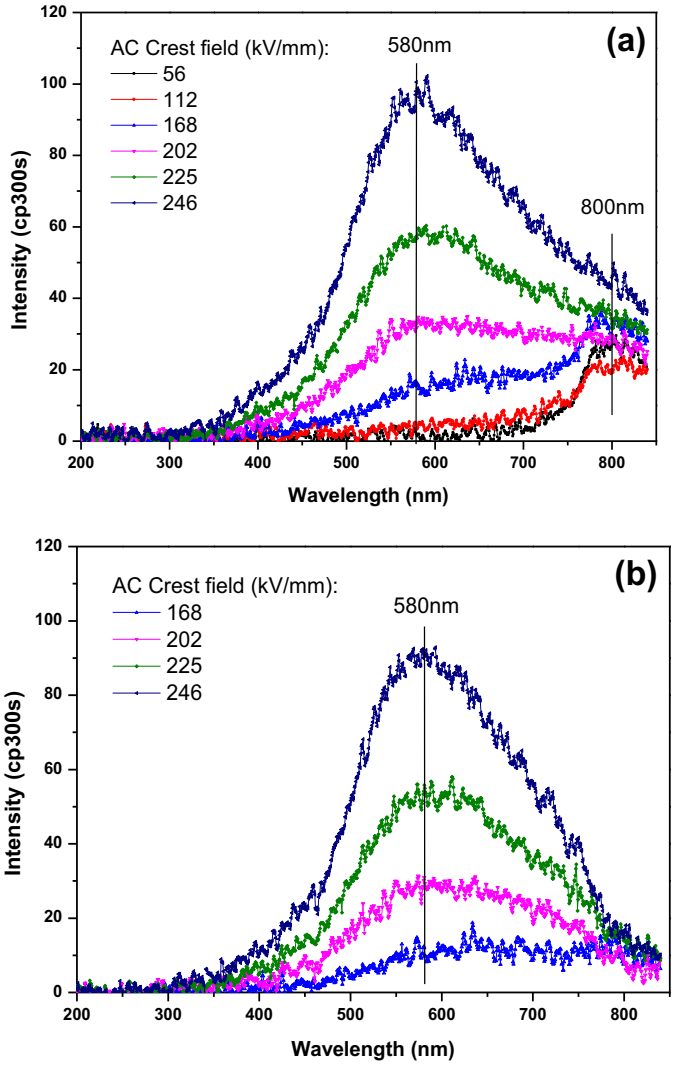

Figure 3-13 EL spectra of BOPP films. (a): Rough spectra with gold electrodes under 50Hz AC stress at different fields; (b): same as (a) after removing the red component. Spectra have been integrated for integrated for 300s, hence the units for intensity.

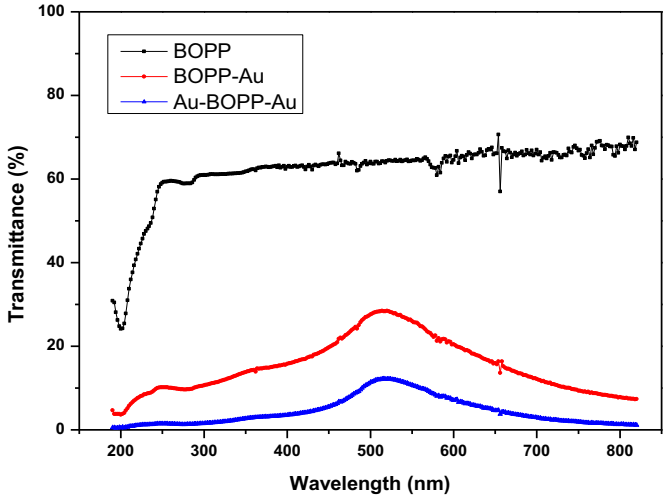

Figure 3-14 Transmittance of PP film and with one or two layers of gold electrode, of which the light pathway is through from one gold layer to another one.

3.4 Discussion

3.4.1 EL characteristics and phase-resolved EL

The EL intensity of BOPP films under DC stress is very faint because the high dielectric strength makes the charge injection very low then very low current go through the materials. However, under AC stress the EL intensity is relative high because the alternative current makes more charge injection to the materials. The EL intensity increases a little with the increase of the frequency. It is interesting that with the increase of the electric field the EL increases nonlinearly with a threshold at a certain electric field of approximately 10 kV/mm. The threshold of EL vs. field is an intrinsic property of the material.

As for the phase-resolved EL, the phase advance will decrease along with the increase of the electric field. The crest of EL intensity is the crest of recombination of charge carriers. The injected electrons combine with the residual holes injected during last period, which makes the crest of recombination in advance of applied voltage. The electrode is another factor that affects the advance of the phase of EL under AC stress. The red component emission contributes relative strong intensity at low AC electric field. Hence, the EL intensity is a sum of both light from material itself and from the red component emission. The red component emission makes the EL crest in phase-resolved EL advanced due to its relative strong intensity at low field. The analyses will be demonstrated in detail in Polyethylene Naphthalate in chapter 4.

3.4.2 EL and PL Spectral analyses

3.4.2.1 Polypropylene

EL emission spectrum can be analyzed as composed of two contributions with different field dependences: a contribution in red domain of the spectrum, centered at 750-800 nm, dominating at low field, and another one centered at about 570-580 nm, dominating at relative high field. The red component emission is due to Surface Plasmons or interface states, the intensity of which varies from sample to sample. They have the same wavelength crest at about 570-580 nm and the same spectra shape except the red emission component, implying they derive from the same or similar luminescent mechanism.

The origin of the main component of the EL emission spectrum at 570-580 nm is worth discussing. The BOPP films contain antioxidant and some other additives and their presence could play a role in the emission process.

One straightforward experiment to check for possible contributions in the emission is to record the UV-induced luminescence spectrum. The UV-absorption spectra, photo-induced fluorescence emission and photo-induced phosphorescence emission of BOPP films are shown in Figure 3-15 and Figure 3-16. The UV-induced fluorescence (FL) spectrum is excited at 230 nm and taken at room temperature. The UV-induced phosphorescence (PHL)

spectrum is excited at 250 nm at liquid nitrogen temperature and is recorded during the natural decay of the phosphorescence (i.e. UV excitation beam off). The phosphorescence of polyolefin quench with the existence of oxygen molecules at room temperature, therefore cannot be detected during light emission analyses. Hence, the EL in BOPP films is due to chromophores not the same with fluorescence and phosphorescence in optical excitations.

Figure 3-16 (a) has shown the UV-absorption spectrum of a film with an absorption maximum at 200 nm and two absorption shoulders at 230 nm and 280 nm. Absorptions at 200 nm and 230 nm are typical of $\pi \rightarrow \pi^*$ transitions in C=C double bonds that are present in polyolefin films through the phenyl ring of Irganox as well as unsaturations of the polyolefin chain. The absorption at 280 nm is rather due to the $n \rightarrow \pi^*$ transition in carbonyl compounds. Figure 3-16 (b) shows the fluorescence emission (transition from the first excited singlet down to the singlet ground state of the excited species) which is at maximum when excited at 230 nm and 280 nm (corresponding to the absorption maxima). Such kind of photo-induced emission is typical of fluorescence with a residual oxidation [38]. Figure 3-16 (c) shows the phosphorescence peak excited at 250 nm (transition from the first excited triplet down to the singlet ground state of the excited species - a forbidden transition associated with a long life time > ms). It exhibits a maximum at 472 nm and two shoulders at 440 nm and 500 nm which have been associated with the presence of unsaturated carbonyls of the di-enone type [38]. Anyway in the context of our discussion, it appears that the EL and CL spectra are not organized around the same components as those revealed in photoluminescence, except may be for the shoulder at 328 nm visible in the CL spectra. A contribution of the natural fluorescence cannot be ruled out.

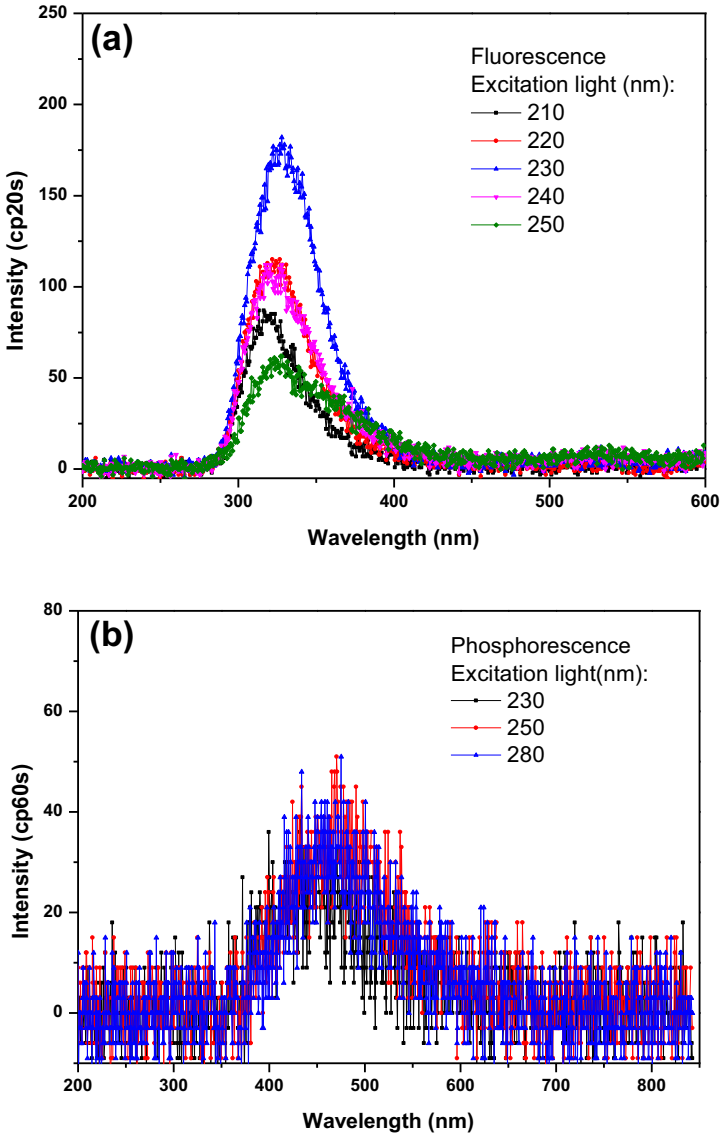

Figure 3-15 (a) photo-induced fluorescence emission with maximum excitation light of wavelength at 230 nm at room temperature and (b) photo-induced phosphorescence emission with maximum excitation light of wavelength at 250 nm at liquid nitrogen temperature of BOPP films.

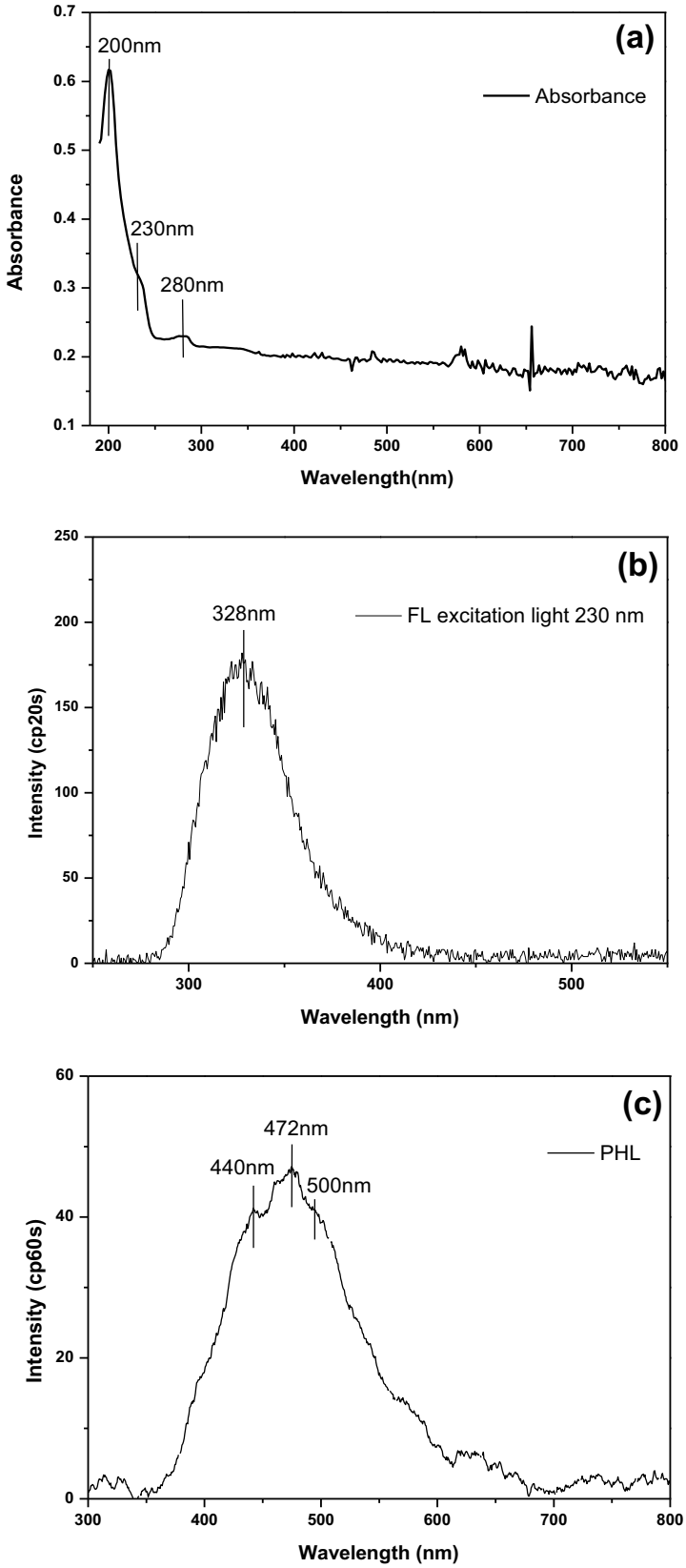

Figure 3-16 (a) UV-absorption spectrum of BOPP measured at room temperature, (b) fluorescence spectra from Figure 3-15 and (c) phosphorescence spectra from Figure 3-15 of BOPP films.

3.4.2.2 **Polypropylene and Polyethylene**

Very close similarities exist between the emission spectra of PP and those obtained on Polyethylene (PE). The LDPE samples exhibit photoluminescence spectra with two maximum excitation light at 230 nm and 280 nm as shown in the two intersections of three white lines in Figure 3-17, which has the same peaks with the BOPP samples in Figure 3-16. The maximum emission spectra is at 328 nm. PE and PP have very close photo-physical properties with photo-induced phosphorescence (transition from excited triplet to singlet ground state in unsaturated species responsible for the emission –see [38]) emission spectra peaking at about 450 nm. In addition, these materials exhibit similar recombination-induced spectra peaking at 505 nm [38] that correspond to the lowest lying triplet states involved in phosphorescence emission.

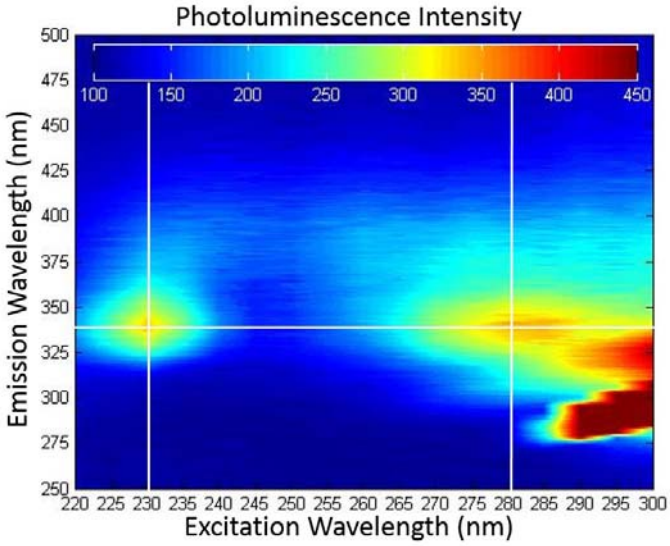

Figure 3-17 Photoluminescence spectra distribution of LDPE films under different excitation light. The emission wavelength vs. excitation wavelength is plotted. The colors from blue to red mean the photoluminescence intensity from low to high.

The EL spectra of LDPE film and XLPE film are measured and plotted in Figure 3-18 and Figure 3-19, respectively. Owing to the similarity between the two polymers, the 570-580 nm EL component in PP could be attributed to the same origin as for PE.

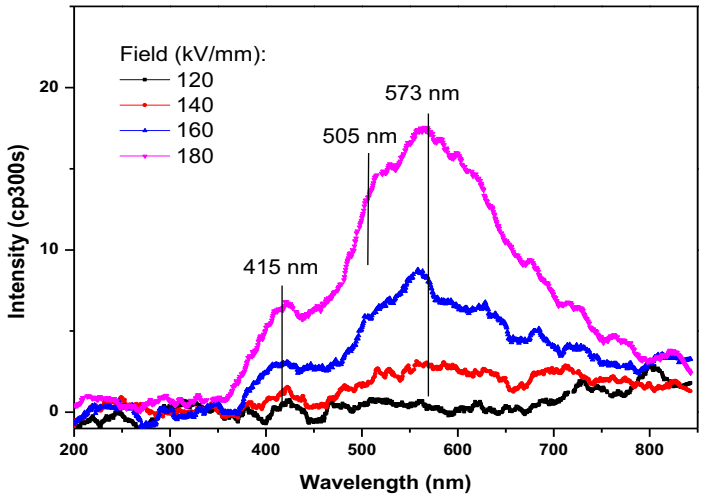

Figure 3-18 EL spectra of LDPE films under 50 Hz AC stress.

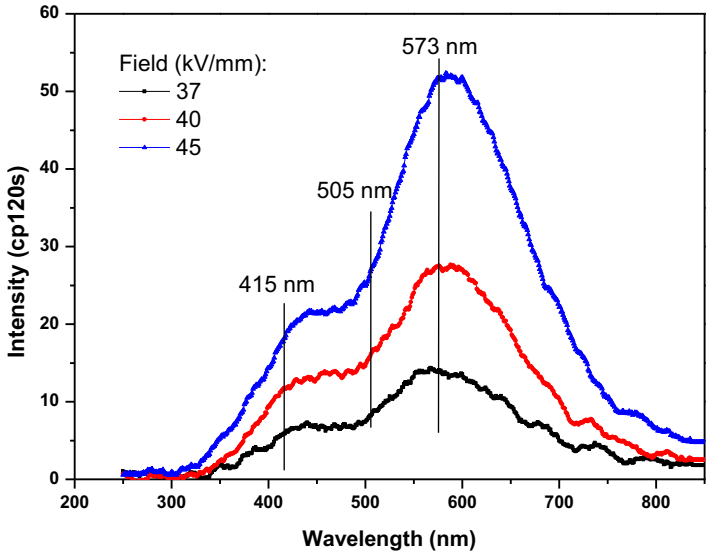

Figure 3-19 EL spectra of XLPE films under 50 Hz AC stress.

Polyethylene and Polypropylene are both polyolefins with similar chemical structures. It can be seen from the EL spectra that they are organized around the same components, although with less apparent contributing shoulders in EL likely due to the low level of light. The fluorescence and phosphorescence emission peak at 328 nm (excitation wavelength 230 nm) and 472 nm (excitation wavelength 250 nm), which is similar in PP and points towards generic species common to both materials as being responsible for the photo-induced emission. It can be seen that they are identically pointing towards a generic excited state in both materials upon high field material degradation. The electroluminescence features in PP and PE reveal their excitation transport and relaxation processes under electric field. PE and PP are both polyolefin, with similar Carbon chain bonds, maybe following the similar degradation route.

Under electric stress, excitons form and release with light emission. An exciton is a bound state of an electron and an electron hole which are attracted to each other by the electrostatic Coulomb force. It is an elementary excitation of materials that can transport energy under electric field. An electron is excited from the valance band into the conduction band, leaving behind a positively charged electron hole. The decay of excitons, i.e. the recombination of the electron and hole, is accompanied by light emission with corresponding energy.

The formation of excitons and subsequent relaxation through a dissociative pathway is one of the likely mechanisms for EL in PP and PE. Indeed, the fate of excitons formed upon recombination of electron/hole pairs has been investigated in Polyethylene materials using density functional calculations and ab-initio molecular dynamics simulations. Two situations were investigated where excitons are self-trapped along a chain [141, 142] or trapped at chemical defects [142]. The relaxation can occur following different pathways depending on the case. When the exciton is trapped on a chemical defect, the relaxation pathway depends of the nature of the chemical defect leading to trapping of the charges, non-radiative recombination or homolitic bond-breaking. This is of course the last process that is relevant for damage. When the exciton is self-trapped along a chain, C-H bonds breaking is promoted according to a recent calculation [143]. With the opening of a chemical route, by-products could be produced in excited states and be responsible for emission in a wavelength range that is not typical of the initial chemistry of the polymer. The electroluminescence features could reveal such degradation process.

3.5 Conclusion

Polyolefin thin films emit light when submitted to DC (weak light emission) or AC (stronger light emission) under uniform field configuration. The electroluminescence versus field characteristic together with the spectral analyses confirms the existence of two contributing mechanisms in the emission process. One is due to an interfacial effect involving Surface Plasmons excited at the metallic electrode upon charge injection/extraction. It is best identified at low field and high AC frequency, with the appearance of a bump in the EL-filed plot that disappears with red censoring.

The other one is related to excited states (excitons) of the polymer promoted upon charge recombination or hot electron effects. Interestingly, we have shown the electroluminescence spectra of BOPP and PE are organized along the same components, indicating the same excited species are at the origin of the emission in both materials. The excitonic states generated under high field in polyolefins (PE and PP) seem to have a common origin which is likely linked with the macromolecular backbone.

Chapter 4
DC and AC Electroluminescence Spectra of Polyethylene Naphthalte: Impact of the Nature of Electrodes

Synopsis

The aim of this chapter is to analyze the impact of the nature of different electrodes on electroluminescence features through EL field characteristics, spectral analyses, and phase angle analyses under AC field. In this way, the origin of the red emission should be unraveled. Polyethylene 2, 6-Naphthalte (PEN, an aromatic polyester), is particularly suitable for understanding electroluminescence in polymeric dielectrics, not only because it gives a high performance with physical, thermal, and chemical characteristics but also EL intensity of PEN under AC and DC field is relatively strong.

One of the unresolved questions in the EL spectrum of insulating materials in general is the occurrence of red emissions under AC electric field when using e.g. silver or gold as metal electrodes. Surface Plasmons (SPs) effects and/or charge recombination on surface states have both been advocated as possible origins for such emissions. In this contribution, EL of 25µm Polyethylene 2, 6-Naphthalte (PEN) films are investigated using Indium Tin Oxide (ITO) and gold (Au) electrodes separately, the singularity of ITO being that it does not exhibit the SPs effects characteristic of noble metals (e.g. gold) in the visible domain. EL spectra and EL-field characteristics were recorded under DC and AC fields, as well as phase-resolved EL patterns. Emission spectra from ITO-PEN-ITO do not reveal the red emission contrary to that of Au-PEN-Au. Results are discussed regarding both the origin of the emissions, and the consequences that SPs-mediated emissions may have on EL features such as EL-field characteristics, spectra, and phase patterns.

4.1 Introduction

The electroluminescence (EL) of insulating polymers is an exciting field of research because it gives insight into electrical ageing and breakdown processes. Various physical and chemical mechanisms have been involved in the aging of electrical insulations under DC and AC stress [4, 5]. Electroluminescence (EL) is a phenomenon involving physical processes such as charge injection, extraction, and transportation, but also chemical reaction through excited states. Electric fields can produce excited or ionized states, some of which have a non-zero probability for light emission during their relaxation and for chemical reaction in their excited states. Hence, on one hand, EL can be a probe of charge excitation and recombination processes, on the other hand, it may provide information on the nature of defects and luminescent sources. Because interfacial electronic states are very important in charge transfer at the electrode-dielectric interface, it should impact on the EL features, especially under AC stress. Therefore, EL can also gather information and be used to probe the physical/chemical processes occurring at the metal-dielectric interface.

Furthermore, electromagnetic properties at metal-dielectric interface undergo an increasing interest in a booming area of sciences called “plasmonics”. Surface Plasmons (SPs, or more exactly Surface Plasmon Polaritons, SPPs) are electro-magnetic excitations that propagate along the interface between a metal and a dielectric. It can be excited by a supply of energy, either photon or electron irradiation on a rough (not perfectly smooth) surface [144]. Therefore, SPs effect can be expected at a dielectric/metal interface submitted to an electric field. For these reasons, electroluminescence phenomena observed in the red region (600-850nm) in insulating polymers with noble metal electrodes (Au, Ag) have been attributed to SP emission [126]. SP processes should not be present in indium tin oxide (ITO), a transparent conducting oxide used as electrode in electroluminescent devices.

4.2 Experimental

All the measurements were performed on PEN films of 25 µm thickness supplied by Dupont (Dupont Teijin Films Teonex® Q51). These PEN films were metallized with ITO electrodes (thickness: 200 nm, diameter: 50 mm) or Au electrodes (thickness: 30 nm, diameter: 50 mm) by sputtering. Samples, sandwich structures were designated as Au-PEN-Au and ITO-PEN-ITO.

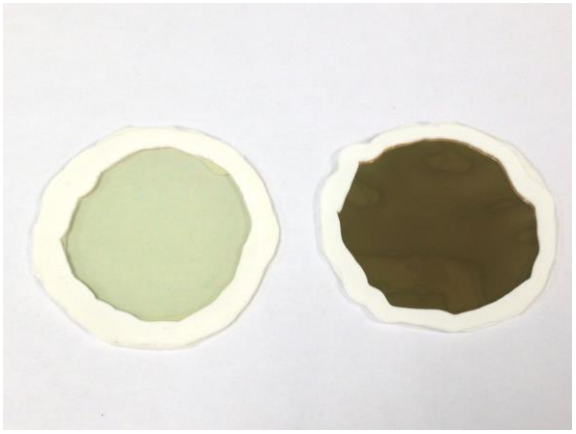

Figure 4-1 PEN samples metalized with ITO (left) and Au (right) electrodes.

EL experiments were performed at room temperature, under high vacuum (10^{-7} mbar) in order to avoid gaseous discharges. Light detection is carried out by two systems: a cooled photomultiplier (PM) working in photon counting mode for integral light detection, and a grating monochromator (4.5 nm in resolution) coupled to a liquid nitrogen cooled charge coupled device (CCD) camera for spectral analyses which covered the wavelength from 200 nm to 850 nm.

For field-dependence EL under DC stress, the field was increased in steps of 20 kV/mm lasting for 10 min from 20 kV/mm to 300 kV/mm. For field-dependence EL of Au-PEN-Au and ITO-PEN-ITO under AC stress, the field was increased in steps of 16 kV/mm lasting for 80 seconds from 16 kV/mm to 272 kV/mm under frequency from 1 Hz to 60 Hz. For field-dependence EL of Au-PEN-Au with filter under AC stress, the field was increased in steps of 8 kV/mm lasting for 80 seconds from 8 kV/mm to 80 kV/mm, then in steps of 16 kV/mm lasting for 80 seconds from 80 kV/mm to 256 kV/mm under frequency from 1 Hz to 60 Hz.

For phase-resolved EL, the measurements were carried out at field of 272 kV/mm under frequency from 1 Hz to 50 Hz; and at frequency of 40 Hz under field from 160 kV/mm to 272 kV/mm.

4.3 Results

4.3.1 Field dependence of EL under DC and AC stress

In Figure 4-2, the EL and current vs. field characteristics of PEN under DC stress are plotted for different electrodes. EL vs. field of PEN under AC stress at different frequencies is also shown in Figure 4-3. Under DC stress, there is no significant difference between two kinds of electrodes. The EL thresholds are both at about 160 kV/mm (though slightly lower for Au-PEN-Au). However, under AC stress, it can be seen clearly that there is an embossment of the characteristic for the Au-PEN-Au sample in the low field region, increasing with an increase in frequency, which does not exist in the ITO-PEN-ITO. It was shown previously that this embossment can be eliminated from the EL spectrum of several polymers with Au electrodes using a cut-off optical filter in the red part of the spectrum [126]. Figure 4-3 (c) shows the characteristics obtained when using a low pass filter cutting at 620 nm (cf. Chap. 2). The UV-visible transmittance spectra of the filter and of a PEN film are shown in Figure 4-4. Clearly the embossment is removed and the characteristics have the same shape as that obtain with ITO electrodes. The impact of red-censoring EL on AU-BOPP-Au or of changing from Au to ITO electrodes presented in the previous chapter in Figure 3-9 goes in the same direction and the effects are even much clearer than with PEN, presumably because PEN has more efficient emission from the material. These features constitute a first indication of the existence of several contributing processes, with distinct field dependencies, to the EL of insulating polymers.

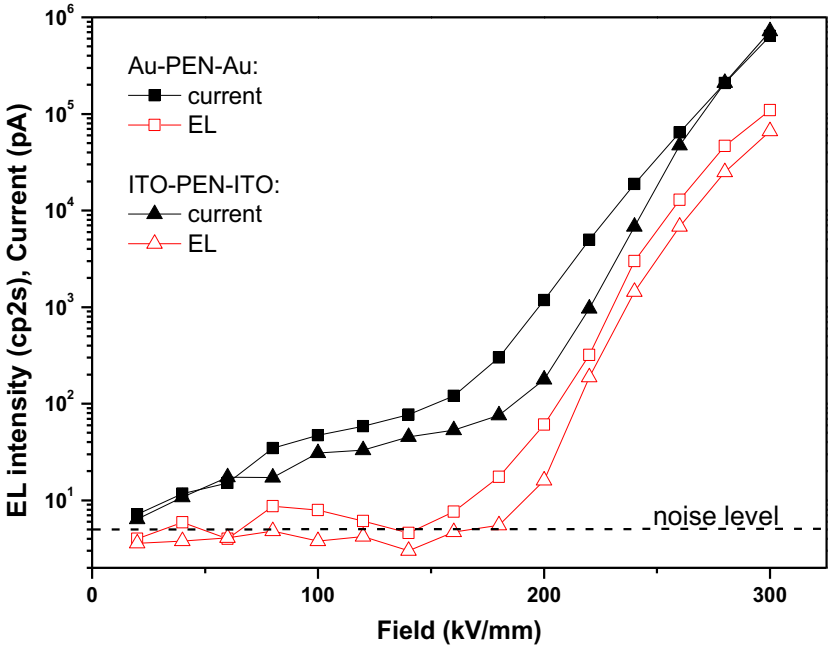

Figure 4-2 Electroluminescence intensity and current vs. field characteristics of Au-PEN-Au and ITO-PEN-ITO under DC stress. The dotted line is EL noise level. "cp2s" stands for counts per 2 seconds. Data are taken after 10 min under constant voltage.

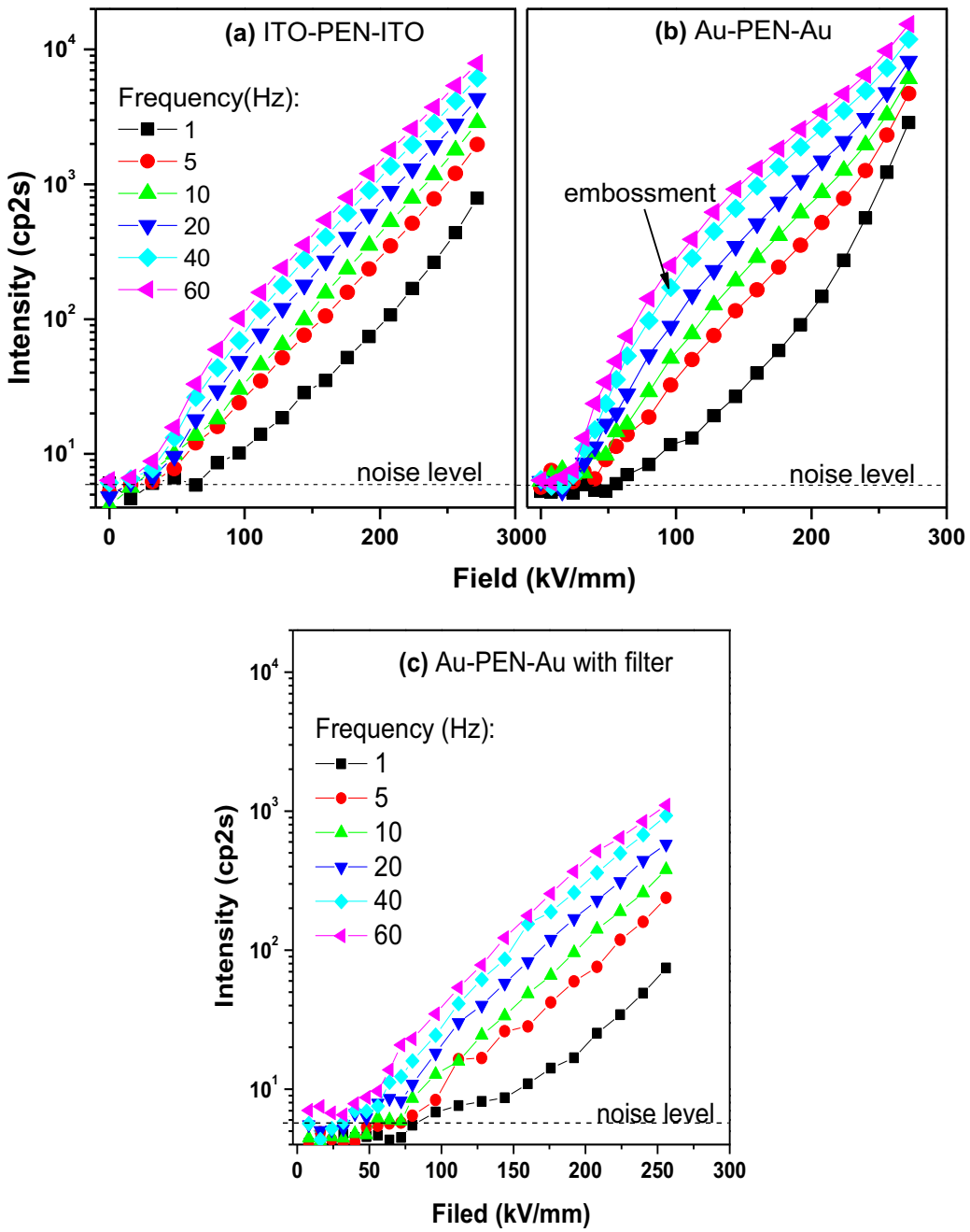

Figure 4-3 Electroluminescence of (a) ITO-PEN-ITO, (b) Au-PEN-Au, and (c) Au-PEN-Au with filter, under AC stress. The dotted line is EL noise level. "cp2s" stands for counts per 2 seconds. Data are taken as an average within 80 seconds under different electric field.

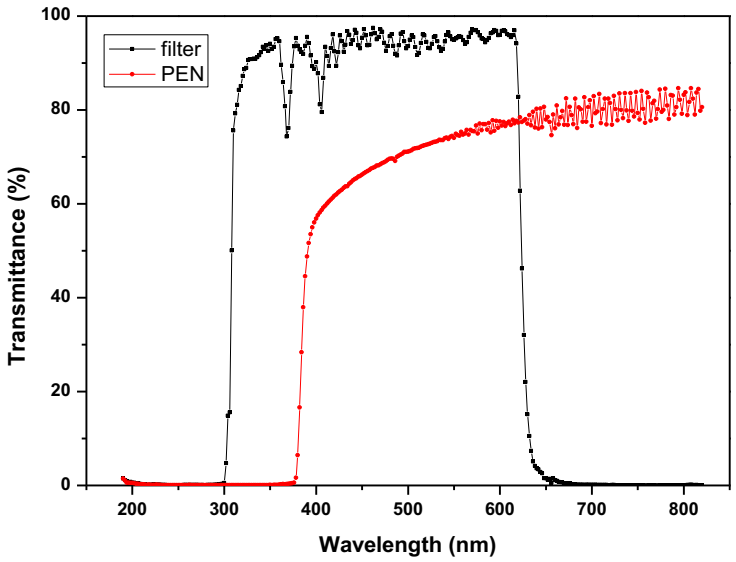

Figure 4-4 Transmittance spectra of filter and PEN.

4.3.2 Phase-resolved EL under AC stress

Interpretation of the EL dependence on voltage waveform can give us information on charge injection and extraction as well as transport and recombination. During the phase-resolved EL measurements, using a cooled photomultiplier to collect the optical signals, the counting dwell time was set suitable for phase-resolved EL measurements with 200 data points in one cycle under AC voltage waveform, and an integration time of 2 seconds per memory channel. The noise level is the same as in Figure 4-2 and Figure 4-3, and is negligible for these measuring conditions under AC.

The frequency-dependence phase-resolved EL is shown in Figure 4-5. There exists an advance of the EL crest comparing to the voltage crest. However, the advancement does not vary with the applied frequency. However, for the field-dependency phase-resolved EL, Figure 4-6 shows the phase-resolved EL patterns of PEN with the two kinds of electrodes under study for sinusoidal waveform voltage. The advancement decreases with the increment of the field.

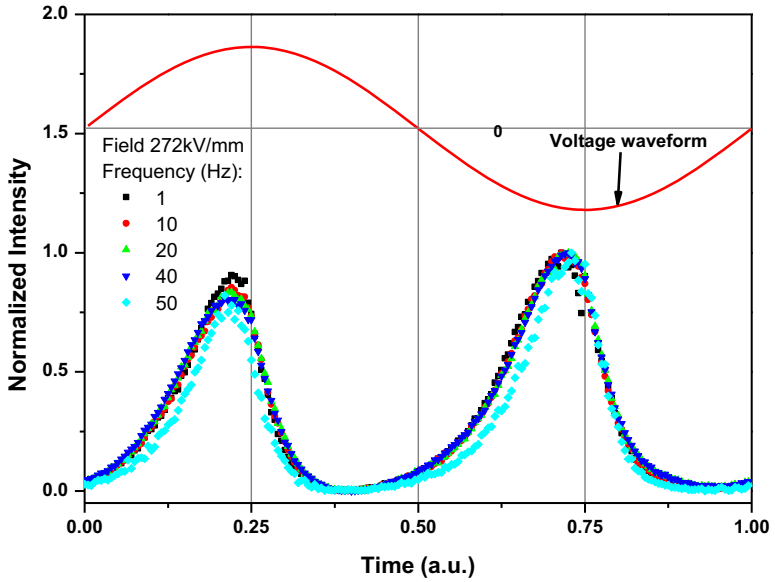

Figure 4-5 Phase-resolved EL of Au-PEN-Au, under AC sinusoidal waveform stress, measured at uniform field 272 kV/mm under different frequency from 1 Hz to 50 Hz. All the data are normalized at EL wave crest.

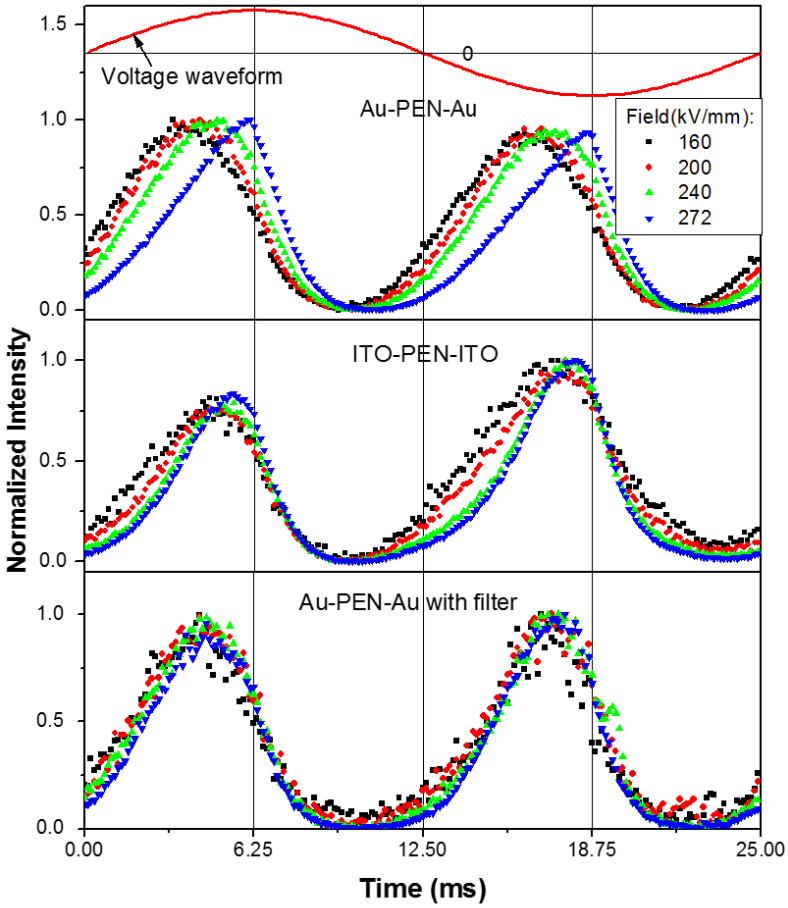

Figure 4-6 Phase-resolved EL of Au-PEN-Au, ITO-PEN-ITO, and Au-PEN-Au with filter under AC sinusoidal waveform stress, measured at uniform frequency 40 Hz under different field. All the data are normalized at EL wave crest.

The light is emitted twice in one voltage cycle as is typical in EL experiments. In one EL cycle, EL intensity increases relatively slowly with the voltage ramping up, then it decreases more rapidly after the crest of voltage. The EL phase angle, defined as the distance between the voltage maxima and EL wave crest is not the same for the three cases. With a red emission light cut-off filter, the phase resolved EL of Au-PEN-Au is more similar to ITO-PEN-ITO, which infers that the red component makes contributions to the left shift phase angle.

The average phase angles for positive and negative voltage half cycle are plotted in Figure 4-7. EL phase angle of Au-PEN-Au changes drastically from 32.4 ° at low field (160 kV/mm) to 1.8 ° at high field (272 kV/mm); that of ITO-PEN-ITO gradually decreases from 18.0 ° to 9.0 °; that of Au-PEN-Au with filter gradually decreases from 23.4 ° to 14 °.

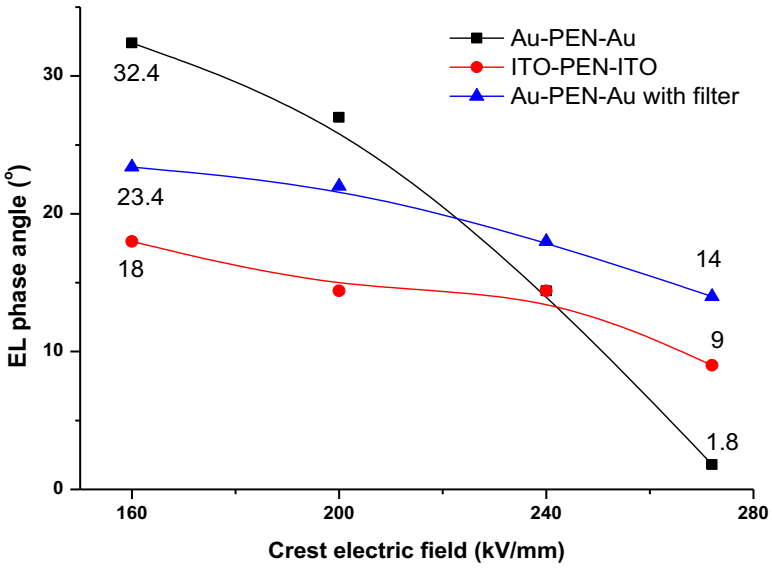

Figure 4-7 Phase angle of Au-PEN-Au, ITO-PEN-ITO, and Au-PEN-Au with filter under AC stress of 40 Hz.

Under AC field, injected charges either are trapped or recombine with carriers of opposite polarity trapped during the previous half cycle. EL is emitted in advance to the crest voltage because the recombination rate of carriers is at maximum there. Interestingly, it can be seen that EL phase angle depends on field and it also depends on electrode nature. EL phase angle has also indeed some relationship with the red component emission. Given the relatively enhanced contribution of red emission at low field, the results tend to show that the phase angle of EL from SPs would be larger than that from PEN emission.

As to the advance of phase of EL, in the literature [85] Baudoin *et. al.* simulated the phase-resolved EL in insulating polymers (especially Polyethylene), based on charge injection transport and recombination model. A hopping mobility of electronic carriers between traps with an exponential distribution in depth was used. The comparison between simulation and

experiment is plotted in Figure 4-8. During one circle of sinusoidal waveform voltage there are several steps for charge transport, trapping, de-trapping, and recombination processes:

a) At t = 0 ms (under zero applied voltage), electric field at the reference electrode is negative (because the net density of charge is positive due to the previous accumulated positive charge within the positive half cycle) and hence electrons begin to be injected and holes begin to be extracted. Injected electrons are then trapped and some of them recombine with trapped holes: hence, the recombination between injected electrons and trapped holes increases in time.
b) At t = 3 ms, electric field at the cathode, recombination rate, injection current for electrons and extraction current for holes are practically at their maximum. The net density of charge begins to be negative and the electric field at the cathode reaches progressively the applied field. This appears prior to the maximum of the applied field.
c) Between t = 3 ms and t = 9 ms, negative carriers are majority carriers in all the cells close to the cathode and this homocharge induces a lowering of the applied field. In this time interval, the recombination rate between injected electrons and trapped holes decreases, i.e. the EL intensity decreases.
d) Between t = 9 ms and t = 13 ms, the electric field at the reference electrode is positive, positive carriers are injected but the net charge density remains negative, acting as an heterocharge that enhances the electric field at the reference electrode relative to the applied field. The recombination between injected holes and trapped electrons begins to increase.
e) At t = 13 ms, the electric field at the reference electrode, recombination rate, injection current for holes and extraction current for electrons are practically at their maximum. The net density of charge begins to be positive and the electric field at the electrode reaches progressively the applied field. As previously, this feature appears before the maximum of the applied field.
f) Between t = 13 ms and t = 19 ms, positive carriers are still injected and reduce the electrode field. Injection current for the holes decreases and hence the recombination between injected holes and trapped electrons decreases.

On the other hand, the impact of the electrode, more precisely Surface Plasmons effect, makes another contributions to the phase shift of the EL. The red component emission from Surface Plasmons has a relatively more contributions under low electric field according to field dependence of EL in Figure 4-3. Hence, the red component emission reaches to the crest of the light emission under relative low electric field, which makes an advance shift in phase-resolved EL.

Moreover, the delay mechanism of EL crest under sinusoidal, triangle and square waveforms of voltage are shown in the annexes at the end of the dissertation, which is due to the rate of the voltage-change. These are supplementary results for phase-resolved EL mechanisms.

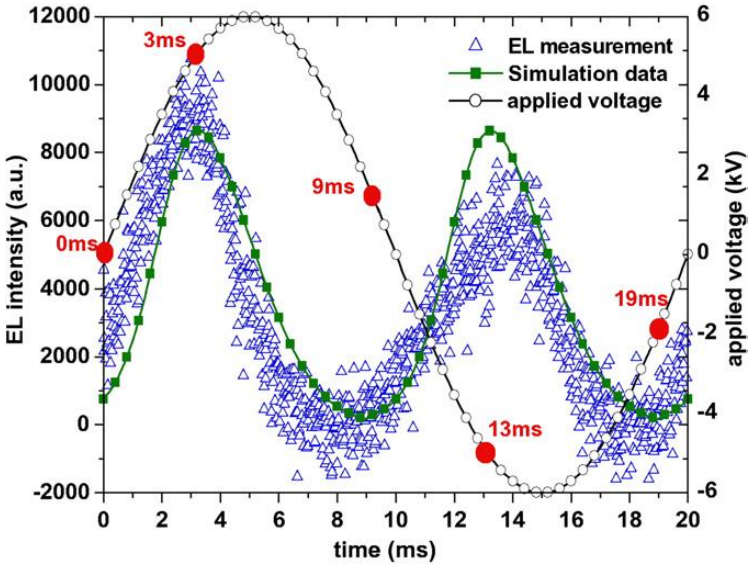

Figure 4-8 Comparison between EL measurement and simulated charge recombination rate for Polyethylene under sinusoidal waveform, simulated by Baudoin et. al. in [85]. The applied field is 60 kV/mm, and the frequency is 50 Hz.

4.3.3 Spectral analyses

The emission spectra of the PEN samples with Au or ITO electrodes under DC stress are shown in Figure 4-9 in order to identify and analyze the light components. The shape of the spectra is fully consistent with those reported earlier, with bands at 500, 578, 618 and 675nm [80]. In both two graphs of Figure 4-9, normalized at 578nm, the bands at 618nm and 675nm are strengthening with the increase of the field. In the same time, the contribution of the wide band at approximately 500 nm clearly decreases. In brief, the two spectra follow the same trends with the field. In order to make clear the relationship between electroluminescence spectra and photoluminescence (PL) spectra of PEN, the PL spectra of the PEN films are measured and plotted in Figure 4-10 at room temperature. The fluorescence spectra peak at 432 nm.

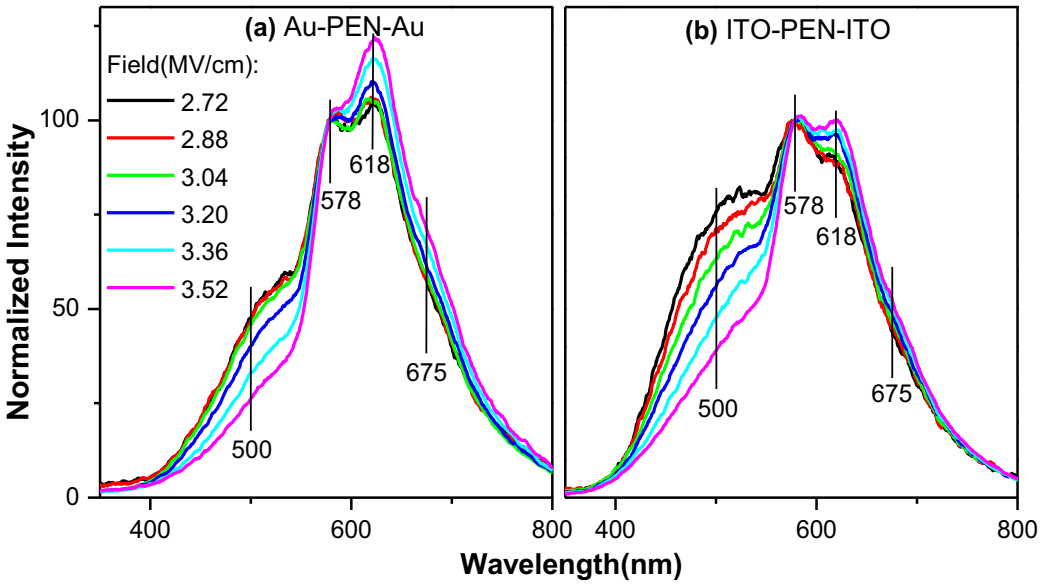

Figure 4-9 Spectra of (a) Au-PEN-Au and (b) ITO-PEN-ITO under DC stress, Spectra normalized to the intensity at 578nm (EL_{578nm}=100).

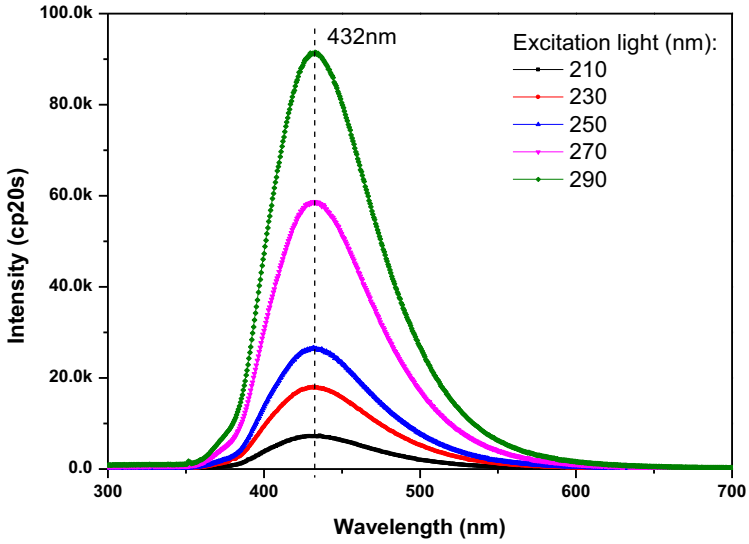

Figure 4-10 Fluorescence spectra of PEN at room temperature.

Under AC stress as in Figure 4-11 the spectra of PEN with Au and ITO electrodes are obviously different. Under low field as in Figure 4-11 (a) and (b), the maximum EL intensity of the broad peak in Au-PEN-Au sample is at about 650 nm, while that of ITO-PEN-ITO sample is rather flat from 450 nm to 650 nm. The EL intensity of the former is also much stronger than the later under the same field. Hence, there exists an additional red component emission (600 nm-750 nm) in the Au-PEN-Au samples, which does not exist in the ITO-PEN-ITO samples and which is also not observed in both two samples under DC stress. It is tempting here to associate the emission in the red to the process at the origin of the embossment in Figure 4-3. From Figure 4-11 (c) and (d), in the high field range, the spectra

are almost the same with different electrodes, demonstrating that the red component has a higher contribution to the EL of low field.

PL spectra of the PEN films at liquid nitrogen temperature are measured and plotted in Figure 4-12. Fluorescence at 432 nm at room temperature of PEN are plotted in Figure 4-10. Phosphorescence at 578 and 638 nm and fluorescence at liquid nitrogen temperature are plotted in Figure 4-12. Due to the low quecning at low temperature, the spectra show more in detail with higher PL intensity. It can be seen that the electroluminescence of PEN is correlated to phosphorescence at approximately 578 nm and not fluorescence at approximately 410 nm. This infers that the electroluminescence is a phosphorescence process. Furthermore, in chapter 5, we will prove that cathodoluminescence can reproduce both the PL spectra and the EL spectra.

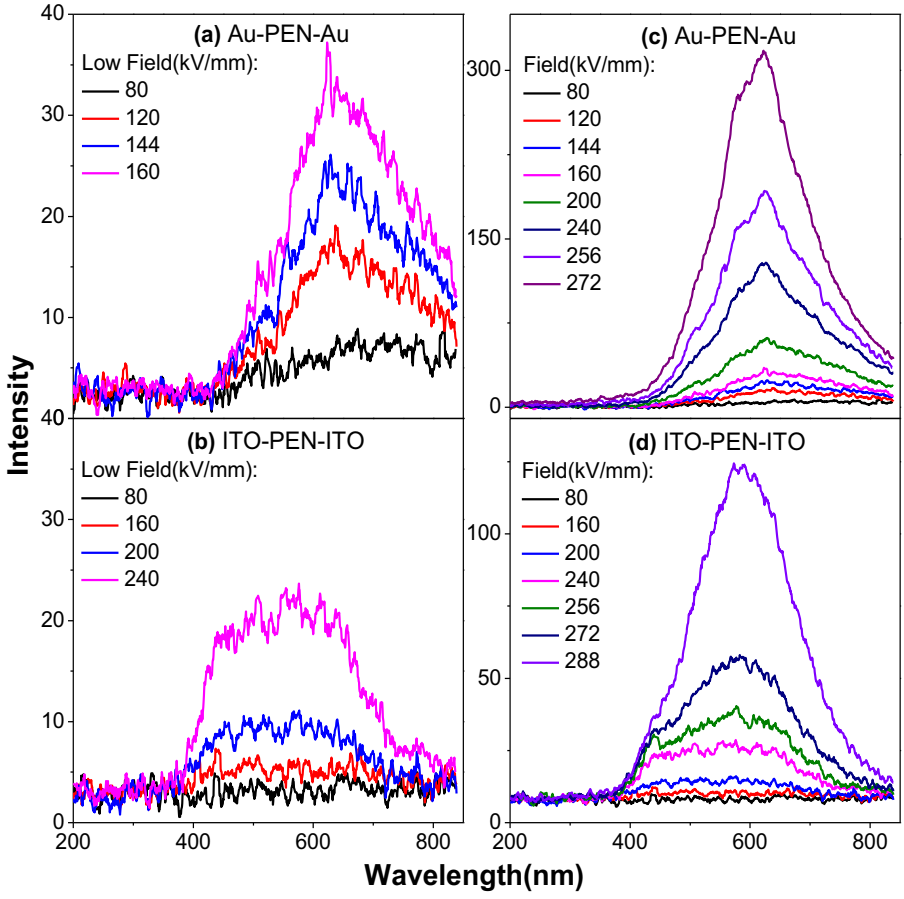

Figure 4-11 EL spectra of Au-PEN-Au and ITO-PEN-ITO under AC stress, frequency: 60 Hz. Intensity is given in counts for an integration time of 5min. (a, c) Au-PEN-Au; (b, d) ITO-PEN-ITO; In (a, b), only spectra with low intensity are shown for sake of clarity.

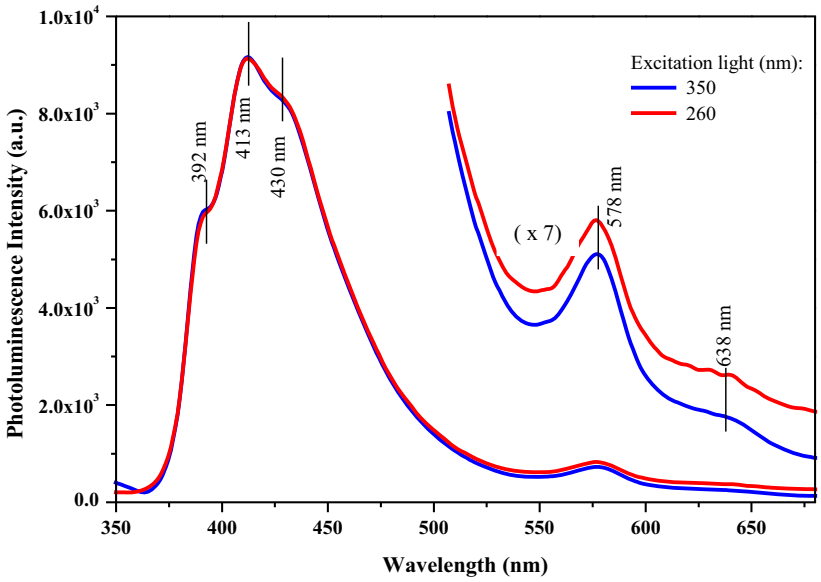

Figure 4-12 Photoluminescence spectra of PEN film at liquid nitrogen temperature for two excitation wavelengths. Adapted from [145].

4.4 Discussion

The PEN films and BOPP films are both detected with red component emission under electric field. The origin of the "red component" in different insulating polymers has also been discussed in several papers [42, 72, 103, 126]. There are many experimental facts inclining for an emission process occurring at the electrode/polymer contact due to charge injection/extraction at the interface. Two emission processes have been advocated in the literature. A first one is linked with the surface states at the contact polymer/metal acting as recombination centers for the injected carriers (changing sign in each half cycle of the AC stress) [72]. A second possibility is the radiative relaxation from Surface Plasmons (SPs) excited by the injection/extraction processes at the electrode surface [42, 103, 126]. SPs are coherent electron oscillations at the surface of the metallic electrode and can relax radiatively [146]. Along a perfectly smooth interface, the momentum k_{sp} of SPs is parallel to the interface and is always greater than the momentum k_{ph} of photons, precluding light emission from SPs (the momentum of both particles, photons and Surface Plasmons, must match for the conversion to occur). Along a rough interface however, the translational invariance of the SP momentum is broken and its components parallel to the interface can match the momentum of photons. Therefore, SPs can radiate at a rough interface. Actually, the fact that the red emission is not detected using ITO electrodes, a material that cannot sustain Surface Plasmons in the visible domain, inclines associating the red emission to the SPs process. However, plasmonics has a further capability, which is to boost luminescence from molecules in close contact with metallic domains [147]. Even if luminescence from surface states is unlikely due to the existence of a quasi-continuum of energy levels at the interface favoring non-radiative relaxation, a weak light efficiency can be greatly enhanced through

plasmonics. Hence, surface-enhanced luminescence can be the process whereby light from surface defects is magnified, boosting therefore luminescence from charges injected alternatively at the electrodes and recombining on surface states or defects from the surface. The red component emission is a universal phenomenon that can impact the EL measurement of insulating polymers with metal electrode.

Whatever the precise mechanism of emission, we have shown that there are two components in the emission spectra. The "red component" dominates at low field and is responsible for the "bump" of the EL vs. field characteristic and contributes the phase angle in phase-resolved EL. It has been cross-proved that the red emission has correlation with the electrode not with the bulk materials.

There are many experimental facts inclining for an emission process occurring at the contact of electrode/polymer under AC, due to charge injection/extraction at the interface [42]. This also explains the fact that the red component is not detected under DC because the EL comes from the bulk of the sample in that case, contrary to the AC case where charge exchange is mainly occurring at the contact. The fact that the red component is not observed with ITO electrodes under AC is another evidence that its source is located at the contact. But there are still two possibilities: either the electrodes themselves are involved in the emission process, or the interface states.

4.4.1 Surface/interface states

In the interface between gold and PEN, there are interface states due to structural disorder, along with possible chemical disorder due e.g. to oxidation. Both of them may lead to specific emission spectra. Under AC field, with the injection and extraction of charge carriers, these states can act as recombination centers and could emit red emission as postulated in [72]. Though the surface states of PEN metalized with Au or ITO should be almost the same, SPs in Au could produce surface enhanced luminescence [147], boosting therefore luminescence from charges recombination on surface states.

4.4.2 Surface Plasmons

The other possibility is direct emission from Surface Plasmons (SPs). Indeed, it is established that SPs, that are coherent electron oscillations can relax radiatively [146]. The optical red emission due to SPs from Cu, Ag, and Au was investigated by P. Dawson *et al*. [148]. The SPs has a close correlation to the surface/interface structure of the electrode. The surface roughness of our PEN film is shown in Figure 4-13. The root mean square roughness, i.e. Rq, is 21.1 nm, the average roughness, i.e. Ra, being 14.5 nm, the maximum of roughness, i.e. Rmax, being 331 nm, which should be almost the same with the roughness of electrode. The interface under study possesses different scales of roughness, providing the conditions for coupling SPs and light. More sharp tips at nanoscale may improve the light emission due to SPs. In chapter 3, the BOPP films appear with crater-like surfaces, which also have a rough surface. The polymers appear different rough surface at micro-scale due to

manufacturing processes. Hence, the surface structure enhanced SPs is universal among the polymer-Au electrode structures under electric field.

The spectral distribution of light emitted by SPs depends on the surface roughness of electrodes itself and the energy distribution of charge injection/extraction produced by the field. Hence, the roughness of electrode surface and the field applied on it are two key factors. Under AC stress, due to alternative injection at the surface of electrodes, high density of carriers always exists here. So under AC low field, the energy distribution meets the requirement of SPs. However, under DC stress, charge injection starts, then due to screening effect, the current density of injected carriers is much less than in the AC case. The peak of current density happens in each half cycle as modeled in [85]. Hence, we consider that the red emission is mediated with SPs effect.

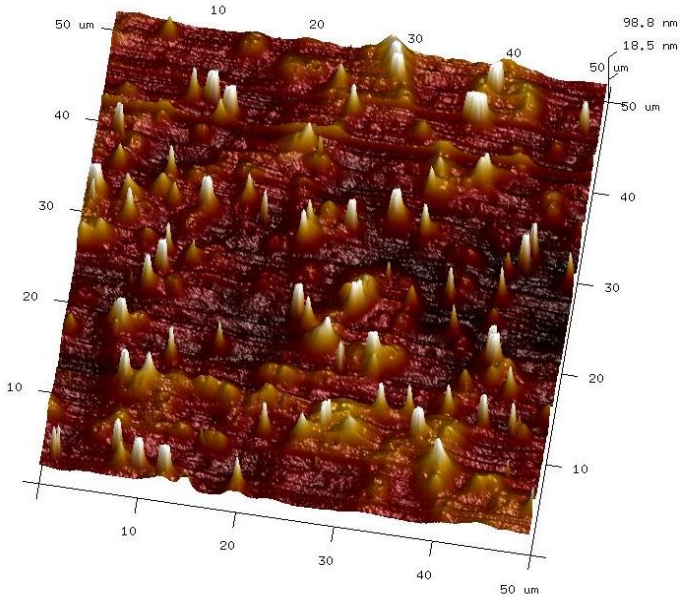

Figure 4-13 Topography of a PEN film obtained by AFM. The size of the image is 50×50μm². Statistics on the image are as follows: root mean square roughness Rq=21.1 nm, average roughness Ra=14.5 nm, max. amplitude Rmax=331 nm.

4.5 Conclusion

Electroluminescence characteristic and spectra under DC and AC stress have been investigated in Polyethylene Naphthalte (PEN) with gold and ITO electrodes. Under low AC field, an additional red emission component is revealed with Au electrode and not with ITO. The red emission is added to the original EL intensity and spectral distribution of PEN. It can be removed by using a 620 nm cut-off filter, accompany with the embossment in EL and left shift of phase angle. Hence, it may derive from a new source. We have proposed that Surface Plasmons at the surface of gold emit the red emission whereas ITO electrodes cannot radiate light due to its optical properties. The roughness of electrode surface and the energy distribution of charge injection/extraction produced by the field are two key factors that should affect Surface Plasmons.

Phase-resolved EL is emitted twice in one AC sinusoidal waveform field cycle. EL intensity peaks are in advance of voltage maxima, the phase advance depending on the field. This is controlled by the recombination of injected carriers and trapped carriers with opposite charges. Injected charges either are trapped or recombine with trapped carriers of opposite polarity from last half field cycle, generating advance of EL crest. More interestingly, with Au electrodes the phase angle changes with field more drastically than with ITO. At the ramping region of field, the SPs-mediated red emission exists and may contribute an additional light, result in their different phase angles. This can be an indirect evidence of SPs-mediated red emission. Further work is needed to fully understand the SPs-mediated red light emitting process.

Chapter 5
Cathodoluminescence, a Reproduction of the Electroluminescence Spectrum

Synopsis

In this chapter, the nature of luminescent centers involved in electron beam induced luminescence i.e. cathodoluminescence (CL) of two types of polyolefin thin films - Polypropylene and Polyethylene, along with aromatic polyesters –Polyethylene Naphthalte and Polyether Ether Ketone, are investigated, comparing wavelength-resolved emission spectra to those obtained under electric field excitation named electroluminescence (EL).

The CL mechanisms in insulating polymers will be analyzed. The CL and EL spectra components will be identified and quantitatively characterized. Eventually we will show that both CL and EL spectra of polyolefins can be reconstructed quantitatively in a series of elementary spectra involving unsaturated groups, which can be a breakthrough to uncover the nature of both EL and CL mechanisms in insulating polymers and its correlation to electrical ageing.

5.1 Introduction

Insulating polymers are used in a variety of applications in electrical engineering, such as cables, generators, transformers and capacitors [1, 2]. Electrical ageing and breakdown in insulating polymers is of fundamental interest to the researchers, the design engineers, the manufacturers and the customers. In this respect, Partial Discharge (PD) is a harmful process leading to ageing and failure of insulating polymers. However, with the development of the materials and apparatus, PDs can be weakened or avoided in some situations, e.g. extra high voltage cables, capacitors, etc. Therefore, there is urgent demand for understanding electrical degradation mechanisms under high energy particles or electric field intensity, pushing the limit of electrical properties in insulating polymers.

Electroluminescence (EL) is an exciting field of research for probing insulating polymers, because it gives insight into electrical ageing and breakdown process, since firstly reported in 1967 by Hartman [3]. They are original techniques, contributing to uncover the nature of charge transport mechanisms and electrical ageing. It provides very interesting information of photo-physical nature, revealing excited states in the polymer, coupled to the electrical behavior of the material, especially with charge carriers in the material that are at the origin of the excitation through the exchange of kinetic or potential energy. Various physical and chemical mechanisms have been involved in the aging of electrical insulations under DC and AC stress [4, 5]. EL is a phenomenon involving physical processes such as charge injection, extraction, and transportation, but also chemical reaction through excited states. Electric fields can produce excited or ionized states, some of which have a non-zero probability for light emission during their relaxation. Hence, on one hand, EL can be a probe of charge excitation and recombination processes, on the other hand, it may provide information on the nature of defects and luminescent sources. EL is associated with electrical ageing and could provide the signature of excited species under electric field. Because interfacial electronic states are very important in charge transfer at the electrode-dielectric interface, it should impact on the EL features, especially under AC stress. Therefore, EL can also gather information and be used to probe the physical/chemical processes occurring inside dielectrics or at the metal-dielectric interface.

However, the essence of EL and the links between EL and electrical ageing or breakdown are still debatable. Especially, there are contributions in the EL spectrum that are not interpreted due to the impossibility to excite such levels by other means and produce the same emission bands. We investigate more specifically in this section light detected when exciting the material under electron beam. Although cathodoluminescence (CL) is known for very long [90, 149], thorough investigations of CL from polymeric materials are seldom. The interest of analyzing CL in the perspective of interpreting EL spectra as the main excitation source is clearly identified, being optical signature produced by impact of electrons of high kinetic energy [37, 90, 91, 150, 151]. Hence, CL is a supplementary technique with another excitation source for probing insulating polymers.

5.2 Experimental

The cathodoluminescence measurements are all carried out in the special-designed multi-purpose chamber demonstrated in chapter 2 in detail. In this chapter, we investigated polyolefin family, i.e. Bi-axially Oriented Polypropylene (BOPP), additive-free Low Density Polyethylene (LDPE) and Cross-linked Polyethylene (XLPE), along with two aromatic polyesters i.e. Polyethylene Naphthalte (PEN) and Polyether Ether Ketone (PEEK). These materials has been introduced in chapter 2 in detail. Attempts of cathodoluminescence measurements have been made also on Polyimide films. However, no light could be detected for this kind material presumably because of its strong absorption in the UV-visible region. For these reasons the results on Polyimide are not reported here.

5.2.1 Materials

Measurements were carried out on different polyolefin materials, being Bi-axially Oriented Polypropylene (BOPP) films of 17.8 μm thickness supplied by KOPAFILM, Germany, Cross-linked Polyethylene (XLPE) films of 150 μm thickness peeled from high voltage cables and issued from EU Artemis project [130], and additive-free Low Density Polyethylene (LDPE) of 50 μm thickness provided by ABB. BOPP films are "hazy" films with rough surfaces to promote impregnation of capacitors, which is demonstrated in chapter 3. Measurements were also carried out on two aromatic polyesters: PEN films with a thickness of 25 μm supplied by Dupont (Dupont Teijin Films Teonex® Q51) and PEEK films with a thickness of 50 μm supplied by Goodfellow Cambridge Limited. These materials are widely used in electrical and electronic industry.

5.2.2 Light analyses setups

Both cathodoluminescence (CL, or called electron beam induced luminescence) and electroluminescence (EL) analyses were performed at room temperature under high vacuum (about $5x10^{-7}$ mbar) in a specially-designed multipurpose chamber in order to avoid discharges in the ambient atmosphere. Light detection is carried out by a grating monochromator (4.5 nm in resolution) coupled to a liquid nitrogen cooled charge coupled device (CCD) camera for spectral analyses which covers the wavelength range from 200 nm to 850 nm. Both surfaces of samples were metallized with semi-transparent layers of gold as shown is Figure 2-8 in chapter 2 deposited by cold sputtering (thickness: 30 nm, diameter: 50 mm) for EL measurement. Otherwise, these samples don't need any pretreatment for the CL measurement.

Electron beam gun which provides focused electron beams as shown in Figure 2-14 in chapter 2 was used to provide electron beam of energy up to 5 keV for the cathodoluminescence measurement. The filament is set to a negative high voltage and the anode at the ground. The distance between the electron gun and the sample on the holder is about 40 mm. The axis of the gun is at 50° to the normal of the sample plane rendering

possible light detection along the normal to the samples. The irradiation area is about 1 mm^2. The beam current is about 1 μA. Emission spectra were recorded for different electron beam energies from 2 keV to 5 keV and for different radiation time up to 210 seconds with the same beam energy.

The specially-designed electrodes - a ring electrode connecting to alternate current (AC) supply and a plane electrode connecting to the ground as shown in Figure 2-8 in chapter 2, provide uniform AC electric field for the electroluminescence measurement. The light emission from the center of the ring electrode through the center hole of the mask can be recorded by the CCD. The internal diameter of the ring electrode is 20 mm, the external diameter 40 mm. EL spectra were recorded under AC electric stress at 50 Hz frequency under field up to 250 kV/mm for BOPP and up to 45 kV/mm for LDPE.

Photoluminescence (PL) measurements can be also achieved in the same specially-designed multipurpose chamber at ambient atmosphere, excited with a xenon lamp which covers the wavelength range from 200 nm to 700 nm.

5.2.3 Electron beam energy, beam current and CL intensity

Electron beam with energy values from 0.5 keV up to 5 keV are irradiated to the samples. During CL measurements, the beam energy was increased from 0 keV to 0.5 keV, then by step of 1 keV lasting for about 30 seconds up from 2 keV to 4 keV, then lasting for more than 400 seconds at 5 keV. Light emission from the samples were recorded simultaneously along the process of electron beam energy irradiation shown as beam energy, current and CL intensity vs. time in Figure 5-2 (a) and (b) for BOPP and XLPE, respectively. Both electron beam current and CL intensity are decreasing with the irradiation time, except for the step at 0.5 keV, where in fact only the incandescence is involved and no electrons exit the gun for current measurement. At the beginning of the irradiation period beam current and light emission decrease very fast and then after a certain time it decreases slowly and is almost stable (cf. result for 5 keV). The beam current at 2 keV is negative which is due to secondary electron emission from the materials. Below a crossover point for the energy of the electron beam, the net electron emission from the surface of the material is higher than the incident electron beam such that the surface of the materials gets charged positively.

The transient beam current and CL intensity infers that the reaction between electron beams and materials change with time. There are two possibilities: firstly the potential involved by trapped electrons on the surface of the sample repel the electron beams and decrease the irradiation; secondly the irradiation of samples induces degradation on the surface of the materials leading to a decrease the CL intensity.

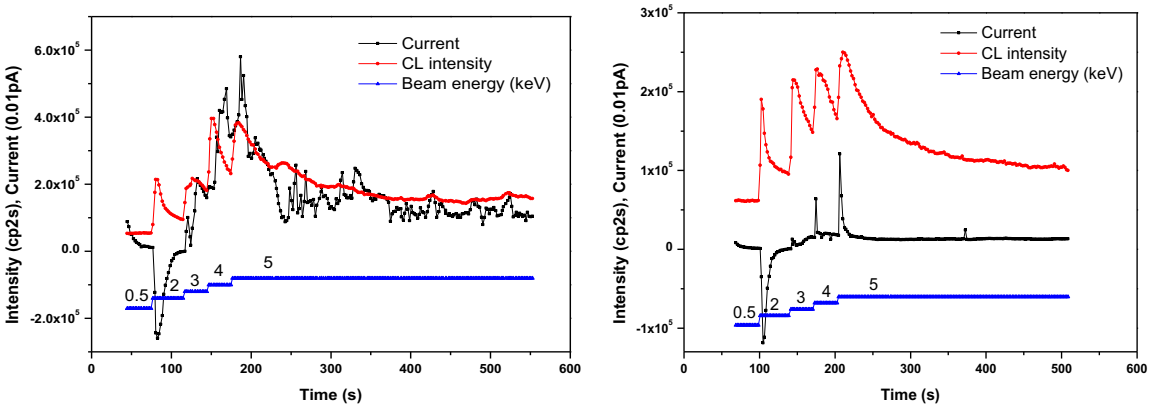

a. CL of BOPP *b. CL of XLPE*

Figure 5-1 CL intensity and beam energy vs. time during the CL measurement, (a) BOPP and (b) XLPE.

5.2.4 Electrical field and EL intensity

EL intensity were recorded under AC stress at different fields a short time after voltage stabilization as shown in Figure 5-2 (a) and (b). Voltage was increased by step of 5.6 kV/mm lasting for 40 seconds up to a level of 33 kV/mm, then by step of 22.4 kV/mm from 44.2 kV/mm to 223.4 kV/mm for BOPP samples. Voltage was increased by step of 1.3 kV/mm lasting for 40 seconds up to a level of 13 kV/mm, then by step of 2.6 kV/mm up to 57 kV/mm for XLPE samples.

The EL intensity increases non-linearly with the increment of electric stress. The EL intensity decreases with the time under electric stress. However, the EL intensity is much more stable than that of CL. Electron beam and electrical field are two excitation sources that both excite the material. The spectra of them will be compared and analyzed in next section.

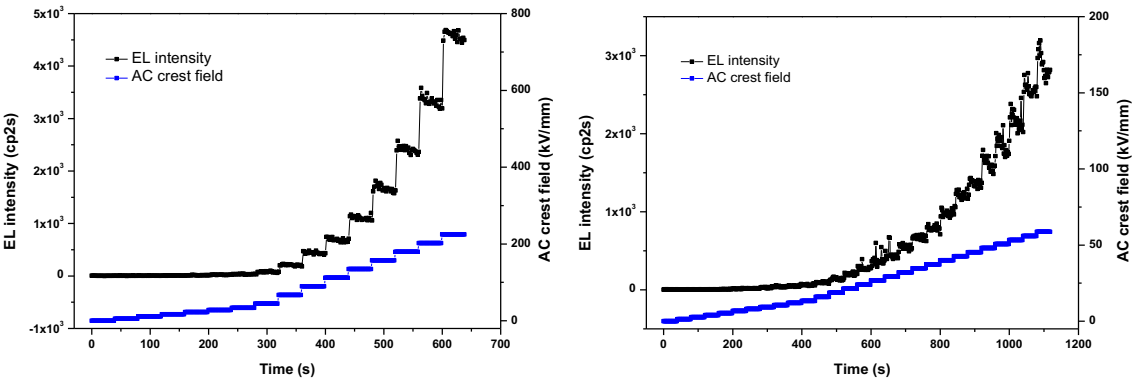

a. EL of BOPP *b. EL of XLPE*

Figure 5-2 EL intensity and electrical field vs. time during the EL measurement, (a) BOPP and (b) XLPE.

5.3 CL spectral analyses of insulating polymers

5.3.1 Polypropylene and Polyethylene

In order to investigate common features in luminescence of PE and PP, we reproduced CL spectra of PP and PE films in Figure 5-3 for different e-beam energies. Figure 5-3 (a) and (b) are the CL spectra of BOPP, while Figure 5-3 (c) and (d) are the CL spectra of XLPE. They are quite well-resolved and reveal a relatively strong emission when comparing to AC EL (intensity is about x600 that of AC EL spectra in Figure 3-13). The CL emission is due to the energetic carriers injected in the samples during the electron beam irradiation. A main peak at 573 nm and several shoulders at lower wavelengths 505 nm, 415 nm and 320 nm are evidenced.

For PP samples, a main peak at about 573 nm and several shoulders at lower wavelength, i.e. 505 nm, 415 nm, and 328 nm are evidenced; for PE samples, the main peak is also at about 573 nm but the shoulders components are weaker than in PP. The main peak in CL spectra also has the same wavelength vs. that in EL spectra, which infers that EL also derives mainly or partly from hot electron carriers. Both the BOPP films and XLPE films contain antioxidant and some other additives, but the nature is not the same in the two materials.

CL spectra exhibit high sensitivity to impurities, point defects, structural modifications, etc [90]. Exposure of materials to electron beam with energy of some keV induces a number of processes in the samples, which lead to the formation of characteristic radiation and bremsstrahlung, and Auger electrons, which were studied in detail in [152, 153]. The electron beam can excite the deep traps to excited states or create electron-hole pairs at luminescent centers, which could then go back to ground level through transition, simultaneously emitting light. From normalized CL spectra of PP in Figure 5-3 (b), we can see that the shoulders have a dependence on the electron beam energy. These shoulders will be analyzed and decomposed below.

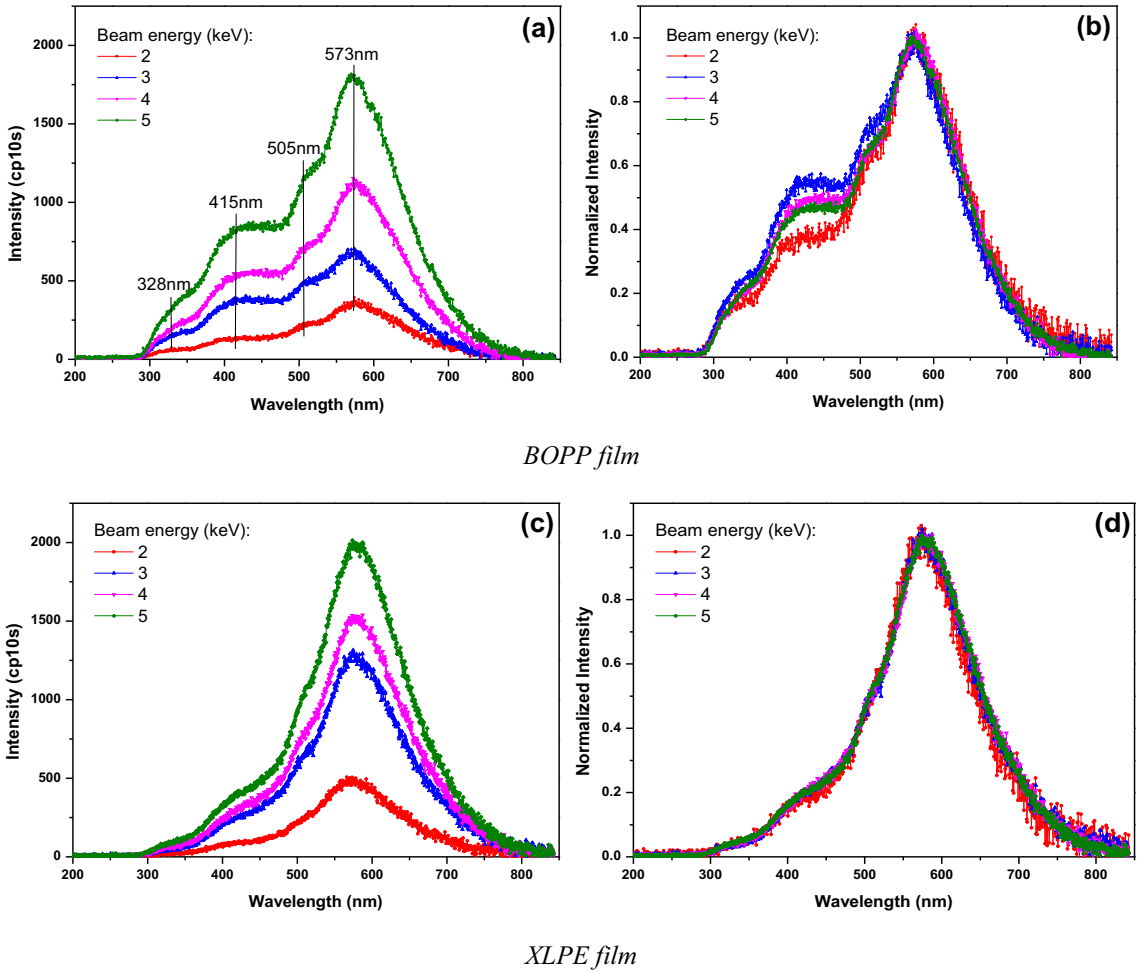

Figure 5-3 CL spectra of BOPP and XLPE, (a) Spectra of BOPP films under different electron beam energies with irradiation time 10 seconds, (b) Normalized spectra of BOPP films from (a), (c) Spectra of XLPE films under different electron beam energies with irradiation time 10 seconds, (d) Normalized spectra of XLPE films from (c).

In order to uncover the correlations between CL intensity and irradiation, we investigated the time-resolved spectral analyses of both BOPP and XLPE. CL spectra were carried out after different irradiation time with electron beam as shown in Figure 5-4 (a) and (c). The relative intensities of the four peaks or shoulders are not evidently variable as shown in normalized intensity in Figure 5-4 (b) and (d), while CL intensity of both BOPP and XLPE decreases a lot within about 60 seconds and then decrease slowly with the irradiation time as shown in Figure 5-5. The samples emit much less light after about 60 seconds. It can be speculated that at that time the samples have been almost aged. In our experiment, the irradiated area on both PE and PP samples have turned to be light brown from transparent, which directly proves that they have been aged during the electron beam irradiation. Along with the CL intensity decreasing with time, we can infer the CL emission is accompanied by electrical degradation of the insulating polymers. Furthermore, the CL spectrum - especially the main peak at 573 nm may be a signature of electrical degradation in these polymers.

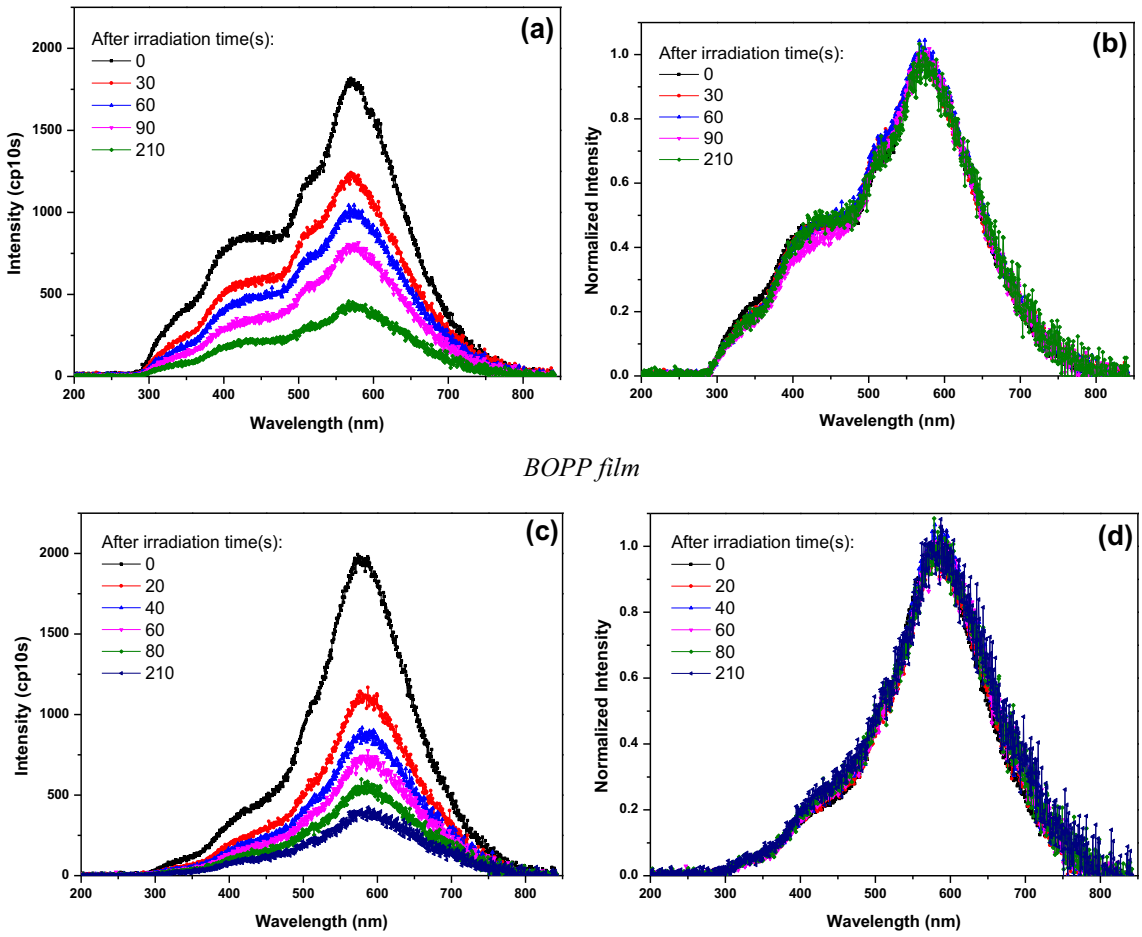

Figure 5-4 CL spectra under electron beam energy 5 keV after different irradiation time, (a) Spectra of BOPP films, (b) Normalized spectra of BOPP films from (a), (c) Spectra of XLPE films, (d) Normalized spectra of XLPE films from (c).

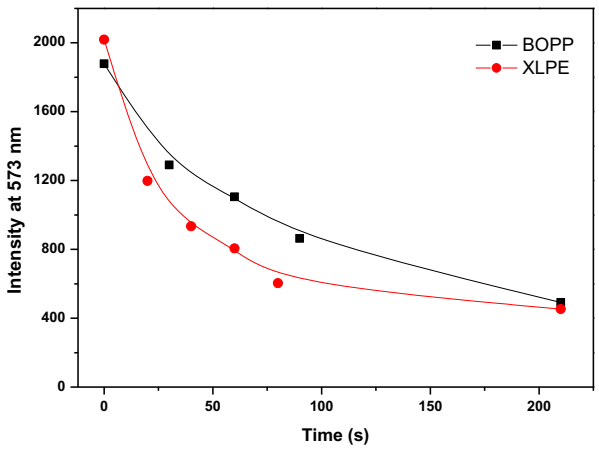

Figure 5-5 CL intensity at 573 nm of BOPP and XLPE films after different irradiation time.

We have compared the normalized CL spectra of PE and PP in Figure 5-6. Their spectra both contain the same main peak at 570-580 nm. However the three shoulders in PE are weaker than those of PP.

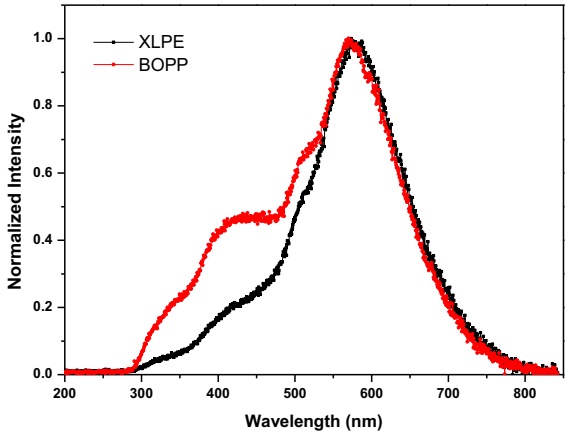

Figure 5-6 Normalized CL spectra of XLPE films and BOPP films from Figure 5-3.

5.3.2 Aromatic polyesters

CL spectra for insulating polymers have also been proved a reproduction of EL in two aromatic polyesters: Polyethylene Naphthalate and Polyether Ether Ketone. It is a universal technique for probing polymers.

5.3.2.1 **Polyethylene Naphthalte**

The PEN films are irradiated under electron beams with energy from 2 keV to 5 keV. The CL spectra of PEN are plotted in Figure 5-7. The spectra intensity increase with the increment of beam energy. However, according to the normalized spectra we can see that the relative intensity at approximately 430 nm increase much faster than the peak at 631 nm. The peak at 430 nm is exact its photoluminescence crest as shown in Figure 4-10 and Figure 4-12 in chapter 4. The peak at 631 nm and two shoulders of phosphorescence have also been achieved in EL spectra investigated in Chapter 4. The CL is a reproduction of both PL and EL, but with more spectra information and higher resolution.

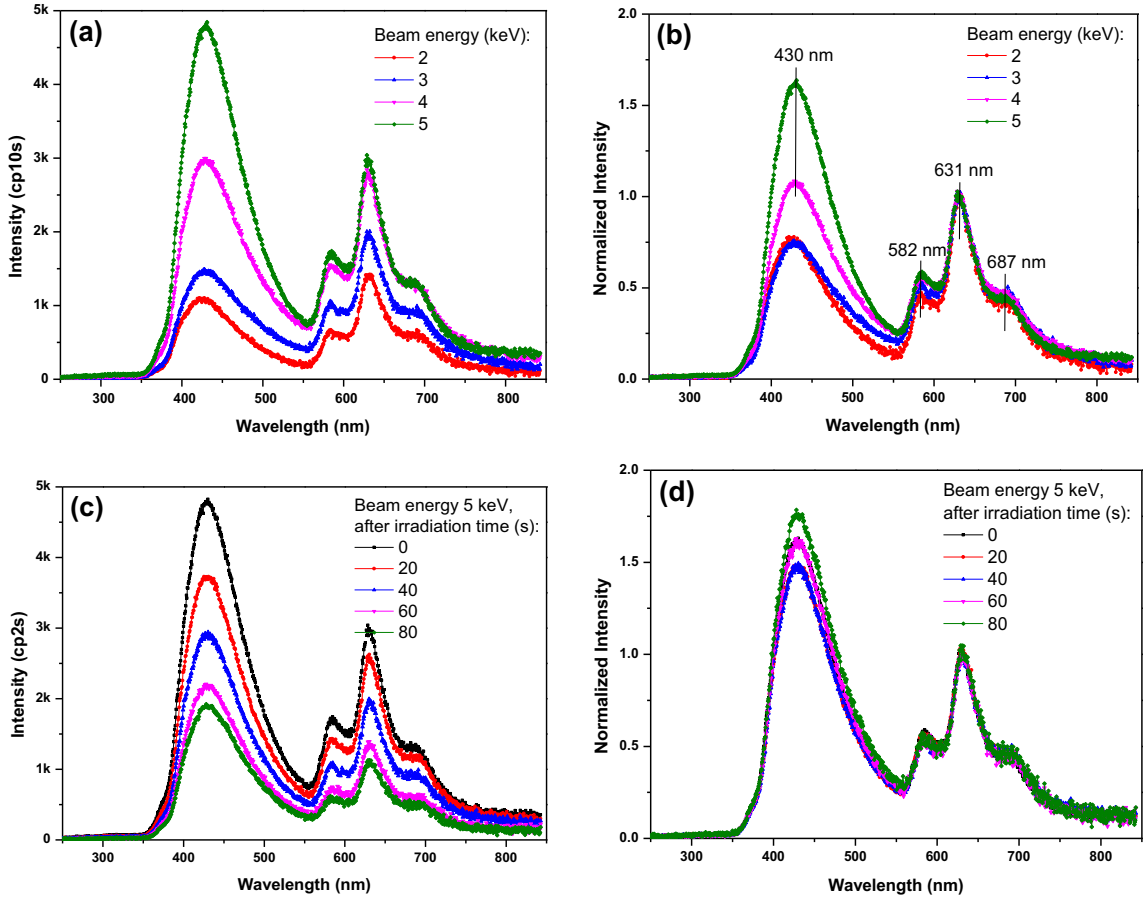

Figure 5-7 CL spectra of PEN films, (a) Spectra of PEN films under different irradiation electron beam energy, (b) Normalized spectra at 631 nm of PEN films from (a), (c) Spectra of PEN films after different irradiation time, (d) Normalized spectra at 631 nm of PEN films from (c).

5.3.2.2 **Polyether Ether Ketone**

The Polyether Ether Ketone (PEEK) films are irradiated under electron beams with energy from 2 keV to 5 keV. The CL spectra are plotted in Figure 5-8. The CL intensity increases with the increment of the electron beam energy. From the spectra normalized at 496 nm, the peak at 622 nm decreases with the increase of the electron beam energy. During the irradiation time 240 seconds, the 622 nm peak decreases much faster than 496 nm peak, and then disappears as seen in Figure 5-8 c and d. This could be similar to PEN, the two peaks depend on different mechanisms. The CL contains PL components at approximately 490 nm and other components, which demonstrates that CL in insulating polymers is a reproduction of both EL and PL.

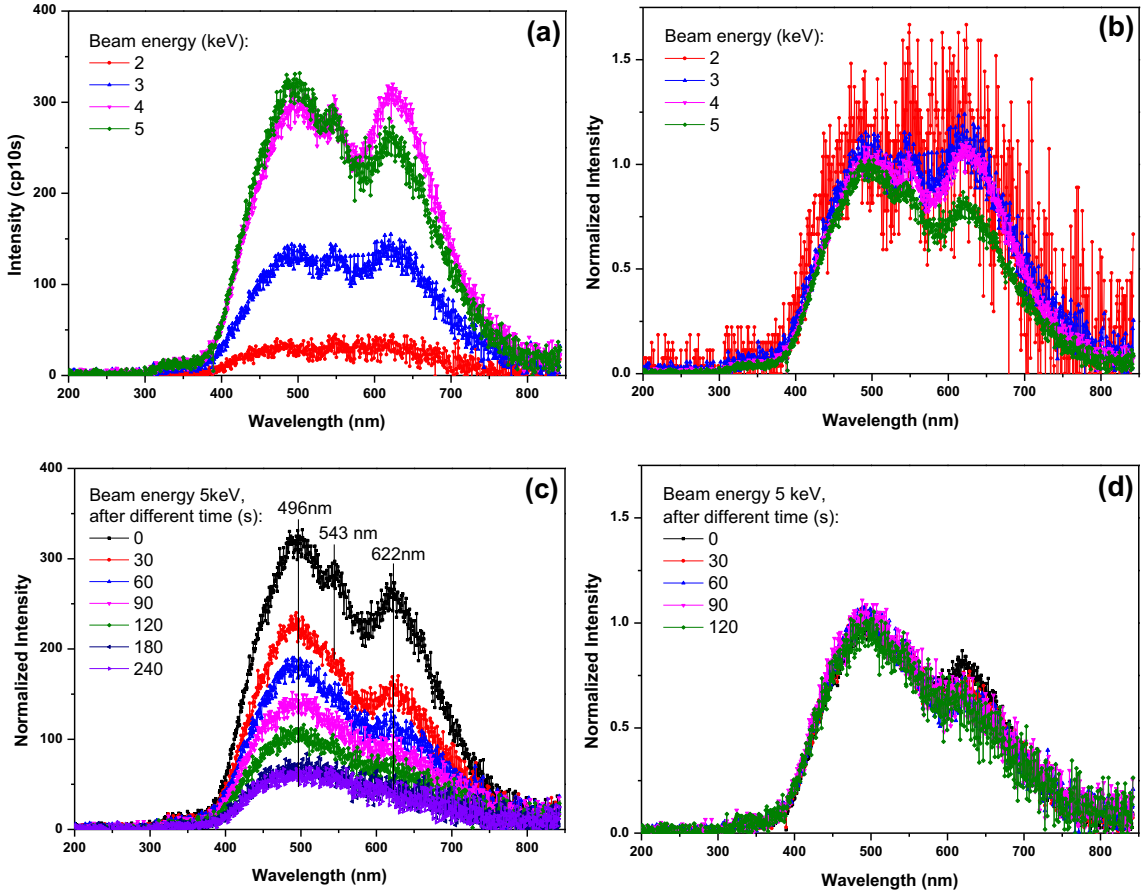

Figure 5-8 CL spectra of PEEK films, (a) Spectra of PEEK films under different irradiation electron beam energy, (b) Normalized spectra at 496 nm of PEEK films from (a), (c) Spectra of PEEK films after different irradiation time, (d) Normalized spectra at 496 nm of PEEK films from (c).

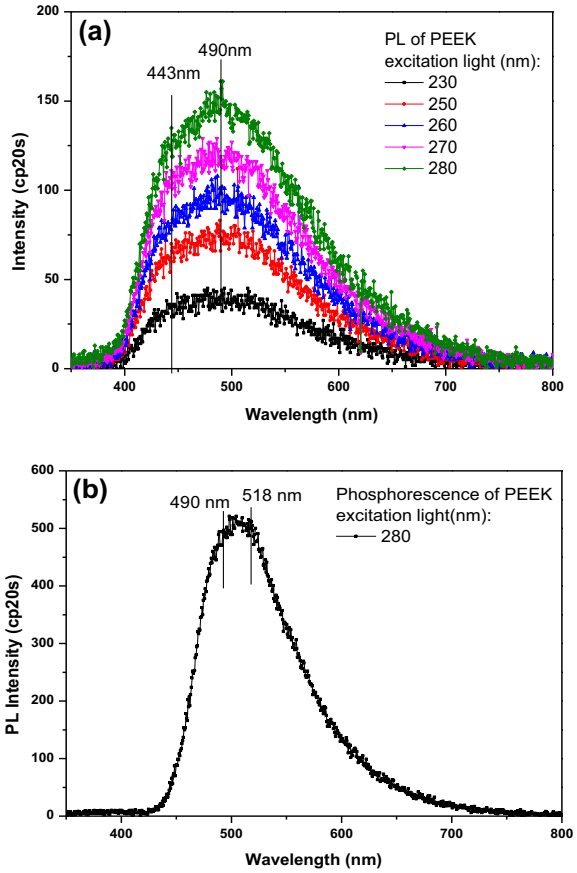

Figure 5-9 PL Spectra of PEEK (a) at room temperature and (b) at liquid nitrogen temperature.

5.4 Spectral reconstruction of polyolefins on the basis of elementary components

5.4.1 Identification of elementary components in spectra of polyolefin

In order to investigate the origin of the CL spectra peaks of PE and PP, we compared CL and EL spectra of PP to emission spectra produced using different excitation sources. These are Fluorescence (FL) obtained in photoluminescence experiments, Chemi-luminescence (CHL), recorded along thermal oxidation [74] and Recombination-induced Luminescence (RL) [38] of PP films as shown in Figure 5-10. For the peak at about 570 nm, it has not been identified according to previous works. However, it has a direct correlation with electrical degradation according to our experiments forward. The symmetrical component peaking at 573 nm is extracted from the CL spectra of BOPP as shown in Figure 5-11.

The FL in Figure 5-10 can account for the component at 328 nm in CL. The photo-induced luminescence derives from a physical process and does not contribute to the electrical ageing. The UV-visible transmission spectrum of BOPP films reveal an absorption maximum at 200 nm, and two absorption shoulders at 230 nm and 280 nm as shown in Figure 3-16 (a) in chapter 3, which are exactly the same two excitation peaks for the Fluorescence.

The CHL spectrum shown in Figure 5-10 was obtained on commercial PP film, 17.8 µm thick during the thermal oxidation at 125 °C [74]. It involves formation of carbonyl functions with a typical peak at 415 nm. We consider that the spectrum is characteristic of PP in the early stage of the oxidation process (when isolated carbonyl groups are being formed) [154].

The RL has been investigated by contacting the samples with a cold plasma in Helium powered at a frequency of about 5 kHz [38]. The light emission is due to the recombination of deposited charge carriers. It is at 505 nm [74], inferring the charge recombination luminescence. In recombination-induced luminescence experiments where the light comes from charge recombination on the natural chromophores of PP the emission is broad and peaks at 505 nm as shown in Figure 5-10 [38].

Consequently, the EL and CL spectra of PP could be interpreted as the superposition of four contributions: the fluorescence of the natural chromophore, a chemiluminescence component, the phosphorescence of enone compounds among the natural chromophore which act as recombination centers, and a fourth component at longer wavelengths tentatively attributed to excitation of by-products of the PP molecules.

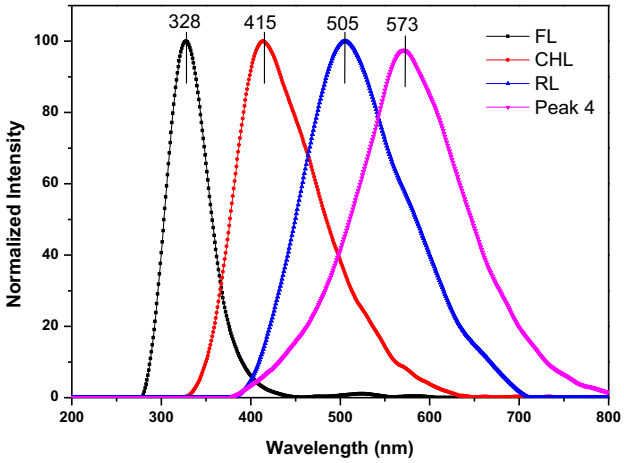

Figure 5-10 Spectral components associated with the fourth elementary processes. FL: Fluorescence spectrum –taken from Figure 3-16; CHL: chemiluminescence spectrum -taken from reference [154]; RL: recombination-induced luminescence –taken from reference [38]; Peak 4: unknown component –derived from fitting CL spectrum. Note that the spectra have been smoothed for eliminating noise.

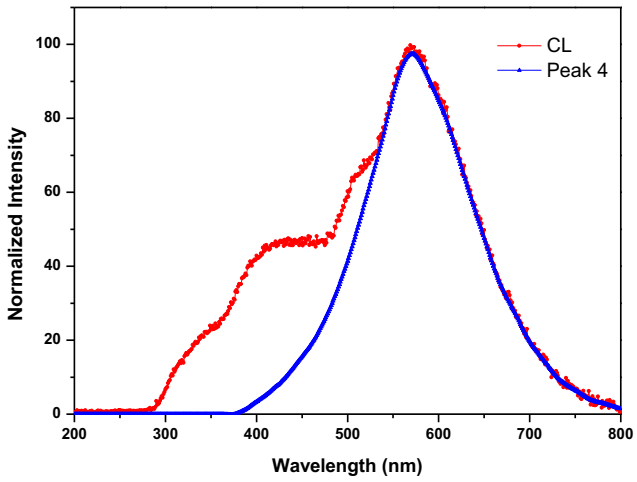

Figure 5-11 The symmetrical component peaking at 573 nm extracted from the CL spectra of BOPP.

5.4.2 Correcting the EL spectra for the SPs contribution

The emission spectra of EL and CL are superimposed for PE and PP in Figure 5-12 (a) and (b). It is evident that they are all organized around a common component peaking at 573 nm, with the extra-contribution in the red part of the spectrum for EL. We then corrected the EL spectra for SPs contribution according to our previous analyses on CL and EL excitation mechanisms; the difference in light intensity between EL and CL above 573 nm was entirely assigned to SPs related emission. Emission spectra due to SPs in metal-insulator-metal structure of different nature as plotted in Figure 5-13 are compared to the calculated SPs component from Figure 5-12. The luminescence due to radiative decay of SPs at the surface of gold can have different spectral features depending on the roughness scale of the surface and the conditions of excitation [148]. SPs excited at the surface of electrodes in the configuration of our experiments are thought to be due to charge injection/extraction at the interface metal/dielectric. For a given excitation condition i.e. the applied field, the intensity of the light can change from sample to sample (depending on details at a microscopic level) but the spectral shape has always been reported with maxima at 750 nm and decreasing intensity into the visible domain.

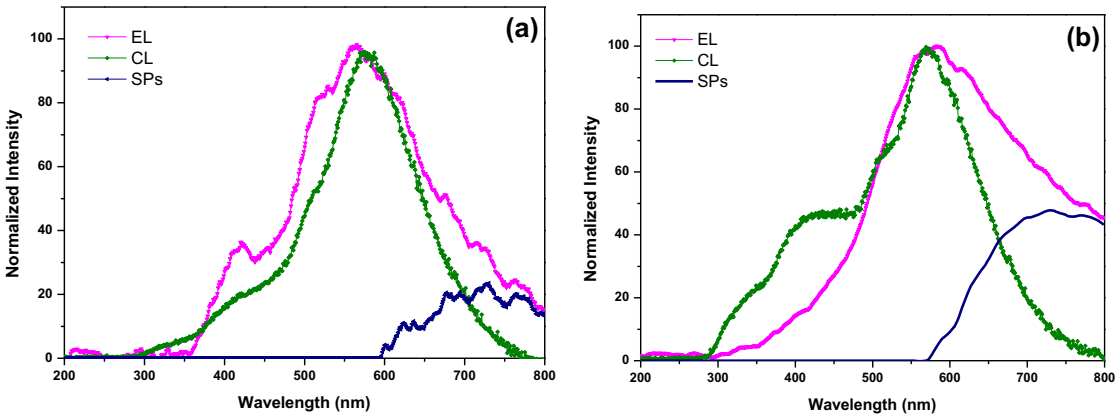

Figure 5-12 Correction of EL spectra by the contribution of Surface Plasmons emission in XLPE and BOPP. (a) Superposition between EL and CL spectra in the case of XLPE; (b) Superposition between EL and CL spectra in the case of BOPP.

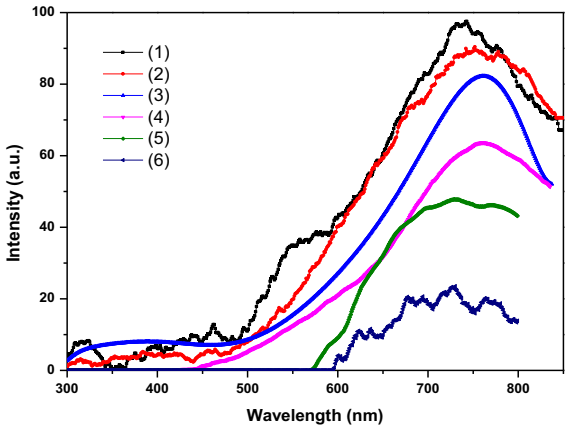

Figure 5-13 Emission spectra due to SPs related emission in Metal-Insulator-Metal structure of different nature. Low field EL spectra of (1) Ag-Polyethylene Naphathalate-Ag, (2) Ag-PE-Ag and (3) Au-PE-Au, (4) due to surface plasmon in a MIM structure. From [42]. (5) SPs from BOPP in Figure 5-12 (b), (6) SPs from XLPE in Figure 5-12 (a).

5.4.3 Reconstruction of EL and CL spectra with four components

We reconstruct the emission spectra of CL and EL on the basis of the previous analyses. The spectra associated with fluorescence, chemiluminescence and recombination-induced luminescence are shown in Figure 5-10. The fit to CL and EL spectra of PP and PE films are shown in Figure 5-14 a, b, c, and d respectively. All the spectra are nicely reproduced. The relative contribution of each elementary component is given in Table 5-1. The different mechanisms do not contribute with the same weight in both processes: fluorescence and chemiluminescence have a stronger relative contribution to the CL spectrum.

The EL and CL spectra of both PE and PP sample are reconstructed from the four previous components as shown in Figure 5-10. The shape of each elementary component has been

approximated by a Gaussian peaking at the same wavelength during the peak fitting processes. The Gaussian function is as follow:

$$f_{(x)} = ae^{\frac{-(x-b)^2}{2c^2}} \quad (5\text{-}1)$$

Where a stands for the intensity, b for the wavelength and c for the width. The peak of the Gaussian function is the same with that of the elementary component spectra.

Then "Least square method" is programmed in "Matlab" to verify if the difference of fitting spectra and original spectra is at the minimum. W is the difference between the sum of the four spectra and the target spectra (EL or CL spectra).

$$W = \sum_{x=200}^{799}(a * y_{1(x)} + b * y_{2(x)} + c * y_{3(x)} + d * y_{4(x)} - y_{5(x)})^2 \quad (5\text{-}2)$$

where, a, b, c and d are four unknown parameter; $y_{1(x)}$, $y_{2(x)}$, $y_{3(x)}$ and $y_{4(x)}$ are intensity of the four elementary spectra; $y_{5(x)}$ is the intensity of the target spectra. We Program in "Matlab" to calculate to achieve W to be the minimum, and get a, b, c and d.

Hence, the simulation spectra are as:

$$\text{Simulation}=a*FL+b*CHL+c*RL+d*EL. \quad (5\text{-}3)$$

The weight of each elementary component in the best fitting figure is calculated with integration method in "Originlab" (integration of the area of the curve) and demonstrated in Table 5-1.

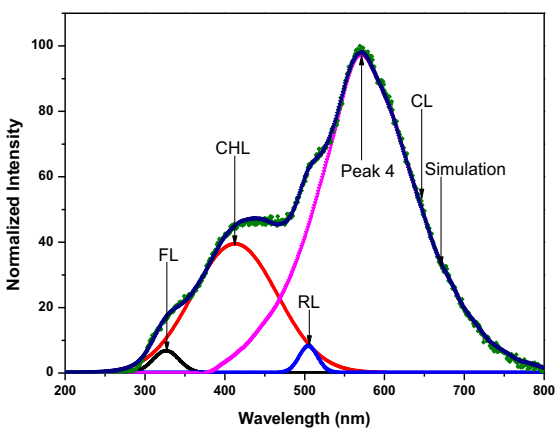

a. Reconstruction of the CL spectrum in PP films

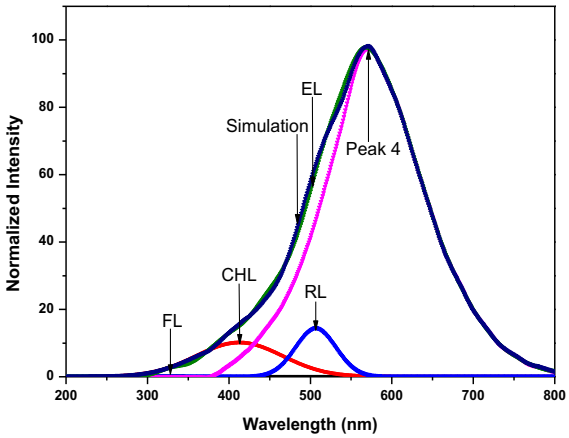

b. Reconstruction of the EL spectrum in PP films

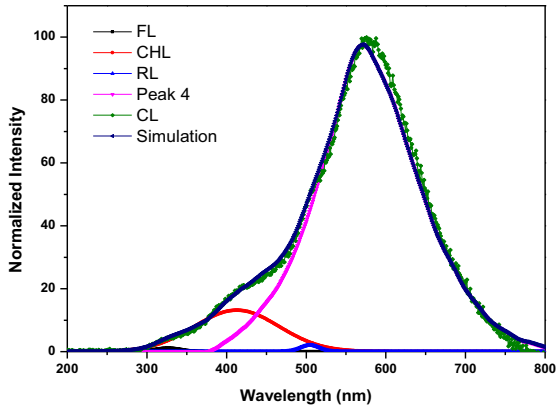

c. Reconstruction of the CL spectrum in PE films

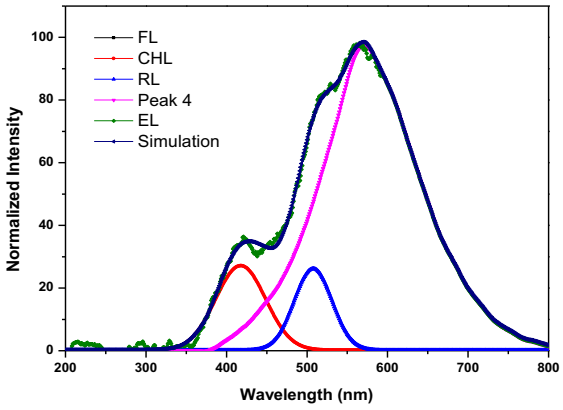

d. Reconstruction of the EL spectrum in PE films

Figure 5-14 Reconstruction of the CL and EL spectra in PP and PE films on the basis of four elementary components. FL stands for fluorescence, CHL for chemiluminescence, RL for recombination-induced luminescence and peak 4: unknown component associated to the generation of by-products in excited states.

Table 5-1 Relative contributions of the four elementary components in CL and EL spectra in PP and PE films.

Materials	**Luminescence type**	**Fluorescence of natural chromophore** **Peak max at 328 nm**	**Chemiluminescence in its early stage** **Peak max at 415 nm**	**Recombination-induced luminescence** **Peak max at 505 nm**	**Polymer by-products** **Peak max at 573 nm**
PP	**CL**	1.5%	25%	1%	72.5%
	EL	0%	7.7%	5.2%	87.1%
PE	**CL**	0.3%	8%	0.2%	91.5%
	EL	0%	11.5%	8.5%	80%

5.4.4 Reconstruction of EL spectra with SPs contribution

EL spectra were acquired under AC stress for collecting enough light to be analyzed. In such a case, we have shown that Surface Plasmons (SPs) [155] developing at the metallic electrodes contribute to the EL at low electric field through a broad spectral component peaking at about 750 nm [42]. From samples to samples, there is some variation of the SP contribution to the light intensity. SPs dominates the spectra at low field and their relative contribution decreases for an increasing field. We are therefore forced to consider a fifth elementary component in the EL spectra when compared to the CL spectra.

The Surface Plasmons effect is universal in all the not perfect smooth dielectric-metal interfaces under electric field, which is also unavoidable during the electroluminescence measurement. The nature of impact of the electrode has been studied in chapter 4, Surface Plasmons and interface states are important factors to impact the light emission. Therefore, electroluminescence spectra of both PP and PE films are reconstructed using five elementary components: i.e. Fluorescence, Chemiluminescence, Recombination-induced Luminescence, Peak 4, and Surface Plasmons, which is plotted in Figure 5-15. The contributions of elementary components are calculated with integration method in "Originlab" and demonstrated in Table 5-2. It can be seen that from samples (PP) to samples (PE) there is some variation of the SP contribution to the light intensity. Even in the samples, for example PP, the SP contributions can also be variable, which is due to the diversity of the surface structures of films.

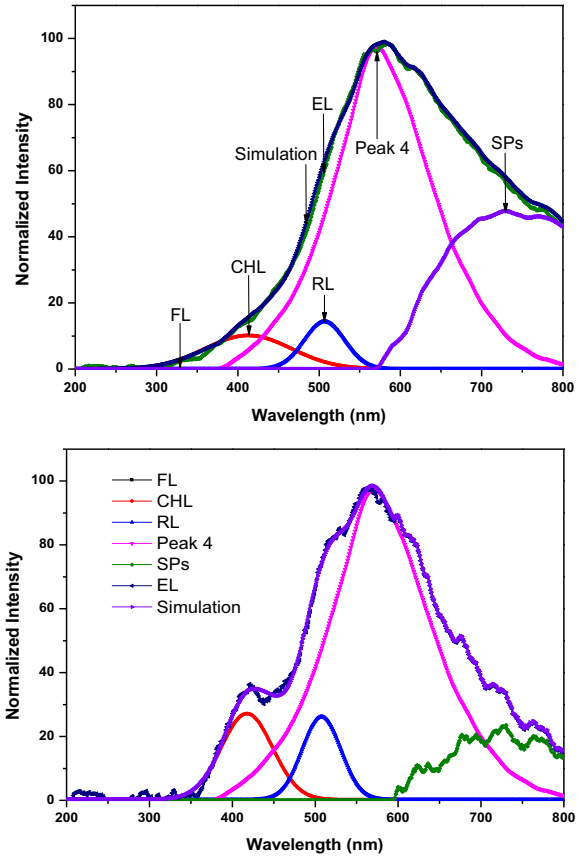

a. Reconstruction of the EL spectrum in PP films *b. Reconstruction of the EL spectrum in PE films*

Figure 5-15 Reconstruction of the EL spectra in PP and PE films on the basis of five elementary components. FL stands for fluorescence, CHL for chemiluminescence, RL for recombination-induced luminescence, peak 4: unknown component associated to the generation of by-products in excited states, and red emission associated to Surface Plasmons.

Table 5-2 Relative contributions of the five elementary components in EL spectra of PP and PE films.

Materials	**Fluorescence of natural chromophore Peak max at 328 nm**	**Chemiluminescence in its early stage Peak max at 415 nm**	**Recombination-induced luminescence Peak max at 505 nm**	**Polymer by-products Peak max at 573 nm**	**Surface Plasmons Peak max at 750 nm**
PP	0%	5%	4%	60%	31%
PE	0%	9.9%	7.4%	68.8%	13.9%

5.4.5 Discussion

These results and their interpretation raise several points. Comparing the general shape of the emission spectra, it appears that EL spectra are less resolved and appear broader when compared to CL. This is certainly due to the level of light that is much less in EL than in CL

(BOPP CL is 600x stronger than BOPP EL in the conditions of our experiments). Now, the analyses allows discussing the relative contributions of each of the four elementary components (and Surface Plasmons component) to the material luminescence in CL and EL.

Table 5-1 and Table 5-2 show the contributions of the different components. Fluorescence contributes little, almost 0%, to electroluminescence, especially comparing to cathodoluminescence spectra. It imply that electroluminescence in insulating polymer is not due to chromophore in the samples but a mixture of chemiluminescence, Recombination-induced luminescence, and other components. The shoulder components are much less evidenced in EL when compared to CL. In the latter case, there is a dependency of the chemiluminescence component on the beam energy which can be explained taking into account the severity of the degradation mechanisms. Excitation conditions under electric field are much less severe and this can explain the small contribution of the shoulder components to the EL spectra. It will be especially interesting to monitor the evolution of the shoulder components vs. time/field in EL experiments as a probe for the onset of hot electron processes and extent of degradation through oxidation reaction. As regards the latter process, the contribution of chemiluminescence in the EL spectra is somehow variable from sample to sample. However, the degassing time of the samples has not been controlled either in cathodo- or electro-luminescence experiments. The concentration of residual oxygen in the samples at the beginning of each experiment is probably different from sample to sample. The oxygen molecules that react with excited states of the polymer are those dissolved in the amorphous part of PP. Note also that chemiluminescence is a very sensitive technique with a quantum yield for light emission of 10^{-9} in polyolefins.

The fluorescence of the natural chromophores of PP has been considered as an elementary component in the emission spectra of PP but not their phosphorescence. The first reason is bound to the fact that such extra component was not needed to approach the emission spectra but also to the fact that phosphorescence at room temperature is easily quenched by the oxygen molecule due to its paramagnetic property. This is why the phosphorescence emission of the natural chromophores is revealed by decreasing the temperature which acts in two ways, decreasing both the oxygen mobility in the polymer network (especially below the glass transition temperature) and its reactivity. Experiments at different temperatures should give some answer to the question. Now, the component of the emission spectra due to charge recombination is also in the domain of the phosphorescence of the natural chromophores of PP. Indeed charge recombination preferentially occurs on those chromophores acting as deep traps [28] which are of unsaturated carbonyls of the enone and di-enone types in PP. Ionization will preferentially affect these species because of the presence of a non-bonding electron on the oxygen atom which is the first ionization level in enone compounds [156].

Upon recombination, the excited state will be a triplet level excited directly through the recombination process or indirectly by transfer from the first excited singlet state. This

explains why recombination processes give rise to phosphorescence of specific chromophores even at room temperature.

The main component in the emission in CL or EL has not been identified. We think it is a signature of material degradation either through the formation of by-products under an excited form or through their excitation upon charge recombination. Indeed, the fate of excitons formed upon recombination of electron/hole pairs has been investigated in a cousin material (Polyethylene) using density functional calculations and ab-initio molecular dynamics simulations. Two situations were investigated where excitons are self-trapped along a chain [141, 143] or trapped at chemical defects [142]. The relaxation can occur following different pathways depending on the case. When the exciton is trapped on a chemical defect, the relaxation pathway depends of the nature of the chemical defect leading to trapping of the charges, non-radiative recombination or homolitic bond-breaking. This is of course the last process that is relevant for damage. When the exciton is self-trapped along a chain, C-H bonds breaking is promoted according to a recent calculation [142]. With the opening of a chemical route, by-products could be produce in excited states and be responsible for emission in a wavelength range that is not typical of the initial chemistry of the polymer. The main peak in electroluminescence could reveal such degradation process.

The electroluminescence and cathodoluminescence of polyolefins appear with the same spectral peak at about 570-580 nm, even with different contributions of shoulders. This implies the generic mechanism of electrical ageing in polyolefin materials. In cathodoluminescence, the kinetic energy of electrons in the beam is the main source of excitation. They lose their energy through a diversity of channels among which impact excitation and impact ionization of the molecules. Impact excitation on the natural chromophores of PP will generate excitonic states that will further relax to their ground states (generating fluorescence and/or phosphorescence emission depending on the nature of the exciton) or react with the dissolved oxygen. It follows the possibility to emit light through the formation of carbonyl functions (chemiluminescence). Impact ionization will be a source of positive charges and there is the possibility of geminate recombination (generating light) when the incoming electron has already lost its kinetic energy, being trapped in the vicinity of the positive charge. Recombination can also occur between trapped electrons and trapped holes in diffusive recombination processes. In recombination processes, the emitting species will be those able to act as recombination centers i.e. those providing deep traps for electric charges. In insulating polymers, these centers are bound to CO species. Owing to the chemical degradation of the material under the electron beam, all these recombination processes can concern by-products leading to new components in the CL spectra. The CL experiment provides therefore the full set of excitation. In electroluminescence, the all set of processes can also be involved depending on the experimental conditions. We have shown that recombination between charges of opposite polarity provides the conditions for EL in polyolefins [42]. It has to be realized that recombination opens the way to chemiluminescence as well through the excitonic states created by the recombination process

itself that can react with dissolved oxygen. Because a chemical pathway is open through reactive excited species, recombination can further affect newly formed chemical groups. In case of hot electron processes and although the kinetic energies is not comparable in CL experiments (a few eV in EL vs. a few keV in CL), there is still the possibility for impact processes, with or without ionization. Impinging electrons with a kinetic energies of a few eV will not have the energy require for impact ionization (15 eV) but they can excite species that will relax through fluorescence and phosphorescence emission, or be stabilized to form transient ions (negative attachment -see [154]) able to subsequently dissociate into molecular fragments.

There is a great similarity between electroluminescence and cathodoluminescence spectra in insulating polymers although one cannot clearly distinguish the different shoulder components and there is an extra-component in the red part of the spectra in electroluminescence spectra. In electroluminescence, the all set of processes active in CL can also be involved depending on the experimental conditions. In case of hot electron processes [157] and although the kinetic energies is not comparable in CL experiments (a few eV in EL vs. a few keV in CL), there is still the possibility for impact processes, with or without ionization. Impinging electrons with a kinetic energies of a few eV will not have the energy require for impact ionization (15 eV) [158], but they can excite species among which the natural chromophores that will relax through fluorescence and phosphorescence emission, or be stabilized to form transient ions (negative attachment) able to subsequently dissociate into molecular fragments [154]. A priori, all the components present in CL have to be envisaged in EL.

To end up, we underline the analyses does not consider more complex situation such as reabsorption of the emission, transfer process, etc. Moreover, it is well known that a luminescent species can have a slightly different emission spectrum depending on its environment, being chemically or physically modified. This is of particular importance in semi-crystalline polymer like PP where the microstructure changes on a micrometer scale. This can explain some slight changes in the emission spectra in addition with some experimental parameters that can differ, i.e. width of the entrance slit of the dispersive system, etc.

5.5 Conclusion

Electroluminescence (EL) and Cathodoluminescence (CL) of Polyethylene and Polypropylene, along with two other aromatic polyesters, have been recorded and compared. We have shown that the CL and EL spectra of PP along with PE involves several bands already identified with other excitation sources and related to carbonyl and unsaturated groups. Cathodoluminescence is a reproduction of electroluminescence for insulating polymer. Emission spectra of PE and PP exhibit the same contributing processes, pointing towards chain defects and degradation products as luminescent species. The common and unique feature of EL and CL spectra is the appearing of a band at about 570 nm, inferring that they derive from the same luminescence mechanisms and physical/chemical processes due to the same unsaturated groups.

The elementary components in both EL and CL spectra of polyolefin materials are identified. Eventually we quantitatively reconstruct the EL and CL spectra on the basis of elementary components: Fluorescence, Chemiluminescence, Recombination-induced Luminescence, and a luminescence peak associated to electrical ageing. The reconstruction spectra fit quite well with the CL and EL spectra. The analyses of spectra components uncover the nature of electroluminescence and generic electrical ageing mechanisms in insulating polymers, especially the initiation of electrical ageing through location at chemical structures of nano-scale in the materials.

General Conclusion and Perspecctives

General conclusion

Electroluminescence and cathodoluminescence along with other luminescence-family techniques are carried out for probing polyolefins, i.e. Polyethylene and Polypropylene and other insulating polymers, i.e. aromatic polyesters - Polyethylene Naphthalte and Polyether Ether Ketone.

The firstly chapter reviews the advanced experimental and theoretical achievements on luminescence mechanisms and electrical ageing, degradation and breakdown processes. The insulating polymers and their electrical applications are introduced. Luminescence with different excitation sources such as photoluminescence (optical excitation) - fluorescence and phosphorescence, electroluminescence (electric field excitation), cathodoluminescence (electron beam excitation), chemiluminescence (plasmas induced chemical oxidation processes), and recombination induced luminescence (plasmas induced recombination processes) are reviewed and their mechanisms and physical/chemical processes are demonstrated. In addition, Surface Plasmons (SPs) are demonstrated as an unavoidable electrode-dielectric interface process. The concept, classification and mechanisms of electrical ageing, degradation and breakdown are presented and analyzed. The diagnostic methods for pre-breakdown signs are reviewed, such as partial discharge detection, space charge diagnostic methods and luminescence techniques. The relationship between electrical ageing and electroluminescence are described and analyzed. The onset of electroluminescence is exactly the threshold of electrical ageing. Spectral analyses is an elegant way to represent the physical and chemical processes in the materials under stress and to uncover the relationship between electroluminescence and electrical ageing.

Chapter two presents the experimental materials and techniques used in the work. Polyolefin materials, cross-linked Polyethylene (XLPE), additive-free low density Polyethylene (LDPE), Bi-axially Oriented Polypropylene (BOPP), and aromatic polyesters -Polyethylene Naphthalte and Polyether Ether Ketone and their chemical structures are introduced. The setups for gold and Indium Tin Oxide (ITO) metallization are described. The electrical and optical properties such as thickness, transparency and electric resistance per centimeter of gold and ITO are demonstrated. The luminescence diagnostic system with different excitation sources and other inspection equipment are illustrated.

Chapter three is a topic on excitons formation in polyolefin films under electric stress and its relationship to electrical degradation. Sandwich structures with BOPP are carried out and analyzed under both DC and AC stress. Field dependence, phase-resolved EL and spectral analyses are carried out and discussed. Spectral analyses of Polypropylene is compared to that of Polyethylene. The same spectral main peak at approximately 570 nm of them infers that the similar chemical structures and defect of them and EL in polyolefins follow the same physical or chemical route under electrical field.

In order to uncover the nature of electrode effect during EL measurement chapter four is investigated on electroluminescence of Polyethylene Naphthalte (PEN). The electrode interface effects in other polymers such as Polypropylene are also discussed. The Surface Plasmons and/or interface state can be considered the source of the red component emission at approximately 750 nm in EL spectra.

Further thorough study is carried out in chapter five on cathodoluminescence of above-mentioned insulating polymers. Thin films of PP, PE, along PEN and PEEK were irradiated under electron beam up to 5 keV to be excited. We could reconstruct EL and CL spectra of both PE and PP using four elementary components: i.e. Fluorescence, Chemiluminescence, Recombination-induced Luminescence, and main component of the EL spectrum at 570nm reported above and constituting an ageing marker. For the first time the nature of both EL and CL in polyolefins is uncovered, containing four basic components with different relative contributions. Identification of these spectral components is helpful to interpret the nature of light emission from polyolefins and other insulating polymers and to bridge the gap between space charge distribution and electrical ageing or breakdown.

Through researches on EL and CL in several insulating polymers, i.e. polyolefins and aromatic polyesters, excitons formation and relaxation processes under electric stress and kinetic electrons are evidenced. More importantly, the spectral components analyses and reconstruction uncovers the nature of luminescence and its correlation to the initiation electrical ageing. In the future, luminescence measurement can be developed to be a standard method to probe and analyze insulating polymers.

Future works

Future works are recommended to further enhance the understanding of electroluminescence and electrical ageing. The diagnostic method for initiation of electrical ageing under electric stress is of significance. Electroluminescence is an elegant way to evidence and uncover the mechanisms of initiation of electrical ageing.

1. The EL intensity under AC stress is much stronger than that under DC stress. Experimental and simulations are interesting to carry out for comparison of EL between under DC stress and under AC stress.
2. It is still of great significance to locate the luminescent centers in accurate chemical groups. The chemical groups in the carbon bone chains and residual are interesting to investigate.
3. More works should be carried out to apply the EL techniques on checking the state of ageing of system in service.

Annexes

Annexe A: Space charge diagnostic methods

Table 0-1 Overview of space charge diagnostic methods, r is the method's resolution, t the sample thickness, adapted from [123].

Method	Disturbance	Scan mechanism	Detection process	r(μm)	t (μm)
Thermal pulse method	Absorption of short light pulse in front electrode	Diffusion according to heat conduction equations	Voltage change across sample	≥2	≈200
Laser intensity modulation method (LIMM)	Absorption of modulated light in front electrode	Frequency-dependent steady-state heat profile	Current between sample electrodes	≥2	≈25
laser induced pressure pulse method (LIPP)	Absorption of short laser light pulse in front electrode	Propagation with longitudinal sound velocity	Current between sample electrodes	1	100-1000
Thermo-elastically generated LIPP	Absorption of short laser light pulse in thin buried layer	Propagation with longitudinal sound velocity	Current or voltage between sample electrodes	1	50-70
Pressure wave propagation method	Absorption of short laser light pulse in metal target	Propagation with longitudinal sound velocity	Voltage or current between sample electrode	10	5-200
Non-structured acoustic pulse method	HV spark between conductor and metal diaphragm	Propagation with longitudinal sound velocity	Voltage between sample electrode	1000	≤10000
Laser generated acoustic pulse method	Absorption of short laser light pulse in thin paper target	Propagation with longitudinal sound velocity	Voltage between sample	50	≤3000
Acoustic probe method	Absorption of short laser light pulse in thin paper target	Propagation with longitudinal sound velocity	Between sample electrodes	200	2000-6000
Piezo-electrically generated pressure step method	Electrical excitation of piezoelectric quartz plate	Propagation with longitudinal sound velocity	Current between sample electrodes	1	25
Thermal step method	Applying two isothermal sources across sample	Thermal expansion of the sample	Current between sample electrodes	150	2000-20000
Electro-acoustic pulse method (PEA)	Force of modulated electric field on charges in sample	Propagation with longitudinal sound velocity	Piezoelectric transducer at sample electrode	100	≤10000
Photoconductivity method	Absorption of narrow light beam in sample	External movement of light beam	Current between sample electrodes	≥1.5	-
Space charge mapping	Interaction of polarized light with field	Parallel illumination of sample volume or movement of light beam or sample	Photographic record	200	-
Spectroscopic measurement	Absorption of exciting radiation in sample	External movement of radiation source or sample	Relative change in the observed spectrum	≥50	-
Field probe method	None	Capacitive coupling to the field	Current	1000	≤20000

*Some parameters have been advanced with the developments of the techniques.

Annexe B: Space charge transport and trapping theory

Profiting by the development of the space charge measurement methods not only in space but also in time scale, a lot of works on space charge distribution measurement and simulation have been carried out. In recent years, the rapid development of computing facilities and database also make contributions to the space charge analyses.

Theoretical models for charge transport in insulating crystals were reported in pioneering work by Mott and Gurney [159], which provided a mechanism for space charge limited currents (SCLC). Among these space charge transport theories, bipolar charge transport (BCT) model has been widely used to simulate time or space evolution of space charges in insulating polymers. It is performed to investigate the relationship between space charge accumulation and conduction, electroluminescence, charge packet formation, electrical breakdown, and surface potential decay properties, etc.

The value of the forbidden gap (between conduction band and valence band, seen in Figure 0-1 and Figure 0-2) in insulating alkanes, such as PE and PP, as derived from calculation or experimental measurement, is approximately 9 eV. The theoretical and ideal conductivity in pure insulating alkanes should be very low at 10^{-45} S/m. However, due to chemical disorders or amorphous phase, by products, impurities, and defects, there exist many trapping centers in the insulating polymers. As a consequence, trapping and de-trapping processes can be possible. These shallow traps and deep traps make critical contributions to the transport, trapping, de-trapping, and recombination processes of space charge.

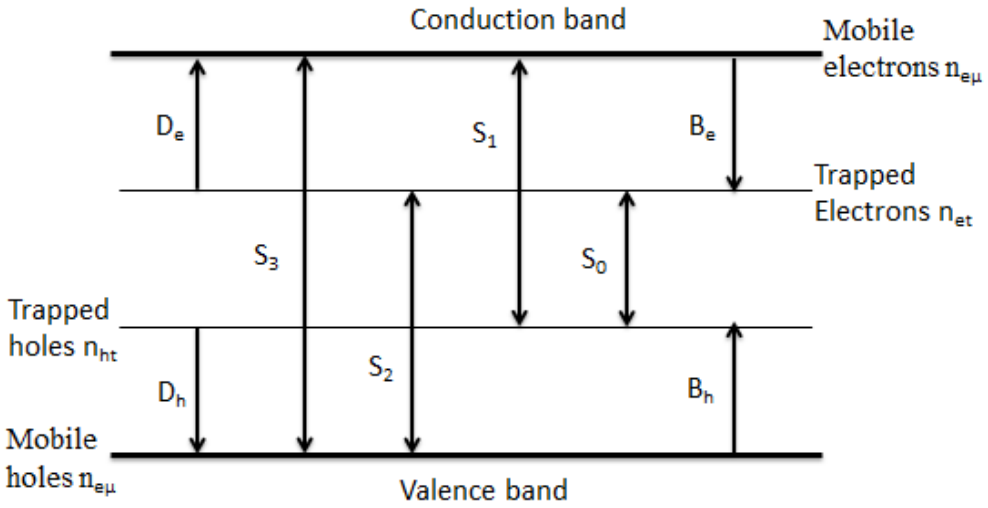

Figure 0-1 Bi-polar model. Conduction is by free charges in transport level - conduction band, associated with an effective mobility. "S", "B", and "D" stand for recombination, trapping and de-trapping coefficients respectively. "n" is the carriers density in transport and trapping levels.

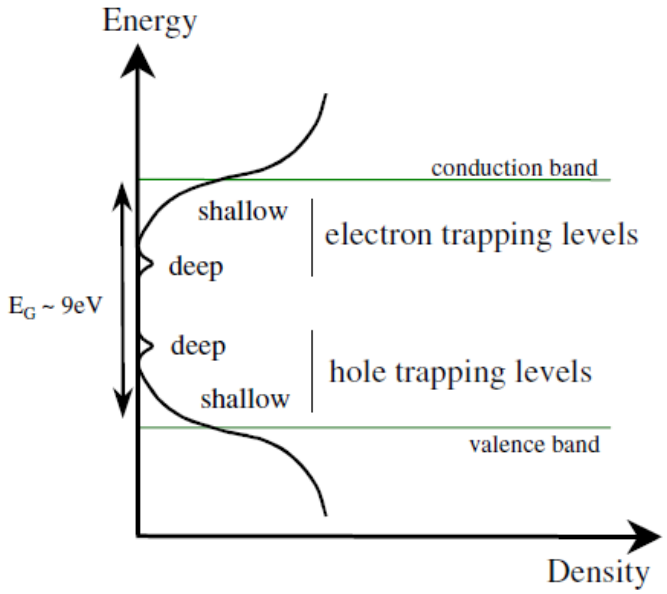

Figure 0-2 Schematic representation of density of state in a disordered material. Shallow and deep traps are related to physical and chemical disorder respectively, taken from [28].

The recombination process of space charge can be indirectly proved by detecting the light emission in insulating polymers under electric field. The light emission process in insulating polymers can be represented using space charge recombination model as shown in Figure 0-3 involving thermal de-trapping and tunneling processes to recombination [160-163].

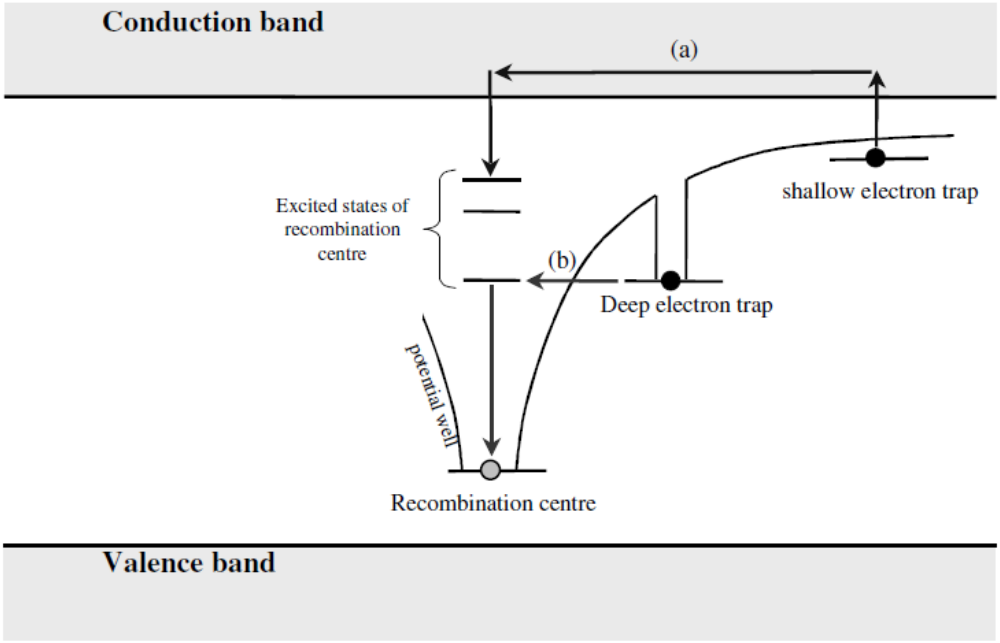

Figure 0-3 Charge recombination processes: (a) thermal de-trapping; (b) tunneling, from [51].

The nature of conduction process or transport of charges in insulating polymers is still the matter of debate. With the development of computing tools, understanding of space charge mechanisms, and the improvement of advanced investigation techniques, more and more theories have been uncovered and developed.

Aside those space charge diagnostic methods presented above, diagnositc methods through electroluminescence along with other luminescence techniques have been pushed as a new way to understand the phenomenon of charge injection and transport in dielectrics and its links with the degradation and ageing under divergent field and uniformed field [66, 164].

Annexe C: Some interesting phase-resolved EL

The PEN films metalized with gold were applied with three waveforms of voltage: sinusoidal (in Figure 0-4), triangle (in Figure 0-5 and Figure 0-6) and square (in Figure 0-7 and Figure 0-8). The three waveforms of voltage are generated by a pulse/function generator, amplified by a high voltage amplifier and display on an oscilloscope, which are demonstrated in chapter 2.

Interestingly, the three waveforms of voltage can be carried out to uncover the phase-resolved EL in insulating polymers. The triangle and square voltage are also of alternative current (AC) but at very special situations. Their differences are the rates of change of voltage (R_v):

a) The R_v of sinusoidal voltage follows the curve of sinusoidal curve.
b) The R_v of triangle voltage is a fixed value.
c) The R_v of square voltage is at the maximum (according to the rate of voltage-change of the pulse/function generator) at the beginning of each half period and zero during each half period.

The crest of EL under triangle voltage of different frequency and intensity is always at the field positive-negative change time. The rate of change of triangle voltage is at a very low value about 3-10 $kV \cdot mm^{-1} \cdot s^{-1}$. The crest of EL under square voltage delays with the increment of field and the frequency. However, the relative delay time should be the same at different frequency under the same electric field. The electrode-insulation-electrode is like a capacitor. For the power supply, there is a maximum current, I_{max} at 20 mA, that it can support. Under electrical voltage, the current, $I = C\frac{dv}{dt}$, where C is the capacitivity of the material, $I \leq I_{max}$.

However, there appears advancement of EL crest under sinusoidal voltage. The phase-resolved EL under sinusoidal voltage in insulating polymers consists of multiple mechanisms. These results based on the rate of voltage-change can be supplementary to study the advancement mechanisms of phase-resolved EL under sinusoidal voltage.

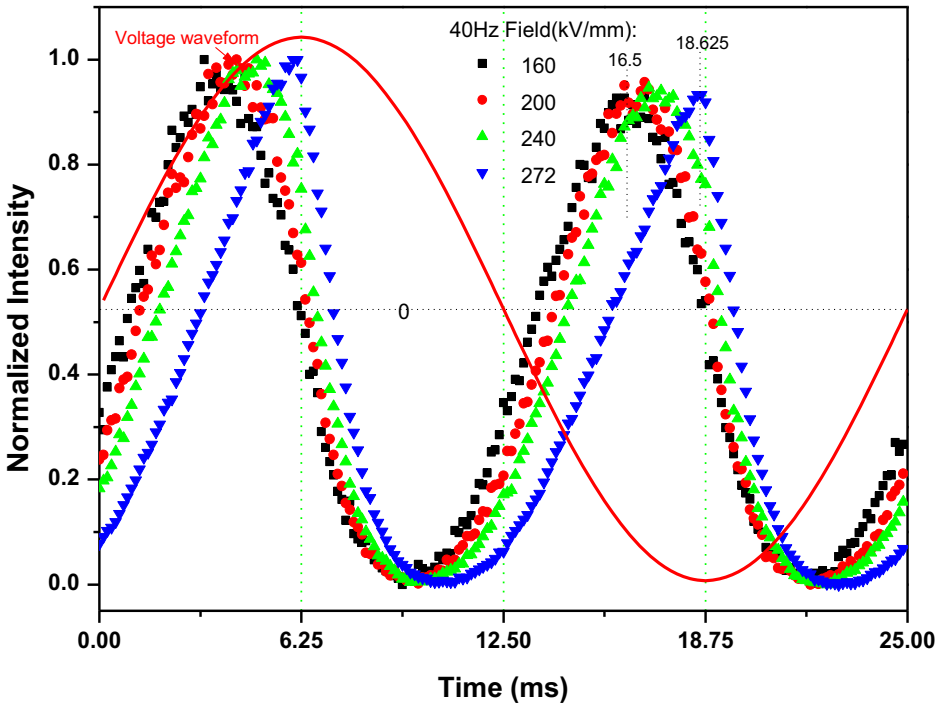

Figure 0-4 Au-PEN-Au under sinusoidal voltage.

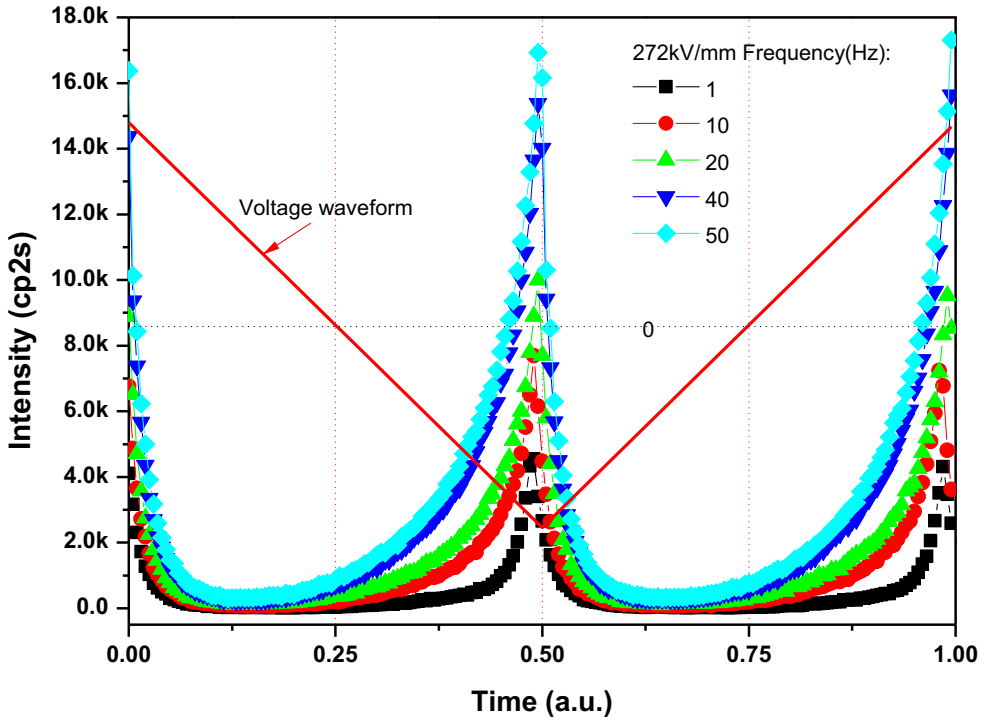

Figure 0-5 Au-PEN-Au under triangle voltage at different frequency.

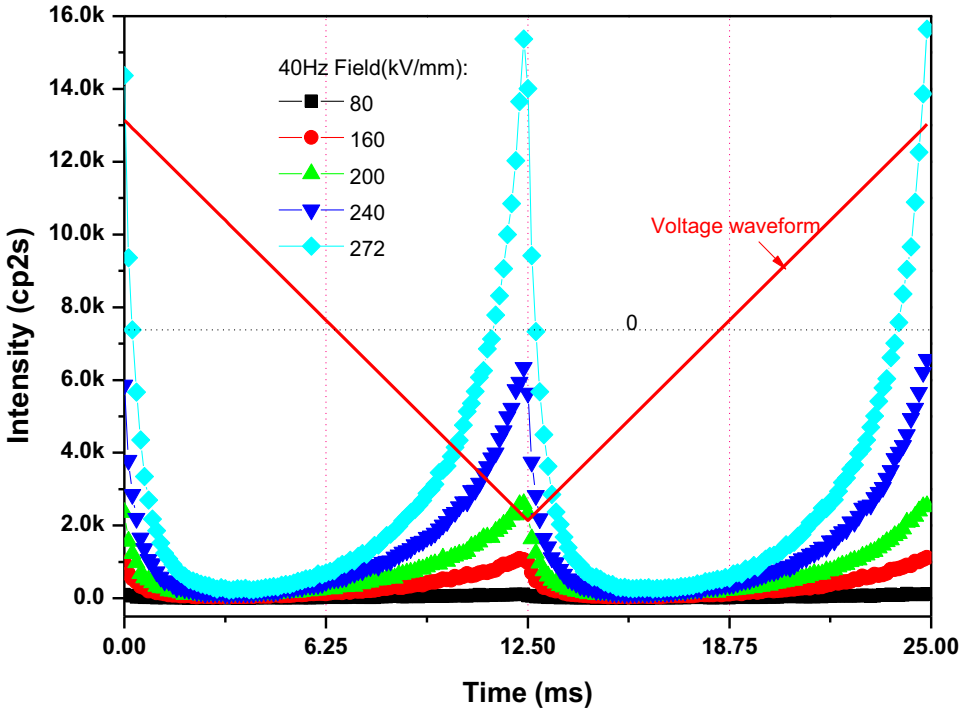

Figure 0-6 Au-PEN-Au under triangle voltage at different field.

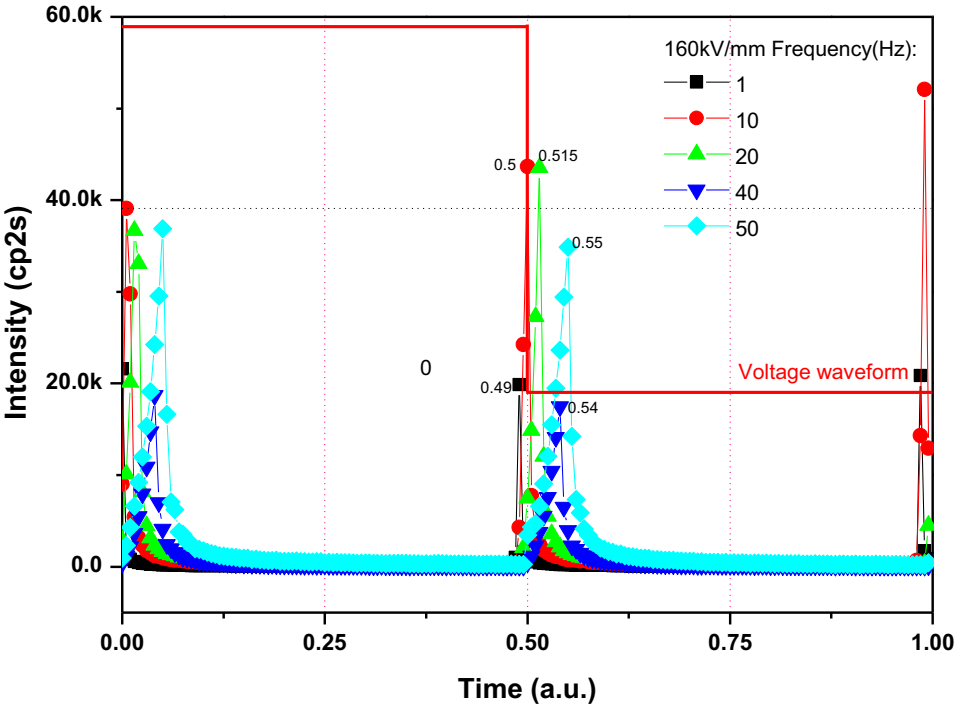

Figure 0-7 Au-PEN-Au under square voltage at different frequency.

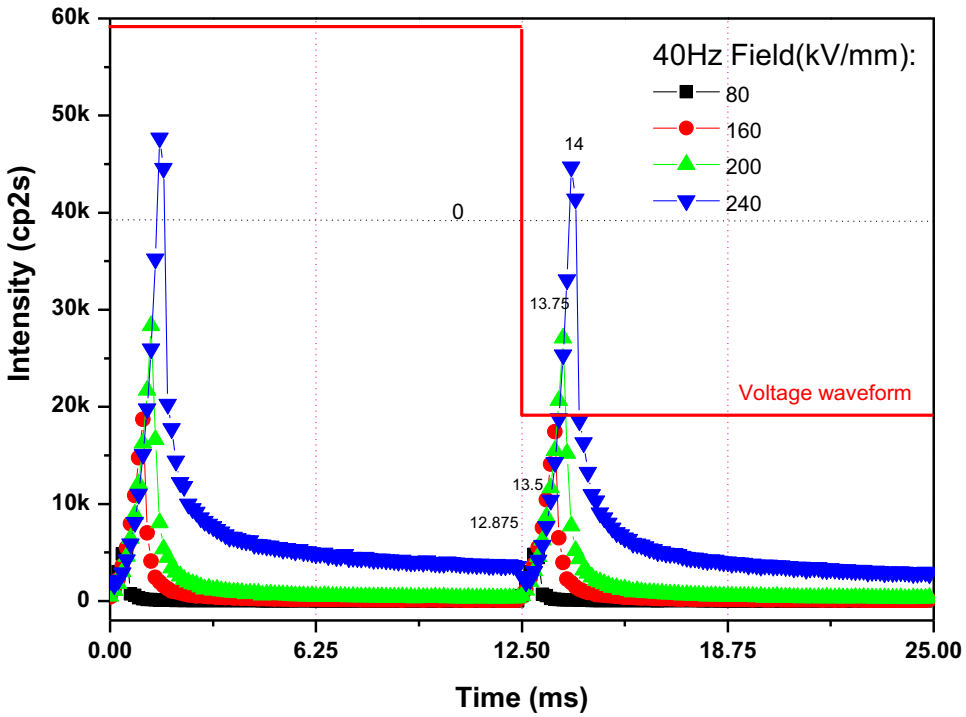

Figure 0-8 Au-PEN-Au under square voltage at different field.

List of Figures

List of Tables

References

[1] G. Teyssedre and C. Laurent, "Advances in high-field insulating polymeric materials over the past 50 years," *IEEE Electr. Insul. Mag.,* vol. 29, pp. 26-36, 2013.

[2] C. Reed, "Advances in polymer dielectrics over the past 50 years," *IEEE Electr. Insul. Mag.,* vol. 29, pp. 58-62, 2013.

[3] W. A. Hartman and H. L. Armstrong, "Electroluminescence in organic polymers," *J. Appl. Phys.,* vol. 38, pp. 2393-2395, 1967.

[4] C. Laurent and G. Teyssedre, "Hot electron and partial-discharge induced ageing of polymers," *Nucl. Instrum. Meth. B,* vol. 208, pp. 442-447, 2003.

[5] E. Aubert, G. Teyssedre, C. Laurent, S. Rowe, and S. Robiani, "Electrically active defects in silica-filled epoxy as revealed by light emission analysis," *J. Phys. D: Appl. Phys.,* vol. 42, p. 165501, 2009.

[6] M. Reading, "An investigation into the structure and properties of polyethylene oxide nanocomposites," Doctoral, School of Electronics and Computer Science, University of Southampton, 2010.

[7] C. Laurent, F. Massines, and C. Mayoux, "Optical emission due to space charge effects in electrically stressed polymers," *IEEE Trans. Dielectr. Electr. Insul.,* vol. 4, pp. 585-603, 1997.

[8] C. K. Chiang, C. R. Fincher, Y. W. Park, A. J. Heeger, H. Shirakawa, E. J. Louis*, et al.*, "Electrical conductivity in doped polyacetylene," *Phys. Rev. Lett.,* vol. 39, pp. 1098-1101, 1977.

[9] R. H. Friend, R. W. Gymer, A. B. Holmes, J. H. Burroughes, R. N. Marks, C. Taliani*, et al.*, "Electroluminescence in conjugated polymers," *Nature,* vol. 397, pp. 121-128, 1999.

[10] D. D. C. Bradley, "Conjugated polymer electroluminescence," *Synth. Met.,* vol. 54, pp. 401-415, 1993.

[11] H. Becker, S. E. Burns, and R. H. Friend, "Effect of metal films on the photoluminescence and electroluminescence of conjugated polymers," *Phys. Rev. B,* vol. 56, pp. 1893-1905, 1997.

[12] D. S. Ginger and N. C. Greenham, "Charge injection and transport in films of CdSe nanocrystals," *J. Appl. Phys.,* vol. 87, pp. 1361-1368, 2000.

[13] P. W. M. Blom and M. Vissenberg, "Charge transport in poly(p-phenylene vinylene) light-emitting diodes," *Materials Science & Engineering R-Reports,* vol. 27, pp. 53-94, 2000.

[14] U. Mitschke and P. Bauerle, "The electroluminescence of organic materials," *J. Mater. Chem.,* vol. 10, pp. 1471-1507, 2000.

[15] B. Ruhstaller, S. A. Carter, S. Barth, H. Riel, W. Riess, and J. C. Scott, "Transient and steady-state behavior of space charges in multilayer organic light-emitting diodes," *J. Appl. Phys.,* vol. 89, pp. 4575-4586, 2001.

[16] S. Reineke, F. Lindner, G. Schwartz, N. Seidler, K. Walzer, B. Luessem*, et al.*, "White organic light-emitting diodes with fluorescent tube efficiency," *Nature,* vol. 459, pp. 234-U116, 2009.

[17] Y.-S. Tyan, "Organic light-emitting-diode lighting overview," *Journal of Photonics for Energy,* vol. 1, 2011.

[18] B. Qiao, "Synthesis of ZnO quantum dots and applications in organic light emitting diodes based on MEH-PPV," Master, School of Science, Beijing Jiaotong University, Beijing, 2012.

[19] M. Aredes, C. Portela, and F. C. Machado, "A 25-MW soft-switching HVDC tap for ±500-kV transmission lines," *ITPD,* vol. 19, pp. 1835-1842, 2004.

[20] T. T. N. Vu, G. Teyssedre, B. Vissouvanadin, S. Le Roy, C. Laurent, M. Mammeri*, et al.*, "Electric field profile measurement and modeling in multi-dielectrics for HVDC application," in *IEEE Int. Conf. Sol. Dielectr. (ICSD)*, pp. 413-416, 2013.

[21] L. Yan and C. Zhe, "A flexible power control method of vsc-hvdc link for the enhancement of effective short-circuit ratio in a hybrid multi-infeed hvdc system," *IEEE Transactions on Power Systems,* vol. 28, pp. 1568-1581, 2013.

[22] G. C. Montanari, L. A. Dissado, and S. Serra, "The hidden threat to hvdc polymeric insulation at design field: Solitonic conduction," *IEEE Electr. Insul. Mag.,* vol. 30, pp. 39-50, 2014.

[23] T. Lueth, M. M. C. Merlin, T. C. Green, F. Hassan, and C. D. Barker, "High-frequency operation of a dc/ac/dc system for hvdc applications," *ITPE,* vol. 29, pp. 4107-4115, 2014.

[24] K. N. Mathes, "A brief history of development in electrical insulation," in *Proc. Electr. Electron. Insul. Conf.*, pp. 147-150, 1991.

[25] T. L. Hanley, R. P. Burford, R. J. Fleming, and K. W. Barber, "A general review of polymeric insulation for use in HVDC cables," *IEEE Electr. Insul. Mag.,* vol. 19, pp. 13-24, 2003.

[26] L. Qi, L. Petersson, and T. Liu, "Review of recent activities on dielectric films for capacitor applications," *Journal of International Council on Electrical Engineering,* vol. 4, pp. 1-6, 2014.

[27] L. Weimers, "HVDC Light: A New Technology for a Better Environment," *IEEE Power Engineering Review,* vol. 18, pp. 19-20, 1998.

[28] G. Teyssedre and C. Laurent, "Charge transport modeling in insulating polymers: from molecular to macroscopic scale," *IEEE Trans. Dielectr. Electr. Insul.,* vol. 12, pp. 857-875, 2005.

[29] J. K. Nelson and J. C. Fothergill, "Internal charge behaviour of nanocomposites," *Nanotechnology,* vol. 15, p. 586, 2004.

[30] G. Teyssedre, G. Tardieu, and C. Laurent, "Characterisation of crosslinked polyethylene materials by luminescence techniques," *JMatS,* vol. 37, pp. 1599-1609, 2002.

[31] G. Teyssedre, C. Laurent, P. Jonnard, and C. Bonnelle, "Comparison between photo-, cathodo-, and electro-luminescence spectra of polyethylene naphthalate films and relationship with electrical aging," in *Proc. IEEE Conf. Electr. Insul. Dielectr. Phenom. (CEIDP)*, pp. 543-546 vol.2, 2000.

[32] N. Shimizu, H. Katsukawa, M. Miyauchi, M. Kosaki, and K. Horii, "The space charge behavior and luminescence phenomena in polymers at 77 k," *IEEE Trans. Electr. Insul.,* vol. EI-14, pp. 256-263, 1979.

[33] T. Lebey, C. Laurent, and C. Mayoux, "Charge injection and electroluminescence threshold field in polymeric material under degradation ac field," presented at the Proc. Symp. Electr. Insul. Mat., 1988.

[34] T. Lebey and C. Laurent, "Charge injection and electroluminescence as a prelude to dielectric breakdown," *J. Appl. Phys.,* vol. 68, pp. 275-282, 1990.

[35] H. Yamamoto, M. Mikami, and S. Nakamura, "Nonlinear cathodoluminescence from insulators," *J. Lumin.,* vol. 102-103, pp. 782-784, 2003.

[36] M. Kuttge, W. Cai, F. García de Abajo, and A. Polman, "Dispersion of metal-insulator-metal plasmon polaritons probed by cathodoluminescence imaging spectroscopy," *Phys. Rev. B,* vol. 80, 2009.

[37] L. J. Brillson, "Applications of depth-resolved cathodoluminescence spectroscopy," *J. Phys. D: Appl. Phys.,* vol. 45, p. 183001, 2012.

[38] G. Teyssedre, L. Cisse, C. Laurent, F. Massines, and P. Tiemblo, "Spectral analysis of optical emission due to isothermal charge recombination in polyolefins," *IEEE Trans. Dielectr. Electr. Insul.,* vol. 5, pp. 527-535, 1998.

[39] G. Teyssedre, C. Laurent, G. Perego, and G. C. Montanari, "Charge recombination induced luminescence of chemically modified cross-linked polyethylene materials," *IEEE Trans. Dielectr. Electr. Insul.,* vol. 16, pp. 232-240, 2009.

[40] J. Jonsson, B. Ranby, C. Laurent, and C. Mayoux, "Influence of thermal and UV aging on electroluminescence of polypropylene films," *IEEE Trans. Dielectr. Electr. Insul.,* vol. 3, pp. 148-152, 1996.

[41] R. C. Smith, C. Liang, M. Landry, J. K. Nelson, and L. S. Schadler, "The mechanisms leading to the useful electrical properties of polymer nanodielectrics," *IEEE Trans. Dielectr. Electr. Insul.,* vol. 15, pp. 187-196, 2008.

[42] C. Laurent, G. Teyssedre, S. Le Roy, and F. Baudoin, "Charge dynamics and its energetic features in polymeric materials," *IEEE Trans. Dielectr. Electr. Insul.,* vol. 20, pp. 357-381, 2013.

[43] G. Blasse, B. Grabmaier, and B. Grabmaier, *Luminescent materials* vol. 44: Springer-Verlag Berlin, 1994.

[44] M. Pope, H. P. Kallmann, and P. Magnante, "Electroluminescence in organic crystals," *The Journal of Chemical Physics,* vol. 38, pp. 2042-2043, 1963.

[45] G. Teyssedre and C. Laurent, "Evidence of hot electron-induced chemical degradation in electroluminescence spectra of polyethylene," *J. Appl. Phys.,* vol. 103, p. 046107, 2008.

[46] B. Qiao, C. Laurent, and G. Teyssedre, "Evidence of exciton formation in thin polypropylene films under AC and DC fields and relationship to electrical degradation," in *Proc. Int. Symp. Electr. Insul. Mat.*, pp. 81-84, 2014.

[47] A. A. El-Saftawy, S. A. A. El Aal, M. S. Ragheb, and S. G. Zakhary, "Studying electron-beam-irradiated PET surface wetting and free energy," *Nucl. Instrum. Meth. B,* vol. 322, pp. 48-53, 2014.

[48] D. Mary, G. Teyssedre, and C. Laurent, "Electroluminescence in saturated polyesters: Temperature dependence and correlation with space charge measurements," in *Proc. IEEE Conf. Electr. Insul. Dielectr. Phenom. (CEIDP)*, pp. 201-204, 2003.

[49] C. Laurent, "Optical prebreakdown warnings in insulating polymers," *IEEE Electr. Insul. Mag.,* vol. 15, pp. 5-13, 1999.

[50] L. Chen, T. D. Huan, C. Wang, and R. Ramprasad, "Unraveling the luminescence signatures of chemical defects in polyethylene," *arXiv preprint arXiv:1503.06688,* 2015.

[51] G. Tardieu, G. Teyssedre, and C. Laurent, "Role of additives as recombination centres in polyethylene materials as probed by luminescence techniques," *J. Phys. D: Appl. Phys.,* vol. 35, pp. 40-47, 2002.

[52] R. Coehoorn, H. van Eersel, P. A. Bobbert, and R. A. J. Janssen, "Kinetic Monte Carlo Study of the Sensitivity of OLED Efficiency and Lifetime to Materials Parameters," *Adv. Funct. Mater.,* vol. 25, pp. 2024-2037, 2015.

[53] L. Ke, H. Liu, M. Yang, Z. Jiao, and X. Sun, "Degradation analysis of Alq(3)-based OLED from noise fluctuations with different driving modes," *Chem. Phys. Lett.,* vol. 623, pp. 68-71, 2015.

[54] R. Singh, K. N. N. Unni, A. Solanki, and Deepak, "Improving the contrast ratio of OLED displays: An analysis of various techniques," *Opt. Mater.,* vol. 34, pp. 716-723, 2012.

[55] H. Sasabe and J. Kido, "Development of high performance OLEDs for general lighting," *Journal of Materials Chemistry C,* vol. 1, pp. 1699-1707, 2013.

[56] B. He, Z. Chang, Y. Jiang, B. Chen, P. Lu, H. S. Kwok*, et al.*, "Impacts of intramolecular B-N coordination on photoluminescence, electronic structure and electroluminescence of tetraphenylethene-based luminogens," *Dyes and Pigments,* vol. 101, pp. 247-253, 2014.

[57] M. R. Andersson, G. Yu, and A. J. Heeger, "Photoluminescence and electroluminescence of films from soluble PPV-polymers," *Synth. Met.,* vol. 85, pp. 1275-1276, 1997.

[58] B. Qiao, C. Laurent, and G. Teyssedre, "Evidence of exciton formation in thin polypropylene films under ac and dc field and relationship to electrical degradation," *IEEJ Transactions on fundamental and materials,* accepted, 2015.

[59] C. Laurent and C. Mayoux, "Light detection during the initiation of electrical treeing at room temperature," *J. Phys. D: Appl. Phys.,* vol. 14, pp. 1903-1910, 1981.

[60] S. S. Bamji, A. T. Bulinski, and R. J. Densley, "Evidence of near-ultraviolet emission during electrical-tree initiation in polyethylene," *J. Appl. Phys.,* vol. 61, p. 694, 1987.

[61] T. Mizuno, Y. S. Liu, W. Shionoya, M. Okada, K. Yasuoka, S. Ishii*, et al.*, "Electroluminescence from surface layer of insulating polymer under ac voltage application," *IEEE Trans. Dielectr. Electr. Insul.,* vol. 5, pp. 903-908, 1998.

[62] Z. Guan-Jun, S. Yan, Z. Wen-Bin, and Y. Zhang, "Surface electroluminescence phenomena of insulating polymers," in *Proc. IEEE Conf. Electr. Insul. Dielectr. Phenom. (CEIDP)*, pp. 253-256, 2003.

[63] D. Mary, G. Teyssedre, L. Cisse, and C. Laurent, "Electroluminescence emission imaging in insulating polymers under uniform field configuration," in *Proc. IEEE Int. Conf. Cond. Break. Soli. Dielectr.*, pp. 261-264, 1998.

[64] M. Kosaki, N. Shimizu, and K. Horii, "Treeing of Polyethylene at 77k," *IEEE Trans. Electr. Insul.,* vol. 12, pp. 40-45, 1977.

[65] N. Shimizu, M. Kosaki, and K. Horii, "Space charge effect on local electric breakdown of polyethylene at 77 K," *J. Appl. Phys.,* vol. 48, pp. 2191-2195, 1977.

[66] C. Laurent and C. Mayoux, "Analysis of the propagation of electrical treeing using optical and electrical methods," *IEEE Trans. Electr. Insul.,* vol. 15, pp. 33-42, 1980.

[67] C. Laurent, C. Mayoux, and S. Noel, "Mechanisms of electroluminescence during aging of polyethylene," *J. Appl. Phys.,* vol. 58, p. 4346, 1985.

[68] S. S. Bamji, A. T. Bulinski, and R. J. Densley, "The role of polymer interface during tree initiation in ldpe," *IEEE Trans. Electr. Insul.,* vol. 21, pp. 639-644, 1986.

[69] S. S. Bamji, A. T. Bulinski, H. Suzuki, M. Matsuki, and Z. Iwata, "Luminescence in crosslinked polyethylene at elevated temperatures," *J. Appl. Phys.,* vol. 74, p. 5149, 1993.

[70] G. C. Stone and R. G. Van Heeswijk, "Electroluminescence from epoxy insulation under impulse voltage," in *Proc. IEEE Conf. Electr. Insul. Dielectr. Phenom. (CEIDP)*, pp. 376-381, 1988.

[71] D. Mary, C. Laurent, J. Guastavino, E. Krause, and C. Mayoux, "Electroluminescence and high-field conduction in poly(ethylene-2, 6-naphthalate)," in *Proc. IEEE Conf. Electr. Insul. Dielectr. Phenom. (CEIDP)*, pp. 298-303, 1994.

[72] T. Mizuno, Y. S. Liu, W. Shionoya, K. Yasuoka, S. Ishii, H. Miyata*, et al.*, "Electroluminescence in insulating polymers in ac electric fields," *IEEE Trans. Dielectr. Electr. Insul.,* vol. 4, pp. 433-438, 1997.

[73] P. Canet, C. Laurent, J. Akinnifesi, and B. Despax, "Light emission from metal-insulator-metal structures," *J. Appl. Phys.,* vol. 73, p. 384, 1993.

[74] P. Tiemblo, J. M. Gomez-Elvira, G. Teyssedre, F. Massines, and C. Laurent, "Chemiluminescence spectral evolution along the thermal oxidation of isotactic polypropylene," *Polym. Degrad. Stab.,* vol. 65, pp. 113-121, 1999.

[75] P. Tiemblo, J. M. Gomez-Elvira, G. Teyssedre, F. Massines, and C. Laurent, "Correlation between polypropylene microstructure, cold plasma interaction and subsequent luminescent emission," *Polym. Int.,* vol. 46, pp. 33-41, 1998.

[76] P. Tiemblo, J. M. Gomez-Elvira, G. Teyssedre, and C. Laurent, "Degradative luminescent processes in atactic polypropylene - I. Chemiluminescence along the thermooxidation," *Polym. Degrad. Stab.,* vol. 66, pp. 41-47, 1999.

[77] P. Tiemblo, J. M. Gomez-Elvira, G. Teyssedre, and C. Laurent, "Degradative luminescent processes in atactic polypropylene II. Chemiluminescence after a cold He plasma attack at-180 degrees C," *Polym. Degrad. Stab.,* vol. 68, pp. 353-362, 2000.

[78] P. Tiemblo, J. M. Gomez-Elvira, G. Teyssedre, F. Massines, and C. Laurent, "Effect of a cold helium plasma at -180 degrees C on polyolefin films - I. Plasma induced luminescence features of polyethylene and polypropylene," *Polym. Degrad. Stab.,* vol. 64, pp. 59-66, 1999.

[79] P. Tiemblo, J. M. Gomez-Elvira, G. Teyssedre, F. Massines, and C. Laurent, "Effect of a cold helium plasma at -180 degrees C on polyolefin films - II. The chemiluminescence component," *Polym. Degrad. Stab.,* vol. 64, pp. 67-73, 1999.

[80] G. Teyssedre, D. Mary, J. L. Auge, and C. Laurent, "Dependence of electroluminescence intensity and spectral distribution on ageing time in polyethylene naphthalate as modelled by space charge modified internal field," *J. Phys. D: Appl. Phys.,* vol. 32, pp. 2296-2305, 1999.

[81] N. Hozumi, G. Teyssedre, C. Laurent, and K. Fukunaga, "Behaviour of space charge correlated with electroluminescence in cross-linked polyethylene," *J. Phys. D: Appl. Phys.,* vol. 37, pp. 1327-1333, 2004.

[82] S. S. Bamji, A. T. Bulinski, and M. Abou-Dakka, "Luminescence and space charge in polymeric dielectrics - [whitehead memorial lecture (2008)]," *IEEE Trans. Dielectr. Electr. Insul.,* vol. 16, pp. 1376-1392, 2009.

[83] S. S. Bamji, "Luminescence and space charge phenomena in polymeric dielectrics," in *Proc. IEEE Conf. Electr. Insul. Dielectr. Phenom. (CEIDP)*, pp. 1-12, 2008.

[84] A. M. Ariffin, P. L. Lewin, and S. J. Dodd, "Electroluminescence measurements of low-density polyethylene (LDPE) films subjected to high electrical stresses in different gas environments," *IEEE Trans. Dielectr. Electr. Insul.,* vol. 18, pp. 130-139, 2011.

[85] F. Baudoin, D. H. Mills, P. L. Lewin, S. Le Roy, G. Teyssedre, and C. Laurent, "Modeling electroluminescence in insulating polymers under ac stress: effect of excitation waveform," *J. Phys. D: Appl. Phys.,* vol. 44, p. 165402, 2011.

[86] F. Baudoin, D. H. Mills, P. L. Lewin, S. Le Roy, G. Teyssedre, and C. Laurent, "Modelling electroluminescence in insulating polymers under sinusoidal stress: Effect of applied voltage, frequency and offset," in *Proc. IEEE Conf. Electr. Insul. Dielectr. Phenom. (CEIDP)*, pp. 820-823, 2011.

[87] F. Baudoin, D. H. Mills, P. L. Lewin, S. Le Roy, G. Teyssedre, C. Laurent*, et al.*, "Modelling electroluminescence in insulating polymers under ac stress: effect of voltage offset and pre-stressing," *J. Phys. D: Appl. Phys.,* vol. 45, p. 325303, 2012.

[88] C. Laurent, "Charge dynamics in polymeric materials and its relation to electrical ageing," in *Proc. IEEE Conf. Electr. Insul. Dielectr. Phenom. (CEIDP)*, pp. 1-20, 2012.

[89] G. Reecht, F. Scheurer, V. Speisser, Y. J. Dappe, F. Mathevet, and G. Schull, "Electroluminescence of a polythiophene molecular wire suspended between a metallic surface and the tip of a scanning tunneling microscope," *Phys. Rev. Lett.,* vol. 112, 2014.

[90] M. V. Zamoryanskaya and A. N. Trofimov, "Cathodoluminescence of radiative centers in wide-bandgap materials," *Opt. Spectrosc.,* vol. 115, pp. 79-85, 2013.

[91] M. Toth, C. Zachreson, and I. Aharonovich, "Role of recombination pathway competition in spatially resolved cathodoluminescence spectroscopy," *Appl. Phys. Lett.,* vol. 105, 2014.

[92] D. J. Lacey and V. Dudler, "Chemiluminescence from polypropylene .1. Imaging thermal oxidation of unstabilised film," *Polym. Degrad. Stab.,* vol. 51, pp. 101-108, 1996.

[93] D. J. Lacey and V. Dudler, "Chemiluminescence from polypropylene .2. The emission wavelengths during prolonged oxidation," *Polym. Degrad. Stab.,* vol. 51, pp. 109-113, 1996.

[94] V. Dudler, D. J. Lacey, and C. Krohnke, "Chemiluminescence from polypropylene .3. Application to the study of antioxidant effectiveness," *Polym. Degrad. Stab.,* vol. 51, pp. 115-124, 1996.

[95] M. Celina, G. A. George, D. J. Lacey, and N. C. Billingham, "Chemiluminescence imaging of the oxidation of polypropylene," *Polym. Degrad. Stab.,* vol. 47, pp. 311-317, 1995.

[96] M. Duran, F. Massines, G. Teyssedre, and C. Laurent, "Luminescence of plasma-treated polymer surfaces at ambient temperature," *Surface & Coatings Technology,* vol. 142, pp. 743-747, 2001.

[97] F. Massines, P. Tiemblo, G. Teyssedre, and C. Laurent, "On the nature of the luminescence emitted by a polypropylene film after interaction with a cold plasma at low temperature," *J. Appl. Phys.,* vol. 81, pp. 937-943, 1997.

[98] J. Jonsson, B. Ranby, D. Mary, F. Massines, C. Laurent, and C. Mayoux, "An interpretation of electroluminescence of polyolefins based on the similarity between electro- and plasma-induced luminescence spectra," in *Proc. IEEE Int. Conf. Cond. Break. Soli. Dielectr.*, pp. 701-705, 1995.

[99] J. M. Alison, J. V. Champion, S. J. Dodd, and G. C. Stevens, "Dynamic bipolar charge recombination model for electroluminescence in polymer-based insulation during electrical tree initiation," *J. Phys. D: Appl. Phys.,* vol. 28, pp. 1693-1701, 1995.

[100] A. E. Miroshnichenko and Y. S. Kivshar, "Applied physics. Polarization traffic control for surface plasmons," *Science,* vol. 340, pp. 283-4, 2013.

[101] P. Canet and C. Laurent, "Electroluminescence from radiative decay of surface plasmons in aluminum insulator indium tin oxide structures," *J. Appl. Phys.,* vol. 75, pp. 7460-7464, 1994.

[102] C. Laurent and P. Canet, "Surface plasmon-induced luminescence: A new way to investigate space charge dynamics in thin dielectric films," *J. Appl. Phys.,* vol. 73, p. 5269, 1993.

[103] B. Qiao, G. Teyssedre, and C. Laurent, "AC electroluminescence spectra of Polyethylene Naphthalate: Impact of the nature of electrodes," in *Proc. IEEE Conf. Electr. Insul. Dielectr. Phenom. (CEIDP)*, pp. 93-96, 2013.

[104] G. Teyssedre, L. Cisse, D. Mary, and C. Laurent, "Identification of the components of the electroluminescence spectrum of PE excited in uniform fields," *IEEE Trans. Dielectr. Electr. Insul.,* vol. 6, pp. 11-19, 1999.

[105] L. A. Dissado and J. C. Fothergill, *Electrical degradation and breakdown in polymers*: IET, 1992.

[106] J. C. Fothergill, "Ageing, space charge and nanodielectrics: ten things we don't know about dielectrics," in *IEEE Int. Conf. Sol. Dielectr. (ICSD)*, pp. 1-10, 2007.

[107] N. Balkan, "Hot electrons in semiconductors," *Physics and Devices, Clarendon Press, Oxford,* 1998.

[108] Y. Sun, C. Bealing, S. Boggs, and R. Ramprasad, "50+ years of intrinsic breakdown," *IEEE Electr. Insul. Mag.,* vol. 29, pp. 8-15, 2013.

[109] S. Boggs and J. Densley, "Fundamentals of partial discharge in the context of field cable testing," *IEEE Electr. Insul. Mag.,* vol. 16, pp. 13-18, 2000.

[110] L. Niemeyer, "A generalized-approach to partial discharge modeling," *IEEE Trans. Dielectr. Electr. Insul.,* vol. 2, pp. 510-528, 1995.

[111] R. J. Densley, "Aging and breakdown of insulation by partial discharges," *J. Electrochem. Soc.,* vol. 122, pp. C72-C72, 1975.

[112] E. C. T. Macedo, J. M. Villanueva, E. G. da Costa, R. C. S. Freire, D. B. Araujo, J. M. R. de Souza Neto*, et al.*, *Assessment of dielectric degradation by measurement, processing and classification of partial discharges*, 2012.

[113] A. Krivda, "Automated recognition of partial discharges," *IEEE Trans. Dielectr. Electr. Insul.,* vol. 2, pp. 796-821, 1995.

[114] F. H. Kreuger, E. Gulski, and A. Krivda, "Classification of partial discharges," *IEEE Trans. Electr. Insul.,* vol. 28, pp. 917-931, 1993.

[115] C. Mauoux and C. Laurent, "Contribution of partial discharges to electrical breakdown of solid insulating materials," *IEEE Trans. Dielectr. Electr. Insul.,* vol. 2, pp. 641-652, 1995.

[116] E. Gulski, "Digital analysis of partial discharges," *IEEE Trans. Dielectr. Electr. Insul.,* vol. 2, pp. 822-837, 1995.

[117] S. A. Boggs and G. C. Stone, "Fundamental limitations in the measurement of corona and partial discharge," *IEEE Trans. Electr. Insul.,* vol. 17, pp. 143-150, 1982.

[118] H. Illias, G. Chen, and P. L. Lewin, "Modeling of partial discharge activity in spherical cavities within a dielectric material," *IEEE Electr. Insul. Mag.,* vol. 28, pp. 5-5, 2012.

[119] W. Sima, C. Jiang, P. Lewin, Q. Yang, and T. Yuan, "Modeling of the partial discharge process in a liquid dielectric: Effect of applied voltage, gap distance, and electrode type," *Energies,* vol. 6, pp. 934-952, 2013.

[120] M. Muhr and R. Woschitz, "Partial discharge diagnostic," in *Proc. Int. Conf. Prop. Appl. Dielectr. Mat.*, pp. 223-226 vol.1, 2000.

[121] P. H. F. Morshuis, "Partial discharge mechanisms in voids related to dielectric degradation," *IEE Proceedings-Science Measurement and Technology,* vol. 142, pp. 62-68, 1995.

[122] E. A. Franke and E. Czekaj, "Wideband partial discharge detector," *IEEE Trans. Electr. Insul.,* vol. 10, pp. 112-116, 1975.

[123] N. H. Ahmed and N. N. Srinivas, "Review of space charge measurements in dielectrics," *IEEE Trans. Dielectr. Electr. Insul.,* vol. 4, pp. 644-656, 1997.

[124] C. Villeneuve-Faure, L. Boudou, K. Makasheva, and G. Teyssedre, "Towards 3D charge localization by a method derived from atomic force microscopy: the electrostatic force distance curve," *J. Phys. D: Appl. Phys.,* vol. 47, 2014.

[125] A. Boularas, F. Baudoin, C. Villeneuve-Faure, S. Clain, and G. Teyssedre, "Multi-dimensional modelling of electrostatic force distance curve over dielectric surface: Influence of tip geometry and correlation with experiment," *J. Appl. Phys.,* vol. 116, 2014.

[126] G. Teyssedre, G. Tardieu, D. Mary, and C. Laurent, "Ac and dc electroluminescence in insulating polymers and implication for electrical ageing," *J. Phys. D: Appl. Phys.,* vol. 34, pp. 2220-2229, 2001.

[127] T. Tanaka and A. Greenwood, "Effects of charge injection and extraction on tree initiation in polyethylene," *IEEE Transactions on Power Apparatus and Systems,* vol. PAS-97, pp. 1749-1759, 1978.

[128] H. Zeller, "Noninsulating properties of insulating materials," in *Proc. IEEE Conf. Electr. Insul. Dielectr. Phenom. (CEIDP)*, pp. 19-47, 1991.

[129] J.-M. Restrepo-Florez, A. Bassi, and M. R. Thompson, "Microbial degradation and deterioration of polyethylene - A review," *Int. Biodeterior. Biodegrad.,* vol. 88, pp. 83-90, 2014.

[130] J. C. Fothergill, G. C. Montanari, G. C. Stevens, C. Laurent, G. Teyssedre, L. A. Dissado*, et al.*, "Electrical, microstructural, physical and chemical characterization of HV XLPE cable peelings for an electrical aging diagnostic data base," *IEEE Trans. Dielectr. Electr. Insul.,* vol. 10, pp. 514-527, 2003.

[131] A. T. Jones, J. M. Aizlewood, and D. Beckett, "Crystalline forms of isotactic polypropylene," *Die Makromolekulare Chemie,* vol. 75, pp. 134-158, 1964.

[132] J. Karger-Kocsis, *Polypropylene structure, blends and composites* vol. 2: Springer, 1995.

[133] S. Boggs, *Private Communication,* 2014.

[134] F. Peng, Q. Xunlin, W. Wirges, R. Gerhard, and L. Zirkel, "Polyethylene-naphthalate (PEN) ferroelectrets: cellular structure, piezoelectricity and thermal stability," *IEEE Trans. Dielectr. Electr. Insul.,* vol. 17, pp. 1079-1087, 2010.

[135] R. Bartnikas and R. Eichhorn, "Engineering dielectrics volume iia: Electrical properties of solid insulating materials: Molecular structure and electrical behavior," 1983.

[136] S. Boggs, C. Bealing, C. Wang, and R. Ramprasad, "Overview of high field aging: Empirical knowledge and theoretical basis," *Abstracts of Papers of the American Chemical Society,* vol. 246, 2013.

[137] S. Tamura and T. Kanai, "Control of well-defined crater structures on the surface of biaxially oriented polypropylene film by adding nucleators," *J. Appl. Polym. Sci.,* vol. 130, pp. 3555-3564, 2013.

[138] S. Tamura, K. Ohta, and T. Kanai, "Study of crater structure formation on the surface of biaxially oriented polypropylene film," *J. Appl. Polym. Sci.,* vol. 124, pp. 2725-2735, 2012.

[139] S. Le Roy, G. Teyssedre, and C. Laurent, "Charge transport and dissipative processes in insulating polymers: Experiments and model," *IEEE Trans. Dielectr. Electr. Insul.,* vol. 12, pp. 644-654, 2005.

[140] F. Baudoin, S. Le Roy, G. Teyssedre, and C. Laurent, "Bipolar charge transport model with trapping and recombination: an analysis of the current versus applied electric field characteristic in steady state conditions," *J. Phys. D: Appl. Phys.,* vol. 41, 2008.

[141] D. Ceresoli, M. C. Righi, E. Tosatti, S. Scandolo, G. Santoro, and S. Serra, "Exciton self-trapping in bulk polyethylene," *J Phys-Condens Mat,* vol. 17, pp. 4621-4627, 2005.

[142] D. Ceresoli, E. Tosatti, S. Scandolo, G. Santoro, and S. Serra, "Trapping of excitons at chemical defects in polyethylene," *J. Chem. Phys.,* vol. 121, pp. 6478-6484, 2004.

[143] C. R. Bealing and R. Ramprasad, "An atomistic description of the high-field degradation of dielectric polyethylene," *J. Chem. Phys.,* vol. 139, p. 174904, 2013.

[144] J. M. Pitarke, V. M. Silkin, E. V. Chulkov, and P. M. Echenique, "Theory of surface plasmons and surface-plasmon polaritons," *Rep. Prog. Phys.,* vol. 70, pp. 1-87, 2007.

[145] G. Teyssedre, D. Mary, and C. Laurent, "Analysis of the luminescence decay following excitation of polyethylene naphthalate films by an electric field," *J. Phys. D: Appl. Phys.,* vol. 31, pp. 267-275, 1998.

[146] R. Ritchie, "Surface plasmons in solids," *Surf Sci.,* vol. 34, pp. 1-19, 1973.

[147] E. Fort and S. Grésillon, "Surface enhanced fluorescence," *J. Phys. D: Appl. Phys.,* vol. 41, p. 013001, 2008.

[148] P. Dawson, D. Walmsley, H. Quinn, and A. Ferguson, "Observation and explanation of light-emission spectra from statistically rough Cu, Ag, and Au tunnel junctions," *Phys. Rev. B,* vol. 30, pp. 3164-3178, 1984.

[149] H. F. Ivey, "Recent Advances in Luminescence (Cathodoluminescence and Electroluminescence)," *IRE Transactions on Component Parts,* vol. 4, pp. 114-129, 1957.

[150] D. Poelman and P. F. Smet, "Time resolved microscopic cathodoluminescence spectroscopy for phosphor research," *Physica B: Condensed Matter,* vol. 439, pp. 35-40, 2014.

[151] M. Pluska, A. Czerwinski, A. Szerling, J. Ratajczak, and J. Katcki, "Effect of Secondary Electroluminescence on Cathodoluminescence and Other Luminescence Measurements," *Acta Phys. Pol., A,* vol. 125, pp. 1027-1032, 2014.

[152] D. Pines, *Elementary excitations in solids: lectures on phonons, electrons, and plasmons* vol. 5: WA Benjamin New York and Amsterdam, 1964.

[153] D. E. Newbury, D. C. Joy, P. Echlin, C. E. Fiori, and J. I. Goldstein, *Scanning electron microscopy and X-ray microanalysis*: Springer, 2003.

[154] L. Sanche, "Dissociative attachment and surface-reactions induced by low-energy electrons," *Journal of Vacuum Science & Technology B,* vol. 10, pp. 196-200, 1992.

[155] H. Raether, "Surface plasmons on smooth and rough surfaces and on gratings," *Springer Tracts in Modern Physics,* vol. 111, pp. 1-133, 1988.

[156] R. S. Becker, "Theory and interpretation of fluorescence and phosphorescence," 1969.

[157] H. R. Zeller, P. Pfluger, and J. Bernasconi, "High-mobility states and dielectric-breakdown in polymeric dielectrics," *IEEE Trans. Electr. Insul.,* vol. 19, pp. 200-204, 1984.

[158] J. W. Allen, "Impact processes in electroluminescence," *J. Lumin.,* vol. 48-9, pp. 18-22, 1991.

[159] N. F. Mott and R. W. Gurney, *Electronic processes in ionic crystals*: Clarendon Press, 1957.

[160] F. Boufayed, S. Leroy, G. Teyssedre, C. Laurent, P. Segur, L. A. Dissado*, et al.*, "Simulation of bipolar charge transport in polyethylene featuring trapping and hopping conduction through an exponential distribution of traps," in *Proc. Int. Symp. Electr. Insul. Mat.*, pp. 340-343 Vol. 2, 2005.

[161] S. Le Roy, V. Griseri, G. Teyssedre, and C. Laurent, "Simulation of charge build up and transport in electron beam irradiated organic dielectrics: Comparison to space charge measurements," in *Proc. IEEE Conf. Electr. Insul. Dielectr. Phenom. (CEIDP)*, pp. 349-352, 2008.

[162] L. A. Dissado, A. Thabet, and S. J. Dodd, "Simulation of DC electrical ageing in insulating polymer films," *IEEE Trans. Dielectr. Electr. Insul.,* vol. 17, pp. 890-897, 2010.

[163] L. A. Dissado and A. Thabet, "Simulation of electrical ageing in insulating polymers using a quantitative physical model," *J. Phys. D: Appl. Phys.,* vol. 41, 2008.

[164] C. Laurent, E. Kay, and N. Souag, "Dielectric breakdown of polymer films containing metal clusters," *J. Appl. Phys.,* vol. 64, pp. 336-343, 1988.

Biography

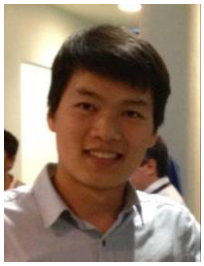

Bo QIAO was born on October 26 in 1988, in Baoding, China. He received his Bachelor of Science degree from Beijing Jiaotong University in 2010. In the same year, he joined the Institute of Optoelectronic Technology following his adviser Dr. Xurong Xu (physicist, academician of the Chinese Academy of Science), and obtained the Master of Engineering degree in material physics and chemistry in 2012. After that, he entered the Laboratory on Plasma and Conversion of Energy (LAPLACE), CNRS and University of Toulouse in France, following his adviser Dr. Gilbert Teyssedre (the director of DSF group), and Dr. Christian Laurent (the director of LAPLACE). Currently, he researches in electrical engineering, engaged in high voltage insulation, using electroluminescence and cathodoluminescence along with other luminescence techniques to understand hot electrons and space charge impacts on electrical ageing and degradation of polymeric insulations under high field for his Ph.D. study.

Journal articles:

1. B. Qiao, G. Teyssedre, C. Laurent, "Uncover the electroluminescence in wide band gap polymers," *J. Phys. D: Appl. Phys.*, vol. 48, pp. 405102, 2015.
2. B. Qiao, G. Teyssedre, C. Laurent, "Electroluminescence and cathodoluminescence from polyethylene and polypropylene films: spectra reconstruction from elementary components and underlying mechanism," *J. Appl. Phys.,* under review, 2015.
3. B. Qiao, C. Laurent, G. Teyssedre, "Evidence of exciton formation in thin polypropylene films under ac and dc field and relationship to electrical degradation," *IEEJ Trans. Fundam. Mat.*, accepted, 2015.

Conference papers:

1. B. Qiao, G. Teyssedre, C. Laurent, "Field- and electron beam-induced luminescence phenomena in polypropylene thin films," in *Proc. IEEE Int. Conf. Prop. Appl. Dielectr. Mat. (ICPADM),* pp. 1-4, Sydney, Australia, 19-22 July, 2015.
2. B. Qiao, G. Teyssedre, C. Laurent, "Contributing mechanisms to cathodoluminescence and AC electroluminescence spectra in polypropylene and polyethylene thin films," in *Conf. Jeun. Cherch. Géni. Electr. (JCGE)*, pp. 1-6, Cherbourg, France, 10-11 June, 2015.
3. B. Qiao, "Contributing mechanisms to cathodoluminescence and AC electroluminescence spectra of polypropylene thin films," in *GEET DAY*, pp. 1-3, Toulouse, France, 9 April, 2015.
4. B. Qiao, C. Laurent, G. Teyssedre, "Evidence of exciton formation in thin polypropylene films under AC and DC fields and relationship to electrical degradation," in *Proc. IEEE Int. Symp. Electr. Insul. Mat. (ISEIM)*, pp. 81-84, Toki Messe, Niigata City, Japan, 1-5 June, 2014.
5. B. Qiao, G. Teyssedre, C. Laurent, "AC Electroluminescence spectra of Polyethylene Naphthalate: impact of the nature of electrodes," in *Proc. IEEE Conf. Electr. Insul. Dielectr. Phenom. (CEIDP)*, pp. 93-96, Shenzhen, China, 21-23 October, 2013.

Title: Electrical ageing of insulating polymers: approach through electroluminescence and cathodoluminescence analyses

Abstract: Electroluminescence (EL) of insulating polymers is a subject of great interest because it is associated with electrical ageing and could provide the signature of excited species under electric field. Electrical ageing and breakdown in insulating polymers is of fundamental interest to the researchers, the design engineers, the manufacturers and the customers of electrical apparatus. In this respect, Partial Discharge (PD) is a harmful process leading to ageing and failure of insulating polymers. However, with the development of the materials and apparatus, PDs can be weakened or avoided in some situations, e.g. extra high voltage cables, capacitors, etc. Therefore, there is urgent demand for understanding electrical degradation mechanisms under high electric field, which can be triggered by energetic charge carriers.

In this work, Electroluminescence, EL, and cathodoluminescence, CL, excited under electron beam, along with other luminescence-family techniques are carried out for probing polyolefins and other insulating polymers. In order to uncover the excitons formation in Polypropylene (PP) and Polyethylene (PE) thin films, the field dependence of EL and current under DC stress and field dependence of EL and phase-resolved EL under AC stress, are investigated. The EL spectra of both PP and PE have the same main peak at approximately 570 nm, pointing towards similar chemical structures and defects in both polyolefins, and same route to degradation. This main peak can be complemented by an emission at approximately 750 nm dominating at low field. Electrode effect on the EL of Polyethylene Naphthalte (PEN) was investigated to understand the origin of the red emission at 750 nm. Through field dependence of EL and phase-resolved EL of Au or ITO electrodes, we proved the red component is due to the nature of electrode, more precisely Surface Plasmons and/or interface states.

Further thorough study was carried out on cathodoluminescence of insulating polymers. Thin films of PP, PE, along with Polyethylene Naphthalate (PEN) and Polyether Ether Ketone (PEEK) were irradiated under electron beam up to 5 keV to be excited. We could reconstruct EL and CL spectra of both PE and PP using four elementary components: i.e. Fluorescence, Chemiluminescence, Recombination-induced Luminescence, and main component of the EL spectrum at 570 nm reported above and constituting an ageing marker. For the first time the nature of both EL and CL in polyolefins is uncovered, containing four basic components with different relative contributions. Identification of these spectral components is helpful to interpret the nature of light emission from polyolefins and other insulating polymers and to bridge the gap between space charge distribution and electrical ageing or breakdown.

Through researches on EL and CL in several insulating polymers, i.e. polyolefins and a polyester, excitons formation and relaxation processes under electric stress and kinetic electrons are evidenced. More importantly, the spectral components analyses and reconstruction uncovers the nature of luminescence and its correlation to electrical ageing. In the future, luminescence measurement can be developed to be a standard method to probe and analyze insulating polymers.

Key words : Electroluminescence; Cathodoluminescence; Hot electrons; Insulating polymers; Space charge; Electrical Ageing; Electrical Degradation.

Titre: Une approche du vieillissement électrique des isolants polymères par mesure d'électroluminescence et de cathodoluminescence

Résumé: L'électroluminescence (EL) de isolants polymères est étudiée car elle peut permettre d'approcher les phénomènes de vieillissement électrique en fournissant la signature optique d'espèces excitées sous champ électrique. Le vieillissement et la rupture diélectrique dans les isolants polymères est d'un intérêt fondamental pour les chercheurs, concepteurs et fabricants de dispositif du génie électrique. À cet égard, les décharges partielles (DPs) sont un des principaux processus conduisant au vieillissement et à la défaillance des isolants. Cependant, avec le développement des matériaux et procédés, les DPs sont évitées dans certaines situations, par exemple, les câbles haute tension, les condensateurs, etc. Par conséquent, le besoin reste prégnant pour la compréhension des mécanismes de dégradation électrique sous forte contrainte électrique, qui peut être initiée par des porteurs énergétiques.

Dans ce travail, l'EL, la cathodoluminescence (CL) excitée sous faisceau d'électrons, ainsi que d'autres techniques de luminescence ont été appliquées à la caractérisation de polyoléfines et d'autres polymères isolants. Afin de comprendre la formation d'excitons dans des films minces de Polypropylène (PP) et Polyéthylène (PE), la dépendance en champ de l'EL et du courant sous contrainte continue, et de l'EL et de sa résolution selon la phase sous contrainte AC, sont étudiées. Les spectres d'EL du PP et du PE ont le même pic principal à environ 570 nm, ce qui implique des structures et des défauts chimiques similaires pour les deux matériaux, et le même processus de dégradation. Le pic principal peut être complété par une émission à environ 750 nm dominante à faible champ. L'impact de la nature des électrodes a été étudiée sur du PEN pour comprendre l'origine de l'émission dans le rouge. A travers la dépendance en champ de l'EL et sa résolution selon la phase avec des métallisations or et ITO, on montre que l'émission dans le rouge est liée à la nature des électrodes et correspond à l'excitation de plasmons de surface ou d'états d'interface.

Une étude plus approfondie est effectuée sur la cathodoluminescence d'isolants polymères. Des couches minces de PP, PE, ainsi que de Polyethylene Naphthalate (PEN) et de Polyether Ether Ketone (PEEK) ont été irradiés par faisceau d'électrons jusqu'à 5 keV. Nous avons pu reconstruire les spectres de CL et d'EL du PE et du PP à partir de quatre composants élémentaires: fluorescence, chimiluminescence, luminescence induite par recombinaison, et composante principale du spectre d'EL à 570nm décrite plus haut et considérée comme signature du vieillissement. Pour la première fois, la nature de l'EL et de la CL de polyoléfines est décomposée en quatre composantes de base avec des contributions relatives différentes. L'identification de ces composantes spectrales est utile pour interpréter la luminescence de polyoléfines et autres isolants polymères, et établir les liens entre distribution de charge d'espace et vieillissement diélectrique.

A travers ces recherches sur l'EL et la CL dans plusieurs isolants polymères, i.e. polyoléfines ou polyesters, la formation d'excitons et les processus de relaxation d'énergie sous contrainte électrique et électrons énergétiques sont mis en évidence. Surtout, l'analyse en composantes spectrales et la reconstruction des spectres donne accès aux mécanismes d'excitation de la luminescence et à une corrélation avec le vieillissement électrique. A l'avenir, les mesures de luminescence peuvent devenir une méthode standard pour sonder et analyser les isolants polymères.

Mots clés: Electroluminescence; Cathodoluminescence; Porteurs chauds; Isolants polymères; Charge d'espace; Vieillissement électrique; Dégradation électrique.